

12-1-2010

# NF- $\kappa$ B translocation in response to different LPS chemotypes in murine macrophages

Elizabeth Carles

Follow this and additional works at: [https://digitalrepository.unm.edu/biol\\_etds](https://digitalrepository.unm.edu/biol_etds)

---

## Recommended Citation

Carles, Elizabeth. "NF- $\kappa$ B translocation in response to different LPS chemotypes in murine macrophages." (2010).  
[https://digitalrepository.unm.edu/biol\\_etds/13](https://digitalrepository.unm.edu/biol_etds/13)

This Thesis is brought to you for free and open access by the Electronic Theses and Dissertations at UNM Digital Repository. It has been accepted for inclusion in Biology ETDs by an authorized administrator of UNM Digital Repository. For more information, please contact [disc@unm.edu](mailto:disc@unm.edu).

**Elizabeth L. Carles**

*Candidate*

**Biology**

*Department*

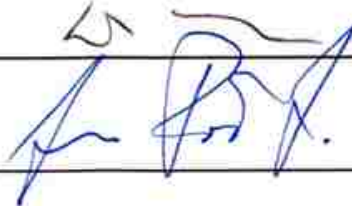
This thesis is approved, and it is acceptable in quality and form for publication:

*Approved by the Thesis Committee:*

Dr. Mary Anne Nelson  ,Chairperson

Dr. Donald Natvig

Dr. Jens F. Poschet



**NF- $\kappa$ B TRANSLOCATION IN RESPONSE TO DIFFERENT LPS  
CHEMOTYPES IN MURINE MACROPHAGES**

**BY**

**ELIZABETH L. CARLES**

**B.S. Biology, University of New Mexico, 2003**

THESIS

Submitted in Partial Fulfillment of the  
Requirements for the Degree of

**Master of Science**

**Biology**

The University of New Mexico  
Albuquerque, New Mexico

**December, 2010**

## **DEDICATION**

I would like to dedicate this thesis to my family, especially my husband Felix and my daughter Natalie. I finished this for you. I would also like to thank my mother, who was always there to help out, whether by feeding me, babysitting, or proofreading.

## ACKNOWLEDGMENTS

I would like to acknowledge the hard work of everyone involved in the MISL Grand Challenge LDRD and the K-Channels LDRD, and thank Sandia National Laboratories for funding and support. I would like to especially thank my advisor, Jens Poschet, for teaching me cell biology, and my colleagues Bryan Carson, Jaclyn Murton, Conrad James, and Igal Brenner for their contributions and guidance. I would also like to acknowledge Cathy Branda, Steve Branda, Mark Van Benthem, Jeff Lucero, Natasha Moonka, Jaewook Joo, Tony Martino, and Anup Singh for their contributions. I want to sincerely thank Dr. Mary Anne Nelson and Dr. Donald Natvig for helping me to collaborate between Sandia and UNM to complete this degree, and to Dr. Susan Rempe for supporting me these last years.

**NF- $\kappa$ B TRANSLOCATION IN RESPONSE TO DIFFERENT  
LPS CHEMOTYPES IN MURINE MACROPHAGES**

**BY**

**ELIZABETH L. CARLES**

**ABSTRACT OF THESIS**

Submitted in Partial Fulfillment of the  
Requirements for the Degree of

**Master of Science**

**Biology**

The University of New Mexico  
Albuquerque, New Mexico

**December, 2010**

## **NF- $\kappa$ B Translocation in Response to Different LPS Chemotypes in Murine Macrophages**

**By  
Elizabeth L. Carles**

**B.A., Biology, University of New Mexico, 2003**

**M.S., Biology, University of New Mexico, 2010**

### **ABSTRACT**

Nuclear Factor  $\kappa$ B (NF- $\kappa$ B) proteins make up a large family of eukaryotic transcription factors that regulate many important cellular functions, including cell signaling, cell growth, development, cell death by apoptosis, and immune and inflammatory responses, and has been shown to be involved in multiple human diseases. NF- $\kappa$ B proteins are subject to careful regulation in the cell, and are regulated at multiple levels. A family of inhibitory proteins exist (called I $\kappa$ B proteins) which bind to NF- $\kappa$ B and cause it to be localized in the cytoplasm. There are multiple signal transduction pathways that can lead to the activation of NF- $\kappa$ B. These signal transduction pathways are induced by contact with a wide variety of molecules, and therefore a huge number of molecules can act as NF- $\kappa$ B activators. One such molecule is lipopolysaccharide (LPS), a bacterial cell wall component, which activates NF- $\kappa$ B via Toll-Like Receptor 4 (TLR4). Following TLR4 activation, I $\kappa$ B is degraded, releasing NF- $\kappa$ B. NF- $\kappa$ B then triggers the transcription of I $\kappa$ B, thus down-regulating its own activity. These complex feedbacks create oscillations that have previously been observed in electrophoretic mobility shift assays (EMSA) and live-cell imaging studies. In order to better understand and characterize NF- $\kappa$ B oscillations, we created macrophage cell lines stably expressing a fluorescently labeled monomer of the NF- $\kappa$ B dimer, RelA-GFP, and conducted time-lapse fluorescence imaging studies of these cells. We examined nuclear NF- $\kappa$ B oscillations in both wild-type and transfected cell lines upon activation by bacterial LPS. LPS chemotypes from various organisms were tested for their effects on oscillatory patterns. Our data show that all LPS' were able to elucidate oscillations, a novel finding for RAW 264.7 macrophage cells. The data also show that while the responses to the

different LPS chemotypes do lead to different oscillatory dynamics, they do not show any easily discernable patterns. This suggests that the temporal profile of NF- $\kappa$ B may not be stimulus specific (at the chemotype level). Our data leads to the conclusion that the oscillatory dynamics of NF- $\kappa$ B may not play as large of a role in immune response as initially thought.



## TABLE OF CONTENTS

LIST OF FIGURES .....	xi
LIST OF TABLES .....	xiii
<b>Chapter 1. Background &amp; Introduction.....</b>	<b>1</b>
1.1 NF- $\kappa$ B Proteins .....	2
1.1.1 NF- $\kappa$ B Target Genes.....	3
1.1.2 NF- $\kappa$ B Regulation.....	4
1.1.3 NF- $\kappa$ B Activators .....	4
1.2 LPS Activation of the TLR4 Signaling Cascade.....	7
1.2.1 LPS Structural Diversity .....	8
1.3 NF- $\kappa$ B Oscillations .....	10
1.4 Purpose of this Work .....	13
<b>Chapter 2. Materials &amp; Methods .....</b>	<b>14</b>
2.1 Cell Culture.....	15
2.2 Fluorescent Construct Preparation, Transfection, and Stable Cell Line Development .....	15
2.3 Endotoxin Preparation .....	17
2.4 Immunocytochemistry.....	17
2.5 Microscopy Experiments.....	19
2.6 Live Microscopy Image Analysis.....	21
2.7 Manual Clustering.....	24
<b>Chapter 3. Results .....</b>	<b>25</b>
3.1 Immunocytochemistry.....	26
3.1.1 NF- $\kappa$ B Response due to LPS in RAW 264.7 Cells:.....	26
3.1.1.1 1nM <i>E. coli</i> LPS.....	26

3.1.1.2 100nM <i>E. coli</i> LPS .....	27
3.1.1.3 1nM <i>Y. pestis</i> 21°C LPS .....	28
3.1.1.4 100nM <i>Y. pestis</i> 21°C LPS .....	29
3.1.1.5 1nM <i>Y. pestis</i> 37°C LPS .....	30
3.1.1.6 100nM <i>Y. pestis</i> 37°C LPS .....	31
3.1.1.7 Summary .....	32
3.1.2 NF- $\kappa$ B Response due to LPS in RAW-RG16 Cells: .....	35
3.1.2.1 1nM <i>E. coli</i> LPS .....	35
3.1.2.2 100nM <i>E. coli</i> LPS .....	35
3.1.2.3 1nM <i>Y. pestis</i> 21°C LPS .....	36
3.1.2.4 100nM <i>Y. pestis</i> 21°C LPS .....	37
3.1.2.5 1nM <i>Y. pestis</i> 37°C LPS .....	38
3.1.2.6 100nM <i>Y. pestis</i> 37°C LPS .....	39
3.1.2.7 Summary .....	40
3.2 Live-Cell Microscopy .....	43
3.2.1 1nM <i>E. coli</i> LPS .....	43
3.2.2 100nM <i>E. coli</i> LPS .....	44
3.2.3 1nM <i>Y. pestis</i> 21°C LPS .....	44
3.2.4 100nM <i>Y. pestis</i> 21°C LPS .....	45
3.2.5 1nM <i>Y. pestis</i> 37°C LPS .....	45
3.2.6 100nM <i>Y. pestis</i> 37°C LPS .....	46
3.3 Live Microscopy Data and Analysis of Oscillatory Behavior .....	46
3.4 Summary .....	47
<b>Chapter 4. Discussion &amp; Conclusions .....</b>	<b>48</b>
4.1 Discussion .....	49

4.1.1 Immunocytochemistry .....	49
4.1.1.1 NF- $\kappa$ B Response due to LPS in RAW 264.7 Cells.....	49
4.1.1.2 NF- $\kappa$ B Response due to LPS in RAW-RG16 Cells .....	50
4.1.1.3 Comparison of NF- $\kappa$ B Response in RAW 264.7 vs. RAW-RG16 Cells .....	50
4.1.2 Live-Cell Microscopy.....	52
4.1.2.1 <i>E. coli</i> LPS.....	53
4.1.2.2 <i>Y. pestis</i> 21°C LPS.....	54
4.1.2.3 <i>Y. pestis</i> 37°C LPS.....	55
4.1.3 Oscillatory Behavior Clustering:.....	56
4.2 Conclusions.....	61
<b>Appendices .....</b>	<b>64</b>
Appendix A. Oscillation Data Plots .....	65
Appendix B. Matlab and CellProfiler Scripts .....	83
References .....	96

## LIST OF FIGURES

Figure 1. Schematic diagram of NF- $\kappa$ B protein structure.....	2
Figure 2. Pathways leading to the activation of NF- $\kappa$ B .....	6
Figure 3. The TLR4 signaling cascade .....	8
Figure 4. The structural diversity of lipid A in Gram-negative microorganisms .....	9
Figure 5. Analysis of NF- $\kappa$ Bn by EMSAs of nuclear extracts prepared at indicated times after stimulation with TNF- $\alpha$ (10 ng/ml) of fibroblasts of the indicated genotype .....	11
Figure 6. Restriction map of p $\beta$ Actin--EGFP-FLAG-RelA.....	16
Figure 7. RAW-RG16 cells at 60X magnification.....	17
Figure 8. NF- $\kappa$ B oscillations in RAW 264.7 macrophages in response to LPS activation .....	20
Figure 9. RAW-RG16 cells at 60X magnification .....	21
Figure 10. The main output windows of CellProfiler™. ....	22
Figure 11. Example of the Matlab® generated plots of the ratio of nuclear to cytoplasmic intensity of each cell over time for a typical dataset .....	23
Figure 12. Example of the Matlab® generated plots of the spatial positions of each cell over time for a typical dataset .....	24
Figure 13. Average percentage of RAW 264.7 cells showing NF- $\kappa$ B translocation into the nucleus after exposure to <i>E. coli</i> LPS at 1nM and 100nM at the stated time intervals. ....	28
Figure 14. Average percentage of RAW 264.7 cells showing NF- $\kappa$ B translocation into the nucleus after exposure to <i>Y. pestis</i> 21°C LPS at 1nM and 100nM at the stated time intervals .....	30
Figure 15. Average percentage of RAW 264.7 cells showing NF- $\kappa$ B translocation into the nucleus after exposure to <i>Y. pestis</i> 37°C LPS at 1nM and 100nM at the stated time intervals .....	32
Figure 16. Plot of the average number of cells (of the 3 replicates) translocated at each time point for the 3 tested chemotypes at 1nM. ....	34
Figure 17. Plot of the average number of cells (of the 3 replicates) translocated at each time point for the 3 tested chemotypes at 100nM. ....	34
Figure 18. Average percentage of RAW-RG16 cells showing NF- $\kappa$ B translocation into the nucleus after exposure to <i>E. coli</i> LPS at 1nM and 100nM at the stated time intervals.....	36
Figure 19. Average percentage of RAW-RG16 cells showing NF- $\kappa$ B translocation into the nucleus after exposure to <i>Y. pestis</i> 21° LPS at 1nM and 100nM at the stated time intervals .....	38
Figure 20. Average percentage of RAW-RG16 cells showing NF- $\kappa$ B translocation into the nucleus after exposure to <i>Y. pestis</i> 37° LPS at 1nM and 100nM at the stated time intervals .....	40

Figure 21. Plot of the average number of cells (of the 3 replicates) translocated at each time point for the 3 tested chemotypes at 1nM .....	42
Figure 22. Plot of the average number of cells (of the 3 replicates) translocated at each time point for the 3 tested chemotypes at 100nM .....	42
Figure 23. Intensity plots from Matlab® for all 18 datasets, with plots for each cell from each unique chemotype/concentration combination overlaid .....	47
Figure 24. Comparison of the average number of wild-type RAW 264.7 cells versus transfected RAW-RG16 cells showing nuclear NF-κB in response to 1nM LPS stimulation .....	51
Figure 25. Comparison of the average number of wild-type RAW 264.7 cells versus transfected RAW-RG16 cells showing nuclear NF-κB in response to 100nM LPS stimulation .....	52
Figures 26 and 27. Comparison of NF-κB oscillation types stimulated by 1nM <i>E. coli</i> , <i>Y. pestis</i> 37°C, or <i>Y. pestis</i> 21°C LPS.....	58
Figures 28 and 29. Comparison of NF-κB oscillation types stimulated by 100nM <i>E. coli</i> , <i>Y. pestis</i> 37°C, or <i>Y. pestis</i> 21°C LPS.....	59

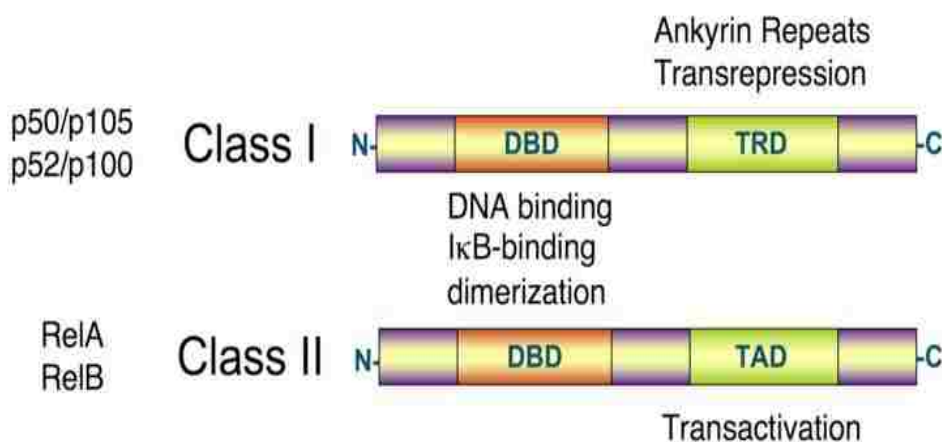
## **LIST OF TABLES**

Table 1. Average percent of RAW 264.7 cells showing NF- $\kappa$ B translocation into the nucleus after exposure to at 1nM or 100nM LPS at the stated time intervals. ....	33
Table 2. Average percent of RAW-RG16 cells showing NF- $\kappa$ B translocation into the nucleus after exposure to at 1nM or 100nM LPS at the stated time intervals. ....	41
Table 3. Percentage of RAW-RG16 cells showing particular NF- $\kappa$ B localization behaviors after exposure to the stated LPS chemotypes at 1nM and 100nM, at the stated time intervals. ...	57

## Chapter 1. Background & Introduction

## 1.1 NF- $\kappa$ B Proteins

Nuclear Factor  $\kappa$ B (NF- $\kappa$ B) proteins make up a large family of eukaryotic transcription factors that share a highly conserved Rel homology (RH) domain. The RH domain contains the DNA-binding domain and the dimerization domain, as well as the sequence needed for nuclear localization and the I $\kappa$ B (inhibitor  $\kappa$ B) binding sequence (Gilmore, 1999). NF- $\kappa$ B proteins are divided into two groups based on their sequence (Figure 1). Class I proteins contain a number of ankyrin



**Figure 1. Schematic diagram of NF- $\kappa$ B protein structure. (Image used with permission of creator, BogHog2, from Wikimedia Commons.)**

repeats and have transrepression activity (p100/p50 and p102/p52; Carlotti et al., 1999), while Class II proteins have transactivation domains (RelA or p65, RelB, and c-Rel). NF- $\kappa$ B proteins form both homo and heterodimers. Class I proteins do not generally activate transcription unless dimerized with a Class II protein. The most common dimer found in cells is the RelA/p50 heterodimer, and this structure is generally what is being referred to when NF- $\kappa$ B is used (Hoffman et al., 2002). These NF- $\kappa$ B dimers bind to segments of DNA 9-10 base pairs long (Gilmore, 2006). The sequence of this DNA segment varies greatly among



organisms, but is generally organized as 5'-GGGRNWYYCC-3', where R is A or G, N is any nucleotide, W is A or T and Y is C or T.

### **1.1.1 NF- $\kappa$ B Target Genes**

Due to its structural diversity, NF- $\kappa$ B has the ability to transcriptionally regulate many important cellular functions, including cell signaling, cell growth, development, cell death by apoptosis, and most commonly, immune and inflammatory responses (Hiscott et al., 2001). NF- $\kappa$ B has been shown to be involved in multiple human diseases like cancer, diabetes, AIDS, arthritis, inflammatory bowel disease, and even asthma, and is therefore being researched as a drug target for several diseases (Baldwin, 2001). NF- $\kappa$ B targets a number of important cytokine genes, including many interleukin genes, like IL-1, IL-2, IL-6, and IL-8 (Baldwin, 2001), several C-C motif chemokines like CCL-5 (Wickremasinghe et al., 2004), CCL-15 (Shin et al., 2005), and CCL-28 (Ogawa et al., 2004), lymphotoxins a and b (Worm et al., 1998 and Kuprash et al., 1996), and tumor necrosis factor  $\alpha$  (TNF $\alpha$ ; Shakhov et al., 1990). NF- $\kappa$ B is also important for the regulation of many genes involved in apoptosis, including inhibitors of apoptosis 1 and 2 (IAP-1 and IAP-2) and TNF-receptor associated factors 1 and 2 (TRAF-1 and TRAF-2; Sethi et al., 2008). NF- $\kappa$ B regulates a large number of other important transcription factors, including the proto-oncogenes c-myc (Duyao et al., 1990) and c-rel (Hannink and Temin, 1990), the tumor suppressor gene p53 (Wu and Lozano, 1994), and various interferon regulatory factors like IRF-1 and IRF-2 (Harada et al., 1994). The lists above are

not intended to be exhaustive, as over 150 target genes regulated by NF- $\kappa$ B have been identified to date (Sethi et al., 2008).

### **1.1.2 NF- $\kappa$ B Regulation**

NF- $\kappa$ B proteins are subject to careful regulation in the cell, and are regulated at multiple levels, including dimerization, nuclear translocation, DNA binding, interaction with other transcription factors, and interaction with transcription mechanism proteins (Chen and Ghosh, 1999). In order to regulate NF- $\kappa$ B translocation into the nucleus, a family of inhibitory proteins exists that bind to it and cause it to be localized in the cytoplasm (Kearns et al., 2006). These inhibitors, the I $\kappa$ B proteins ( $\alpha$ ,  $\beta$ ,  $\epsilon$ , and  $\gamma$ ), interact with NF- $\kappa$ B in many ways, one of which is to cover the nuclear localization sequence of NF- $\kappa$ B, therefore inhibiting its translocation. In response to certain extracellular signals (activators), I $\kappa$ B proteins are phosphorylated by I $\kappa$ B kinase (IKK), leading to their degradation. I $\kappa$ B degradation releases bound NF- $\kappa$ B, which is then free to enter the nucleus and activate genes (Carlotti et al., 1999). It is important to note that hundreds of other molecules have been identified that can inhibit the NF- $\kappa$ B pathway (Gilmore, 2009).

### **1.1.3 NF- $\kappa$ B Activators**

There are multiple signal transduction pathways that can lead to the activation of NF- $\kappa$ B, almost all of which culminate in the activation of IKK (see Figure 2). These signal transduction pathways are induced by contact with a wide variety of molecules, and therefore a huge number of molecules can act as

NF- $\kappa$ B activators. A thorough review of the published literature reveals a long list of activators, including bacteria, fungi, viruses and their products, eukaryotic parasites, inflammatory cytokines, physical and oxidative stress, proteins, receptor ligands, growth factors, hormones, and chemical agents (Pahl, 1999). These molecules bind to many different cell surface receptors, including Toll-Like receptors (TLRs), tumor necrosis factor (TNF) receptors, interleukin-1 (IL-1) receptors, and growth factor receptors, among others (Fischer et al., 1999). One of the most important and well studied activators of NF- $\kappa$ B is lipopolysaccharide (LPS), a major component of the cell wall of Gram-negative bacteria.

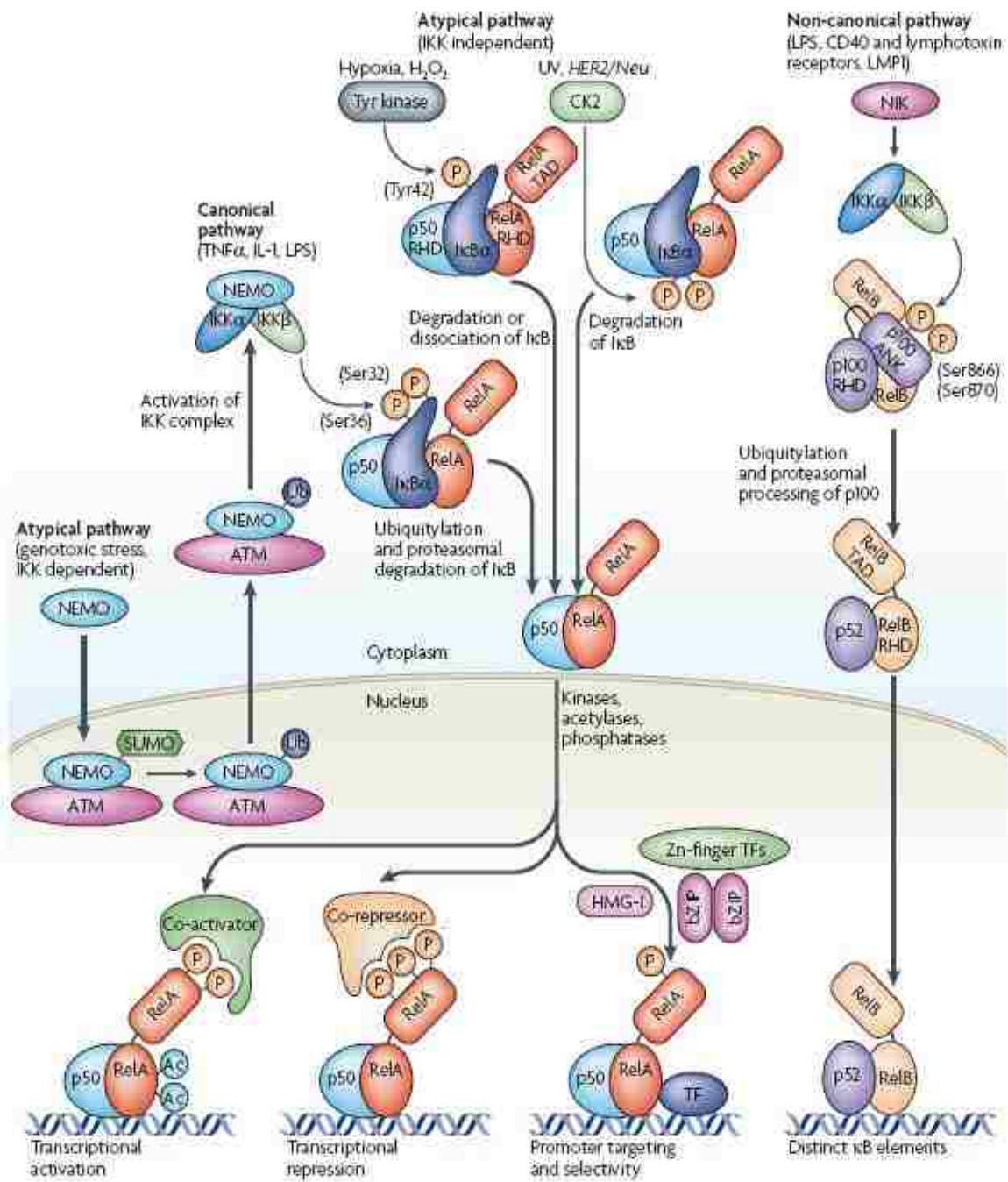


Figure 2. Pathways leading to the activation of NF- $\kappa$ B (image from Perkins, 2007).

## 1.2 LPS Activation of the TLR4 Signaling Cascade

In order to function as an activator, LPS must be extracted from the pathogen's cell wall and transferred to the host's immune cells for recognition. This process is complex and involves multiple proteins. First, LPS is bound to the lipid binding protein (LPB), which removes it from the bacterial membrane (Miyake, 2006). LPS is then transferred to another protein, CD14 (from the cluster of differentiation 14 gene), which delivers it to a heterodimeric membrane protein complex composed of TLR4 (toll-like receptor 4) and MD2 (Park et al., 2009). The TLR4 receptor complex is an important component of innate immunity and pathogen recognition. LPS binding to the TLR4 complex leads to an interaction with the cytosolic adapter proteins myeloid differentiation primary response protein 88 (MyD88) and TIR domain-containing adapter protein (TIRAP; Kawai and Akira 2006). These proteins then recruit interleukin-1 receptor associated kinase 4 (IRAK4), which, upon phosphorylation, is dissociated from MyD88, causing the activation of tumor necrosis factor receptor-associated factor 6 (TRAF6). TRAF6 activates transforming growth factor- $\beta$ -activated protein kinase 1 (TAK1), which then activates I $\kappa$ B kinase (IKK), which phosphorylates I $\kappa$ B. Phosphorylated I $\kappa$ B is ubiquitinated and broken down, causing it to release NF- $\kappa$ B. NF- $\kappa$ B can then translocate into the nucleus, where it acts as a transcription factor leading to the eventual release of inflammatory cytokines (Figure 3).

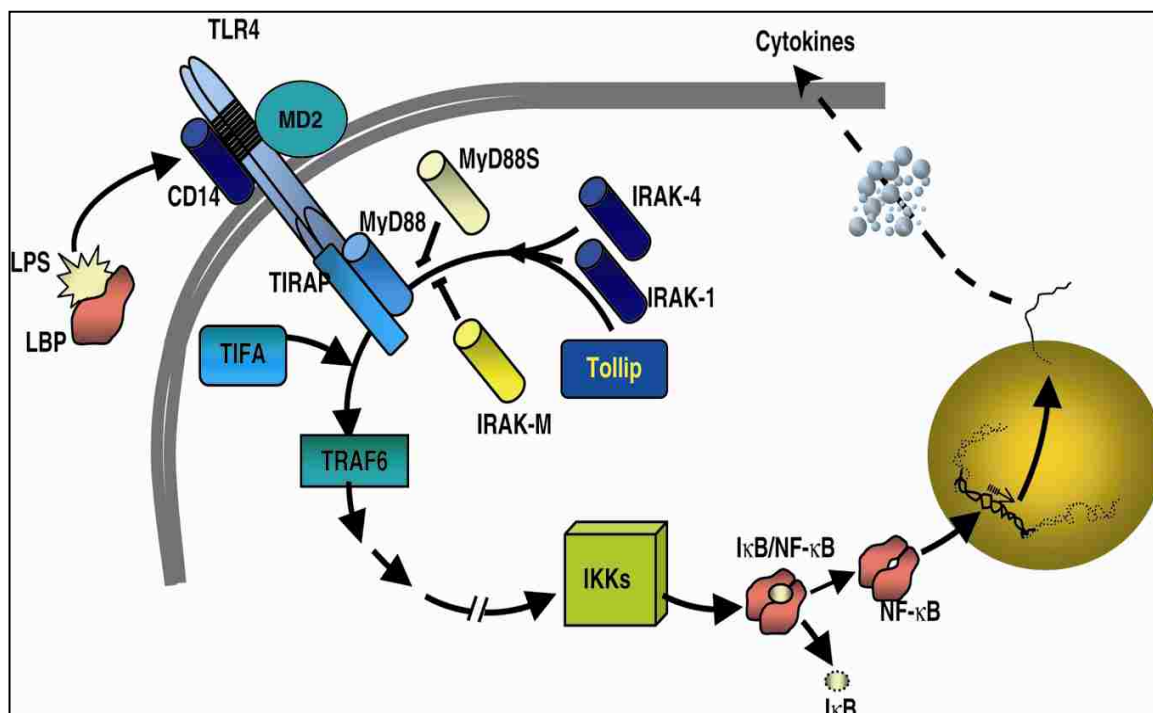
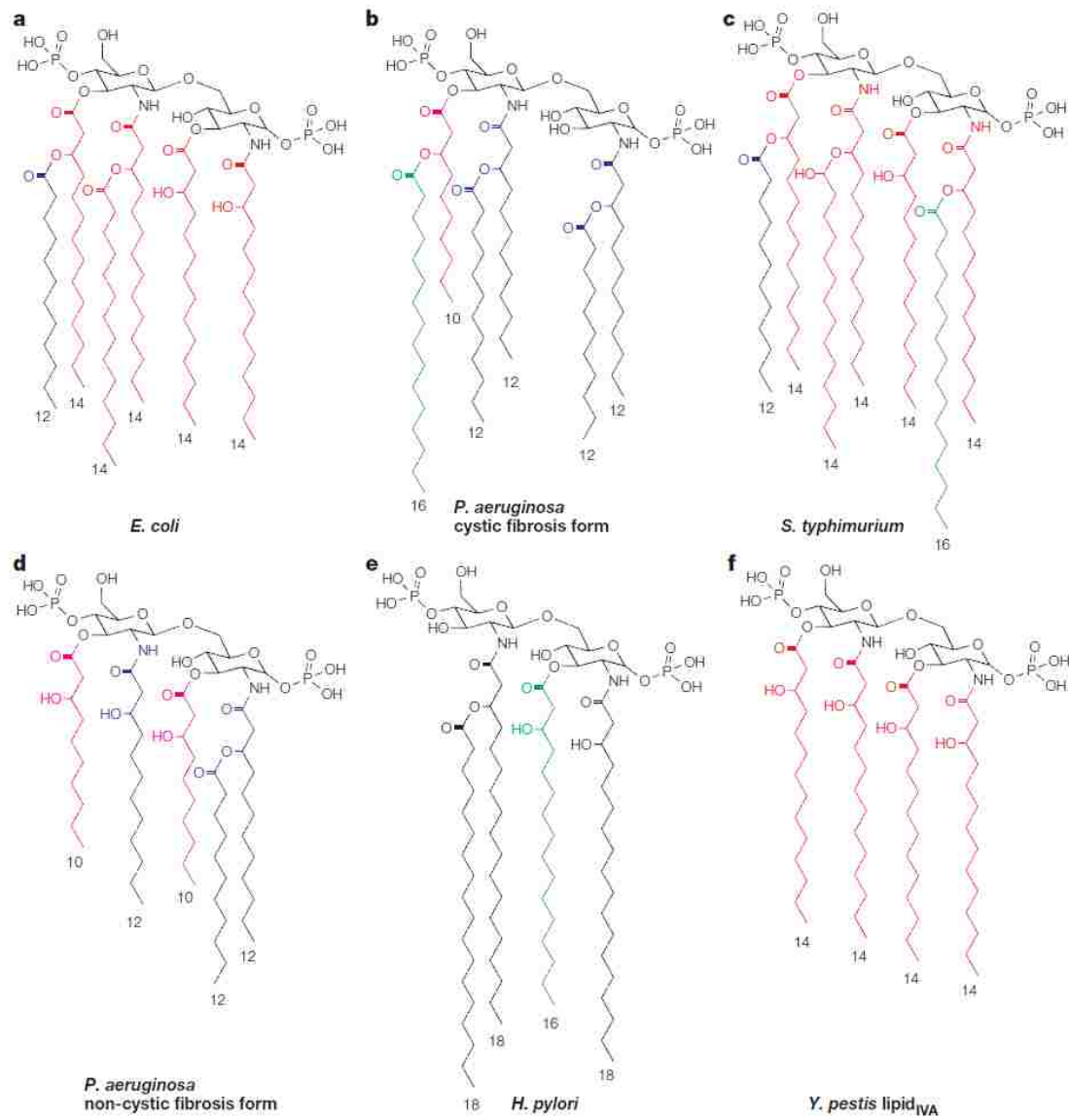


Figure 3. The TLR4 signaling cascade (from Villar et al., 2004).

### 1.2.1 LPS Structural Diversity

LPS molecules synthesized by different gram negative bacteria differ greatly in their structures, particularly in their lipid A component (see Figure 4). These lipids can differ in fatty-acid length and number, and in phosphorylation states (Miller et al., 2005). Some gram negative bacteria are even capable of specifically modifying lipid A using the PhoP–PhoQ two-component regulatory system (Guo et al., 1998). It has even been shown that a single species of bacteria can produce different lipid A structures in response to different environmental conditions. One important example of this is found in *Yersinia pestis*, the organism that causes the plague. *Y. pestis* changes its lipid A structure from hexaacyl to tetraacyl in response to the temperature increase that occurs when it is transferred from the insect vector (21°C) to the mammalian host

(37°C; Rebeil et al., 2004). Alternate lipid A structures may bind to TLR4 differently, giving a possible explanation of how various pathogens initiate different immune responses (Miller et al., 2005).



**Figure 4.** The structural diversity of lipid A in Gram-negative microorganisms (from Miller et al., 2005).

### 1.3 NF- $\kappa$ B Oscillations

Under normal conditions in non-induced cells, NF- $\kappa$ B is kept inactive in the cytoplasm (via bound I $\kappa$ B). To maintain this state, cells keep the concentration of I $\kappa$ B proteins at levels equal to or higher than NF- $\kappa$ B concentrations (Scott et al., 1993). This is accomplished by an increase in I $\kappa$ B transcription, which is controlled by a promoter that is highly responsive to NF- $\kappa$ B activation (Ihekwaba et al., 2004). Therefore as NF- $\kappa$ B concentration increases, so does the concentration of its inhibitor I $\kappa$ B $\alpha$ , creating a negative feedback loop between the proteins (Hoffmann et al., 2002). The differential regulation of NF- $\kappa$ B and I $\kappa$ B $\alpha$  leads to small temporal differences in the transcription and degradation of these proteins, so the translocation of NF- $\kappa$ B tends to be cyclical (Gilmore, 2006) with oscillations in its nuclear concentration (Hoffman et al., 2002). It is thought that the amplitude and period of these oscillations may be important for the transcriptional control of target genes, much in the same way that calcium signaling uses amplitude modulation to control differential gene activation (Berridge, 1997; Nelson et al., 2004). Low concentrations of calcium stimulate the NFAT and ERK pathways, while high concentrations stimulate other regulatory pathways. Oscillatory behavior has been found in a large number of other biological systems as well, including several in the immune system (Stark et al., 2007). Periodic fevers have been shown due to malaria infection and Familial Mediterranean Fever. Neutrophils have oscillations in their NADPH concentration and oscillations have also been seen in the Hes1 transcriptional



repressor and in the p53 tumor suppressor proteins (Adachi et al., 1999; Hirata et al., 2002; Lev Bar-Or et al., 2000).

Because of the complexity of the NF- $\kappa$ B/I $\kappa$ B $\alpha$  system and its negative feedback loop, oscillations in nuclear NF- $\kappa$ B concentrations were predicted, but their existence depends on the cross regulation of the two components (Hoffmann et al., 2002). Recently, Hoffman et al., (2002) completed the first experiments actually demonstrating NF- $\kappa$ B oscillations using an electrophoretic mobility shift assay (EMSA) on human and mouse cell lines exposed to TNF $\alpha$  (Hoffman et al., 2002). Nuclear extracts from TNF $\alpha$ -stimulated cells were allowed to bind to a preparation of oligonucleotides containing an NF- $\kappa$ B consensus sequence (GGGACTTCC). When run on a gel, the amount of protein bound to the oligonucleotides oscillated over time (see Figure 5).

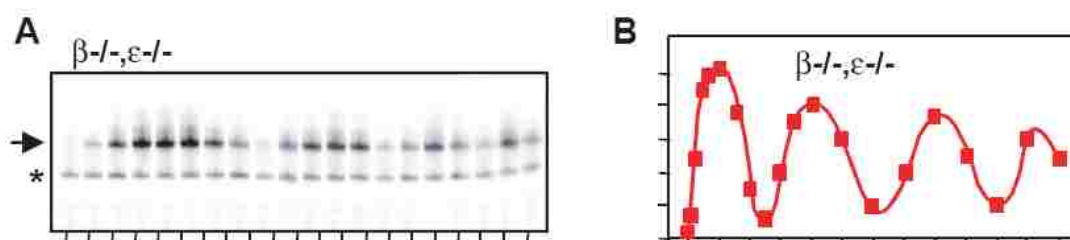


**Figure 5.** Analysis of NF- $\kappa$ Bn by EMSAs of nuclear extracts prepared at indicated times after stimulation with TNF- $\alpha$  (10 ng/ml) of fibroblasts of the indicated genotype (figure from Hoffman et al., 2002).

Although they did observe oscillations, these were seen in mouse fibroblasts that contained only one of the three I $\kappa$ B isoforms (I $\kappa$ B $\alpha$ ), and results in wild type cells were not published. Based on their results, they constructed a computational model that described the temporal control of NF- $\kappa$ B translocation and the role I $\kappa$ B plays in shutting NF- $\kappa$ B off. The model shows that I $\kappa$ B $\alpha$  works to rapidly turn off

NF- $\kappa$ B, allowing strong negative feedback and explaining the oscillatory behavior. It also shows that I $\kappa$ B $\beta$  and I $\kappa$ B $\epsilon$  act to dampen the oscillations over the long term.

In 2004, Nelson et al. published the first paper showing NF- $\kappa$ B oscillations in live HeLa (human cervical carcinoma) and SK-N-AS (human neuroblastoma) cells exposed to TNF $\alpha$  using fluorescent fusion proteins. Their experiments showed that oscillations in cells were asynchronous and that the frequency of oscillations decreased when I $\kappa$ B $\alpha$  concentration increased. This work remains controversial, however, as the Hoffmann model predicts that even small increases in NF- $\kappa$ B concentration can significantly alter the oscillatory dynamics (Barken et al., 2005). The experiments published by Nelson et al. used transfected cell lines estimated to contain as much as 5 times the wild-type RelA concentrations. Nelson et al. (2005) responded to this criticism by stating that their experiments allowed them to know when overexpression would perturb the system, and that that was accounted for.

Further modeling of the NF- $\kappa$ B system has been carried out by Kearns et al. (2006), Covert et al. (2005), and Werner et al. (2005), but these models focus on the dynamics of NF- $\kappa$ B in response to TNF $\alpha$  stimulation. Sensitivity analysis of the Hoffman model was carried out by Ihekwaba et al. (2005), which showed that the system has very complex dynamics, making analysis difficult. They were unable to identify the reactions most significant to the patterns of NF- $\kappa$ B oscillations. Joo et al. (2007) carried out a second sensitivity analysis on a model by Lipniacki et al. (2007), and were able to show that the variables related

to the transcription and translation of I $\kappa$ B $\alpha$  and A20 (another NF- $\kappa$ B inhibitor protein) are the most important for controlling NF- $\kappa$ B oscillations. Models have recently been developed to help understand TLR4 signal transduction in response to LPS (Klinke et al., 2008 and An, 2009), but these models are incomplete without more comprehensive data on the dynamics of NF- $\kappa$ B oscillations in real time in living cells. In fact, it had been reported that LPS did not cause oscillations in NF- $\kappa$ B at all (Covert et al., 2005), but this was refuted by Klinke et al. (2008).

#### **1.4 Purpose of this Work**

The purpose of this work was to conduct a series of experiments examining nuclear NF- $\kappa$ B oscillations in both wild-type and transfected cell lines upon activation by bacterial LPS. Unlike most previous studies, this work was carried out using immune system cells (murine macrophages), as most other somatic cells are incapable of responding to LPS by releasing pro-inflammatory cytokines (Du et al., 1999). The work also explored the different patterns of NF- $\kappa$ B activation and/or oscillation in real-time due to activation by distinct LPS chemotypes from two different gram negative pathogens (*E. coli* and *Y. pestis*), and tried to account for the different immune responses that these chemotypes induce.

## Chapter 2. Materials & Methods

Cell culture and transfection methods were performed as previously described in James et al. (2009) and are described below.

## **2.1 Cell Culture**

Immortalized RAW 264.7 murine macrophage cells were obtained from the ATCC (Part #TIB-71) and cultured in complete Dubelco's Modified Eagle Medium (DMEM, containing 10% FBS, 50U/ml Penicillin, 50 $\mu$ g/ml Streptomycin, and 10mM HEPES buffer) and grown at 37°C in 5% CO<sub>2</sub>. All culture media and supplements were obtained from Mediatech, Inc. Other derivatives of the RAW 264.7 cell line (described below) were cultured under the same conditions, unless noted. All cells were split using a chelating cell dissociation reagent (CellStripper, Mediatech) once they reached 80% confluence.

## **2.2 Fluorescent Construct Preparation, Transfection, and Stable Cell Line Development**

In order to visualize the macrophages and monitor the localization of NF- $\kappa$ B in the cell, a fluorescent fusion protein, RelA-GFP, was developed using the plasmid pECFP-FLAG-RelA. pECFP-FLAG-RelA was a gift from Dr. Allan Brasier (University of Texas Medical Branch). In order to make our construct, p $\beta$ Actin<sup>-</sup>-EGFP-FLAG-RelA (pBA-GFP-RelA, Figure 6), a minimal 106bp human  $\beta$ Actin promoter (Quitschke et al., 1989) was substituted for the cytomegalovirus (CMV) promoter and cloned between the Ase1 and Nhe1 restriction sites, and EGFP was substituted for ECFP between the Age1 and BsrG1 sites in the pECFP-F-RelA construct. For transfection, the plasmid pBA-GFP-RelA was linearized with AflIII (New England Biolabs). The plasmid was then transfected

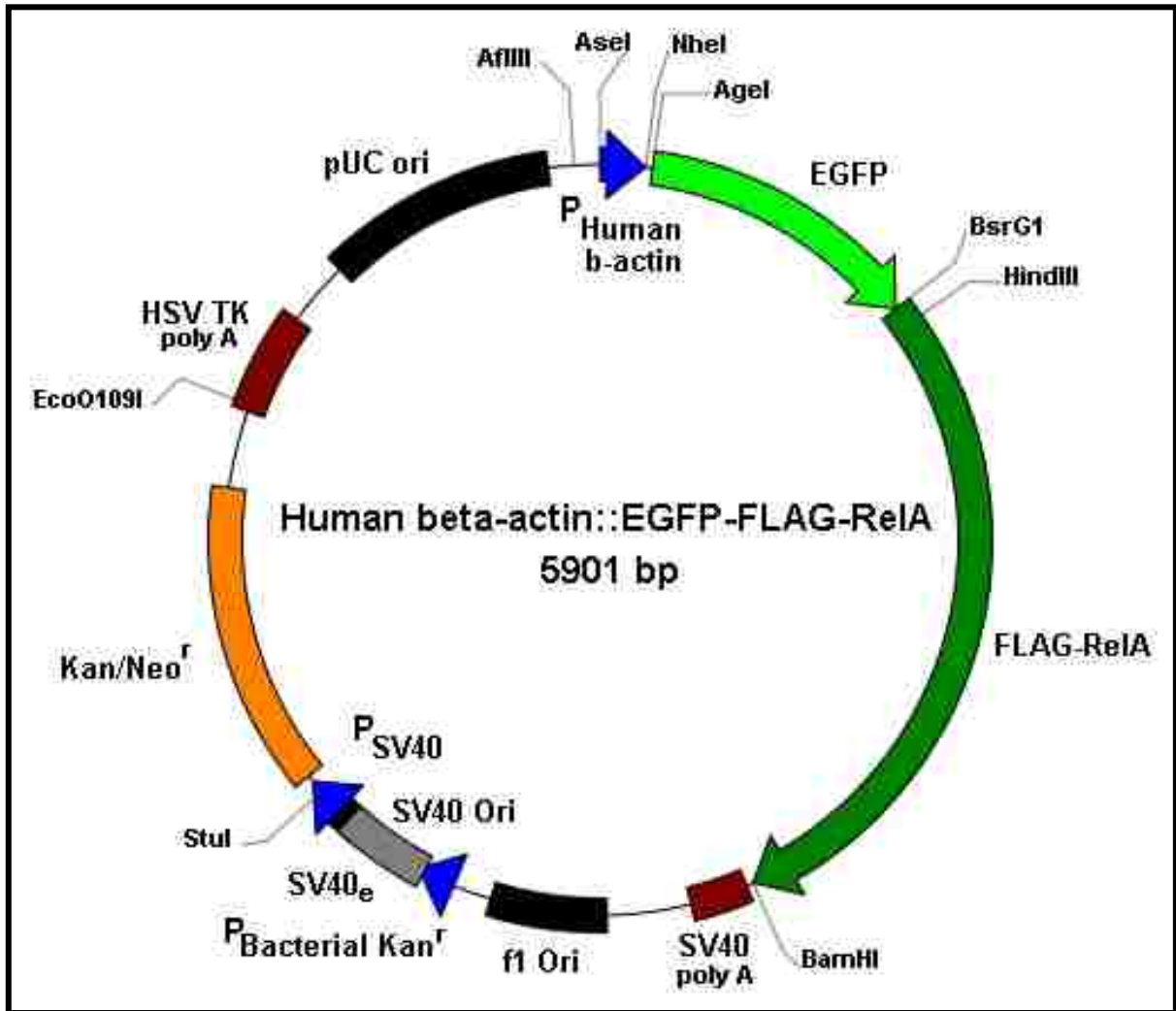


Figure 6. Restriction map of p $\beta$ Actin<sup>-</sup>EGFP-FLAG-ReIA.

into RAW 264.7 cells by Nucleofection using Kit V (Amaxa, Inc.), following the manufacturer's instructions, and cultured with 800 $\mu$ g/ml G-418. Fluorescent macrophage cells were isolated over 12 days in order to establish a stably transfected cell line expressing ReIA-GFP (cells shown in Figure 7). This stable cell line was designated RAW-RG16 and was maintained using 500 $\mu$ g/ml G-418.

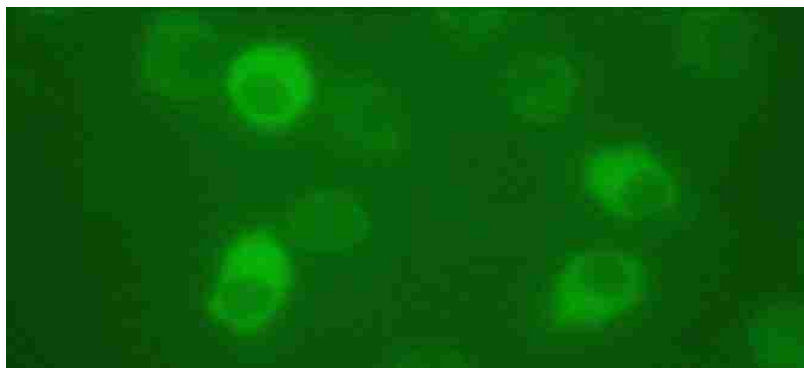


Figure 7. RAW-RG16 cells at 60X magnification. RelA-GFP can be seen in the cytoplasm surrounding the dark nucleus.

### 2.3 Endotoxin Preparation

Purified *E. coli* LPS was purchased from Sigma Aldrich and was diluted to 200 $\mu$ M stocks in 0.1% triethylamine (TEA) in endotoxin-free water using a microtip ultrasonifier (Branson Ultrasonics, 30 seconds at 25% power, 50% duty cycle, repeated twice). Stock solutions were further diluted in endotoxin-free water to 1nM or 100nM concentrations.

Purified *Y. pestis* LPS was a gift from Dr. Roberto Rebeil (Sandia National Laboratories). Extraction and purification are described in Rebeil et al. (2004). Briefly, the LPS was obtained from late exponential phase cultures of *Y. pestis* KIM6+ grown in Luria broth (LB) at pH 7.4 at 21°C or 37°C, without aeration. LPS was purified as described by Darveau and Hancock (1983) and then by phenol extraction (Hirschfeld et al., 2000) and resuspended in endotoxin-free water containing 0.1% TEA.

### 2.4 Immunocytochemistry

Circular microscope coverslips (VWR Scientific) were cleaned for 30 minutes in a 3:1 in a solution of sulfuric acid:hydrogen peroxide and rinsed 4

times with endotoxin free water. The coverslips were then placed into a six-well plate (one per well), and rinsed 3 times with phosphate buffered saline (PBS) to achieve neutral pH.  $5 \times 10^5$  RAW 264.7 cells or RAW-RG16 cells were seeded into each of the wells and cultured overnight according to the methods described above. The following day, the cells were incubated with either 1nm or 100nM LPS in DMEM (2ml) for either 0 min, 15 min, 30 min, 60 min, 90 min, or 120 min. Once incubation was complete, cells were rinsed 3 times with PBS, then fixed for 10 minutes in 2ml of fixing solution (3.8% paraformaldehyde and 5% sucrose in PBS). Fixing solution was removed and cells were rinsed 3 times with PBS. In order to reduce any background staining, a blocking solution containing 5% non-fat dry milk, 0.1% triton X-100, and 0.05% sodium azide dissolved in PBS was added to the wells for 30 minutes at room temperature. Cells were then washed with PBS and incubated with 1-2ml of primary antibody solution at 4°C overnight. Primary antibody solution was a filter-sterilized 1:100 dilution of anti-NFkB-p65 (C-20) (rabbit polyclonal IgG, 200 µg/ml; Santa Cruz Biotechnology Inc., #sc-372) diluted in PBS containing 1% non-fat dry milk, 0.1% triton X-100, and 0.05% sodium azide. The following morning, the primary antibody solution was removed and the cells were rinsed with PBS. In order to visualize the primary antibody, cells were incubated for 30 minutes at room temperature in 1ml of a fluorescent secondary antibody solution. Secondary antibody solution was a filter-sterilized 1:1000 dilution of goat anti-rabbit IgG-Alexa Fluor 568 (Invitrogen Corporation, # A11036) in PBS containing 1% non-fat dry milk, 0.1% triton X-100, and 0.05% sodium azide. Secondary antibody solution was removed and cells



were washed with PBS. Coverslips were then removed from their wells and mounted onto glass microscope slides using PermaFluor (Thermo-Fisher Scientific), following the manufacturer's instructions. Coverslips were then imaged for fluorescence using the methods described in the next section.

## 2.5 Microscopy Experiments

Fluorescence microscopy was carried out using an Olympus IX-71 microscope and a Hamamatsu ORCA-ER High Resolution Digital B/W CCD Camera. The excitation (488nm) and emission (512nm) were controlled using a mercury lamp (Olympus) and filters (Chroma Technology Corp., VT) mounted in a Sutter filter wheel (Sutter Instruments, CA), and controlled by the Slidebook™ program (Version 4.1, Intelligent Imaging Innovations, CO).

For live-cell experiments, 18 hours prior to experimentation,  $5 \times 10^5$  RAW-RG16 cells were seeded on 35mm sterile, disposable, glass-bottom Petri dishes and cultured without G-418. For experiments, the Petri dish containing cells was loaded onto a perfusion chamber (Harvard Instruments, MA) on the microscope where fresh medium was flowed in at 5ml/hr, waste medium was pumped out at 5ml/hr, and a constant temperature of 37°C was maintained. In order to maintain the medium pH at 7.4 during the experiment, complete DMEM was pre-equilibrated to 37°C in room air for at least 2 hrs. The pH of the medium was then adjusted to 7.4 using small volumes of concentrated sodium hydroxide. The medium was then re-sterilized using a 0.2µm filter. All reagents and plasticware used for the assays were either cleaned or purchased endotoxin-free to prevent contaminants from activating the macrophages. Cells were imaged at 60x

magnification at 12 frames per hour (f/hr) for at least 1hr prior to the addition of LPS to watch for any activation by system contaminants. After the control hour was finished, the medium inflow was changed to complete pH-adjusted DMEM containing LPS (either 1nM or 100nM), and imaging continued for 4hr at 30f/hr.

For fixed-cell immunocytochemistry experiments, cells were photographed at 60x magnification using the microscopy system described above. 10 randomly selected images were taken of each coverslip. Images were analyzed visually for NF- $\kappa$ B translocation into the nucleus (activation). The intensity of the fluorophore in the nucleus was noted for every cell in each image (cells on the border were excluded). Translocation was counted when the intensity in the cytoplasm decreased at the same time that the intensity in the nucleus increased and one could see a bright ring in the center of the cell corresponding to the nucleus (see Figure 8). The percentage of activated cells was calculated for

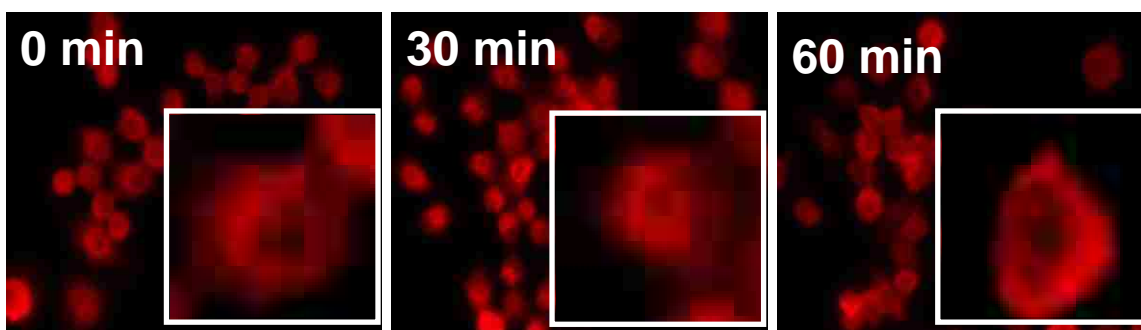


**Figure 8. NF- $\kappa$ B oscillations in RAW 264.7 macrophages in response to LPS activation. The round red objects are cells stained with Alexa Fluor 568. The cutouts represent a single magnified representative cell. The nucleus can be seen at 0 and 60 minutes as a round dark area in the center of the cell. At 30 minutes, the nucleus can be seen as a bright red ring in the center.**

each time point and plotted. These experiments were repeated 3 times each using both the wild-type RAW 264.7 cells and the RAW-RG16 cells for three different LPS chemotypes (*E. coli*, *Y. pestis* 21°C, and *Y. pestis* 37°C) at two

different concentrations (1nM and 100nM). The average percentage of cells translocated and the standard deviations of each experiment were calculated using standard statistical methods in Microsoft Excel®.

## 2.6 Live Microscopy Image Analysis

After imaging was completed, raw images in TIFF format were exported using the Slidebook™ capture software (Intelligent Imaging Innovations, Inc., Denver CO). Images were then imported into Adobe Illustrator CS3® (Adobe Systems, Inc., CA) where nuclei were manually outlined to create a mask for use in further image analysis. All movies captured were screened by hand, and any cells that were not in every frame or that divided during the 4 hours were excluded from further analysis. Remaining cells had their nuclei circled and the rest of the image was blacked out (thus creating the nuclear mask). An example of the first frame of a movie and its corresponding nuclear mask can be seen in Figure 9.

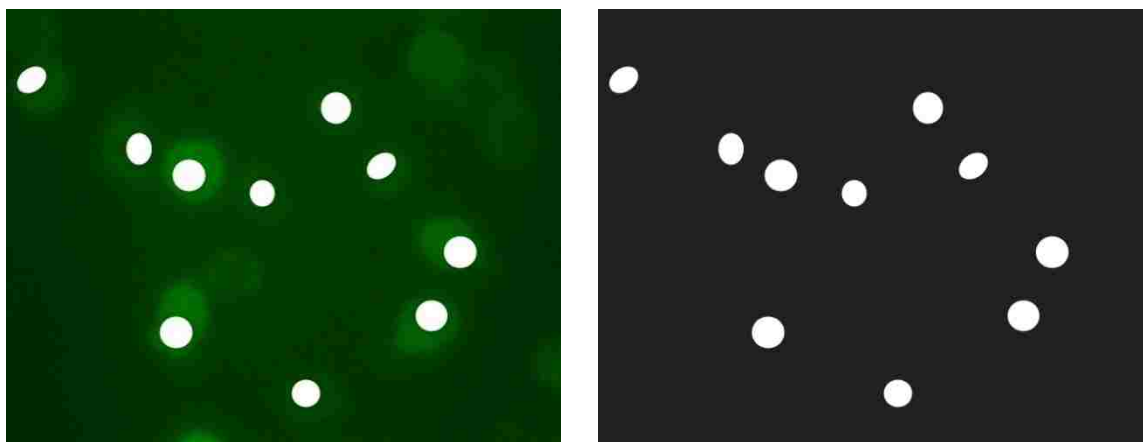


**Figure 9.** RAW-RG16 cells at 60X magnification. Nuclei are identified with white circles (left) and the rest of the image is blacked out to create the mask (right).

In order to obtain intensity data for each frame captured, images were imported into CellProfiler™ (Carpenter et al., 2006). CellProfiler uses preprogrammed image processing modules that can be customized to suit a particular application. For this study, raw images were corrected for uneven illumination and the background was subtracted out. Nuclei were identified using the mask created in the previous step, and their positions were used to extrapolate the position of the cytoplasm. The integrated and mean intensity of each nucleus and its corresponding cytoplasm were calculated for each frame and normalized. Cells were numbered and the data were exported to Excel, where they were visually checked for errors (such as missing frames or missing intensity data). An example of the main output windows for CellProfiler™ for a typical dataset can be seen in Figure 10.

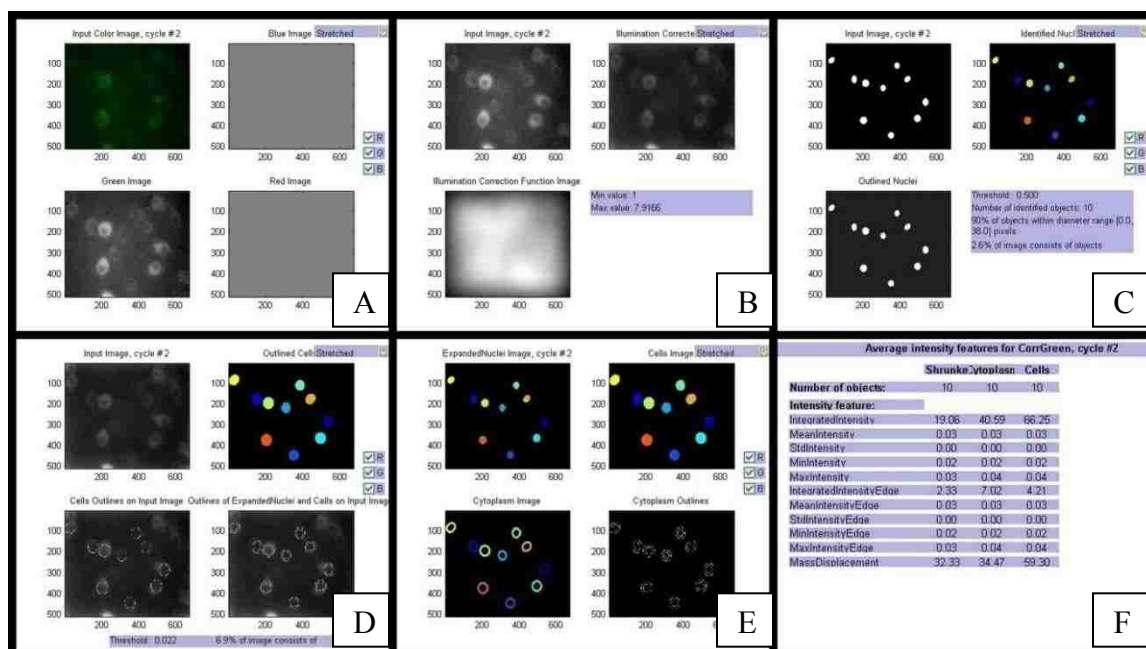


**Figure 10.** The main output windows of CellProfiler™. The images (from left to right) show the import of the raw image (A) and its conversion to grayscale (B), the correction of illumination (C), the identification of nuclei using the imported mask (D), the expansion of nuclei to identify cytoplasmic (E) regions, and the extraction of intensity data (F).

For the next step, the data were imported into Matlab® R2007b (Mathworks, Inc., MA), where the ratio of mean nuclear intensity to mean cytoplasmic intensity was calculated for each cell (script written by Mark Van Benthem and Igal Brenner, 2007). Plots were generated for each cell over the entire 120 frames of an assay. The plots show intensity over time. Modules and the code for the script can be found in Appendix B. An example of the 2 output figures for a typical dataset can be seen in Figures 11 and 12. Figures for all 18 datasets can be seen in Appendix A.

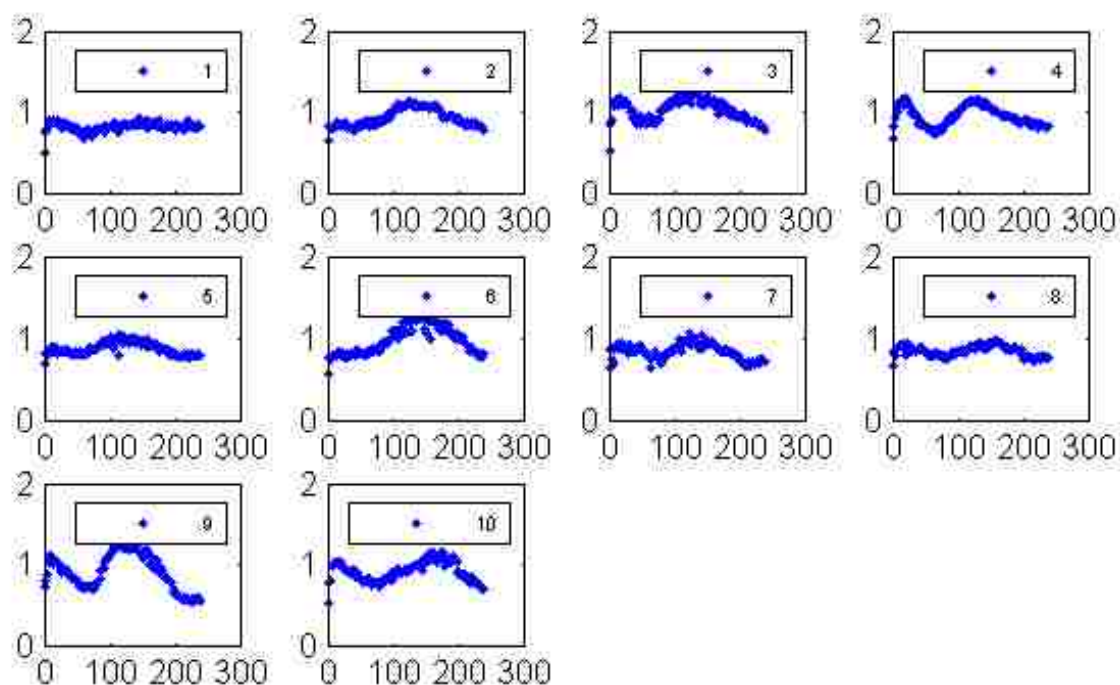


**Figure 11.** Example of the Matlab® generated plots of the ratio of nuclear to cytoplasmic intensity of each cell over time for a typical dataset. The Y-axis shows the nuclear to cytoplasmic intensity ratio and the X-axis shows time (in minutes). Data from 9-18-08 shown.

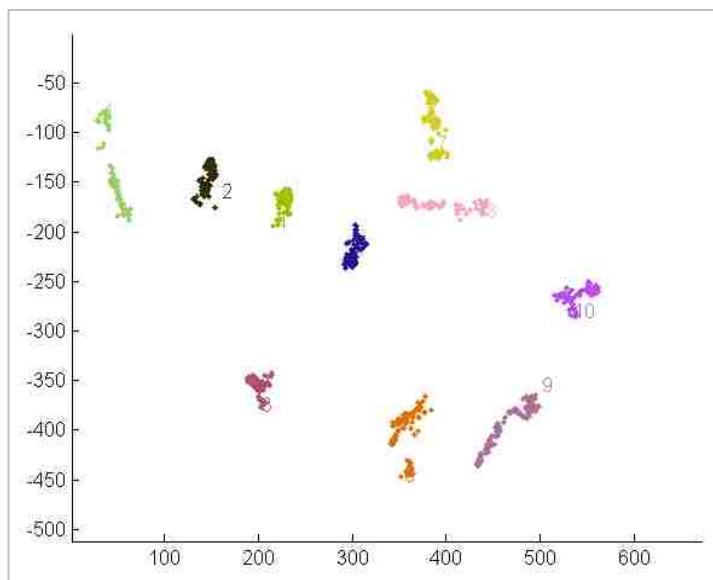


**Figure 12. Example of the Matlab® generated plots of the spatial positions of each cell over time for a typical dataset. Data from 9-18-08 presented (the same cells as seen in Figure 11).**

## 2.7 Manual Clustering

Images were manually analyzed for RelA translocation and for the presence of oscillations. For each assay, cells were assigned numbers by the Matlab® script described above. Each cell was then followed for the full 120 frames by comparing the individual cell plots to the movie, and any translocations of RelA-GFP were noted, as well as how many times it translocated in and out of the nucleus. Cells that showed no translocation were also noted, as well as cells where RelA-GFP went into the nucleus but not back out. Translocation behaviors were grouped into 4 types (0, 1, 2, and 3), and the percentage of cells in each group was calculated in each assay. Type 0 were cells that showed no translocation into the nucleus, type 1 were cells that showed translocation in, then back out of the nucleus, type 2 were cells that showed oscillation in and out of the nucleus more than once, and type 3 were cells that showed translocation into the nucleus and not back out. The percentages of each behavioral type were plotted for the experiments and standard deviations were calculated.

## Chapter 3. Results

### 3.1 Immunocytochemistry

As previously stated, oscillations in nuclear NF- $\kappa$ B concentrations have been observed, but only in non-immune system cells or in biochemical assays. In order to study oscillations in live macrophages in real-time, a fluorescent NF- $\kappa$ B construct (RelA-GFP) was generated, allowing the visualization of NF- $\kappa$ B localization. It was important to verify that this fluorescent construct localized like the wild-type NF- $\kappa$ B transcription factor, and could therefore be used as an indicator of wild-type NF- $\kappa$ B response. To accomplish this, a series of experiments were carried out (with the help of Jaclyn Murton, SNL) using both wild-type RAW 264.7 macrophages and RelA-GFP transfected macrophages (RAW-RG16) and an immunostaining protocol. Briefly, macrophages were cultured and then exposed to LPS and fixed at specific time intervals. Once fixed, the RAW 264.7 cells were stained using an anti-NF- $\kappa$ B antibody and a secondary fluorescent antibody. RAW-RG16 cells were simply fixed. The cells were then imaged using fluorescence microscopy and NF- $\kappa$ B translocation events were counted. All experiments were carried out in triplicate.

#### 3.1.1 NF- $\kappa$ B Response due to LPS in RAW 264.7 Cells:

##### 3.1.1.1 1nM *E. coli* LPS

In RAW 264.7 wild-type cells stained with anti-NF $\kappa$ B-p65/goat anti-rabbit IgG-Alexa Fluor 568, an average of 5% of cells showed nuclear translocation of NF- $\kappa$ B with no *E. coli* LPS present for the 3 repetitions (0 minutes). The standard deviation was 2%. After 15 minutes, an average of 94% of cells showed nuclear translocation of NF- $\kappa$ B in response to 1nM *E. coli* LPS, with a standard deviation



of 2%. After 30 minutes of exposure to 1nM *E. coli* LPS, an average of 98% of cells showed nuclear translocation of NF- $\kappa$ B, with a standard deviation of 3%. An average of 84% of cells showed nuclear translocation of NF- $\kappa$ B in response to 1nM *E. coli* LPS after 60 minutes, with a standard deviation of 2%. An average of 95% of cells showed nuclear translocation of NF- $\kappa$ B in response to 1nM *E. coli* LPS after 90 minutes, with a standard deviation of 1%. At 120 minutes, an average of 93% of cells showed nuclear translocation of NF- $\kappa$ B in response to 1nM *E. coli* LPS, with a standard deviation of 3%. A table and plots of these results can be seen in Figure 13.

#### **3.1.1.2 100nM *E. coli* LPS**

In RAW 264.7 wild-type cells stained with anti-NF $\kappa$ B-p65/goat anti-rabbit IgG-Alexa Fluor 568, an average of 6% of cells showed nuclear translocation of NF- $\kappa$ B with no *E. coli* LPS present for the 3 repetitions (0 minutes). The standard deviation was 1%. After 15 minutes, an average of 90% of cells showed nuclear translocation of NF- $\kappa$ B in response to 100nM *E. coli* LPS, with a standard deviation of 8%. After 30 minutes of exposure to 100nM *E. coli* LPS, an average of 96% of cells showed nuclear translocation of NF- $\kappa$ B, with a standard deviation of 2%. An average of 69% of cells showed nuclear translocation of NF- $\kappa$ B in response to 100nM *E. coli* LPS after 60 minutes, with a standard deviation of 10%. An average of 92% of cells showed nuclear translocation of NF- $\kappa$ B in response to 100nM *E. coli* LPS after 90 minutes, with a standard deviation of 6%. At 120 minutes, an average of 93% of cells showed nuclear translocation of NF-

$\kappa$ B in response to 100nM *E. coli* LPS, with a standard deviation of 4%. A table and plots of these results can be seen in Figure 13.

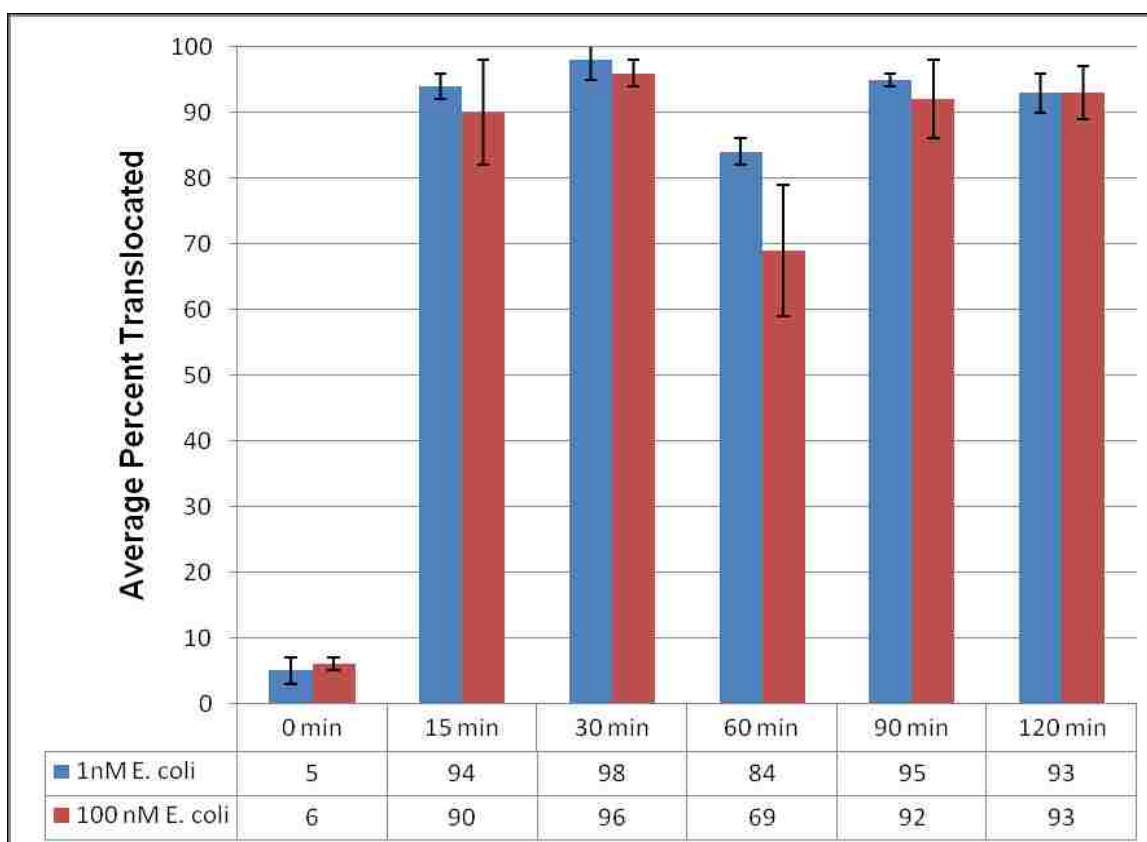


Figure 13. Average percentage of RAW 264.7 cells showing NF- $\kappa$ B translocation into the nucleus after exposure to *E. coli* LPS at 1nM and 100nM at the stated time intervals.

### 3.1.1.3 1nM *Y. pestis* 21°C LPS

In RAW 264.7 wild-type cells stained with anti-NF $\kappa$ B-p65/goat anti-rabbit IgG-Alexa Fluor 568, an average of 3% of cells showed nuclear translocation of NF- $\kappa$ B with no LPS present for the 3 repetitions (0 minutes). The standard deviation was 2%. After 15 minutes, an average of 93% of cells showed nuclear translocation of NF- $\kappa$ B in response to 1nM *Y. pestis* 21°C LPS, with a standard deviation of 8%. After 30 minutes of exposure to 1nM *Y. pestis* 21°C LPS, an average of 98% of cells showed nuclear translocation of NF- $\kappa$ B, with a standard

deviation of 2%. An average of 78% of cells showed nuclear translocation of NF- $\kappa$ B in response to 1nM *Y. pestis* 21°C LPS after 60 minutes, with a standard deviation of 7%. An average of 97% of cells showed nuclear translocation of NF- $\kappa$ B in response to 1nM *Y. pestis* 21°C LPS after 90 minutes, with a standard deviation of 3%. At 120 minutes, an average of 88% of cells showed nuclear translocation of NF- $\kappa$ B in response to 1nM *Y. pestis* 21°C LPS, with a standard deviation of 9%. A table and plots of these results can be seen in Figure 14.

#### **3.1.1.4 100nM *Y. pestis* 21°C LPS**

In RAW 264.7 wild-type cells stained with anti-NF $\kappa$ B-p65/goat anti-rabbit IgG-Alexa Fluor 568, an average of 7% of cells showed nuclear translocation of NF- $\kappa$ B with no LPS present for the 3 repetitions (0 minutes). The standard deviation was 3%. After 15 minutes, an average of 91% of cells showed nuclear translocation of NF- $\kappa$ B in response to 100nM *Y. pestis* 21°C LPS, with a standard deviation of 10%. After 30 minutes of exposure to 100nM *Y. pestis* 21°C LPS, an average of 86% of cells showed nuclear translocation of NF- $\kappa$ B, with a standard deviation of 10%. An average of 70% of cells showed nuclear translocation of NF- $\kappa$ B in response to 100nM *Y. pestis* 21°C LPS after 60 minutes, with a standard deviation of 14%. An average of 95% of cells showed nuclear translocation of NF- $\kappa$ B in response to 100nM *Y. pestis* 21°C LPS after 90 minutes, with a standard deviation of 4%. At 120 minutes, an average of 91% of cells showed nuclear translocation of NF- $\kappa$ B in response to 100nM *Y. pestis* 21°C LPS, with a standard deviation of 2%. A table and plots of these results can be seen in Figure 14.

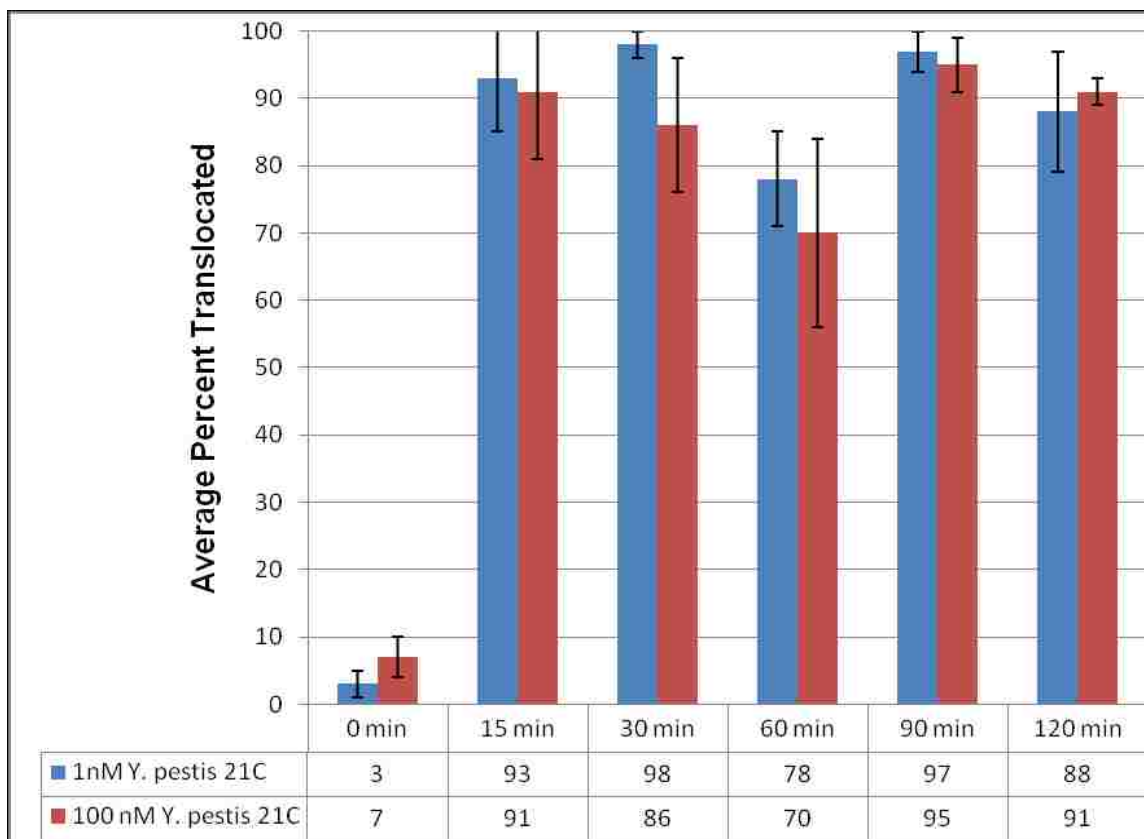


Figure 14. Average percentage of RAW 264.7 cells showing NF- $\kappa$ B translocation into the nucleus after exposure to *Y. pestis* 21°C LPS at 1nM and 100nM at the stated time intervals.

### 3.1.1.5 1nM *Y. pestis* 37°C LPS

In RAW 264.7 wild-type cells stained with anti-NF $\kappa$ B-p65/goat anti-rabbit IgG-Alexa Fluor 568, an average of 1% of cells showed nuclear translocation of NF- $\kappa$ B with no LPS present for the 3 repetitions (0 minutes). The standard deviation was 1%. After 15 minutes, an average of 0% of cells showed nuclear translocation of NF- $\kappa$ B in response to 1nM *Y. pestis* 37°C LPS, with a standard deviation of 0%. After 30 minutes of exposure to 1nM *Y. pestis* 37°C LPS, an average of 10% of cells showed nuclear translocation of NF- $\kappa$ B, with a standard deviation of 5%. An average of 50% of cells showed nuclear translocation of NF- $\kappa$ B in response to 1nM *Y. pestis* 37°C LPS after 60 minutes, with a standard

deviation of 16%. An average of 52% of cells showed nuclear translocation of NF- $\kappa$ B in response to 1nM *Y. pestis* 37°C LPS after 90 minutes, with a standard deviation of 16%. At 120 minutes, an average of 53% of cells showed nuclear translocation of NF- $\kappa$ B in response to 1nM *Y. pestis* 37°C LPS, with a standard deviation of 14%. A table and plots of these results can be seen in Figure 15.

#### **3.1.1.6 100nM *Y. pestis* 37°C LPS**

In RAW 264.7 wild-type cells stained with anti-NF $\kappa$ B-p65/goat anti-rabbit IgG-Alexa Fluor 568, an average of 7% of cells showed nuclear translocation of NF- $\kappa$ B with no *E. coli* LPS present for the 3 repetitions (0 minutes). The standard deviation was 1%. After 15 minutes, an average of 92% of cells showed nuclear translocation of NF- $\kappa$ B in response to 100nM *Y. pestis* 37°C LPS, with a standard deviation of 5%. After 30 minutes of exposure to 100nM *Y. pestis* 37°C LPS, an average of 94% of cells showed nuclear translocation of NF- $\kappa$ B, with a standard deviation of 4%. An average of 77% of cells showed nuclear translocation of NF- $\kappa$ B in response to 100nM *Y. pestis* 37°C LPS after 60 minutes, with a standard deviation of 5%. An average of 93% of cells showed nuclear translocation of NF- $\kappa$ B in response to 100nM *Y. pestis* 37°C LPS after 90 minutes, with a standard deviation of 2%. At 120 minutes, an average of 90% of cells showed nuclear translocation of NF- $\kappa$ B in response to 100nM *Y. pestis* 37°C LPS, with a standard deviation of 5%. A table and plots of these results can be seen in Figure 15.

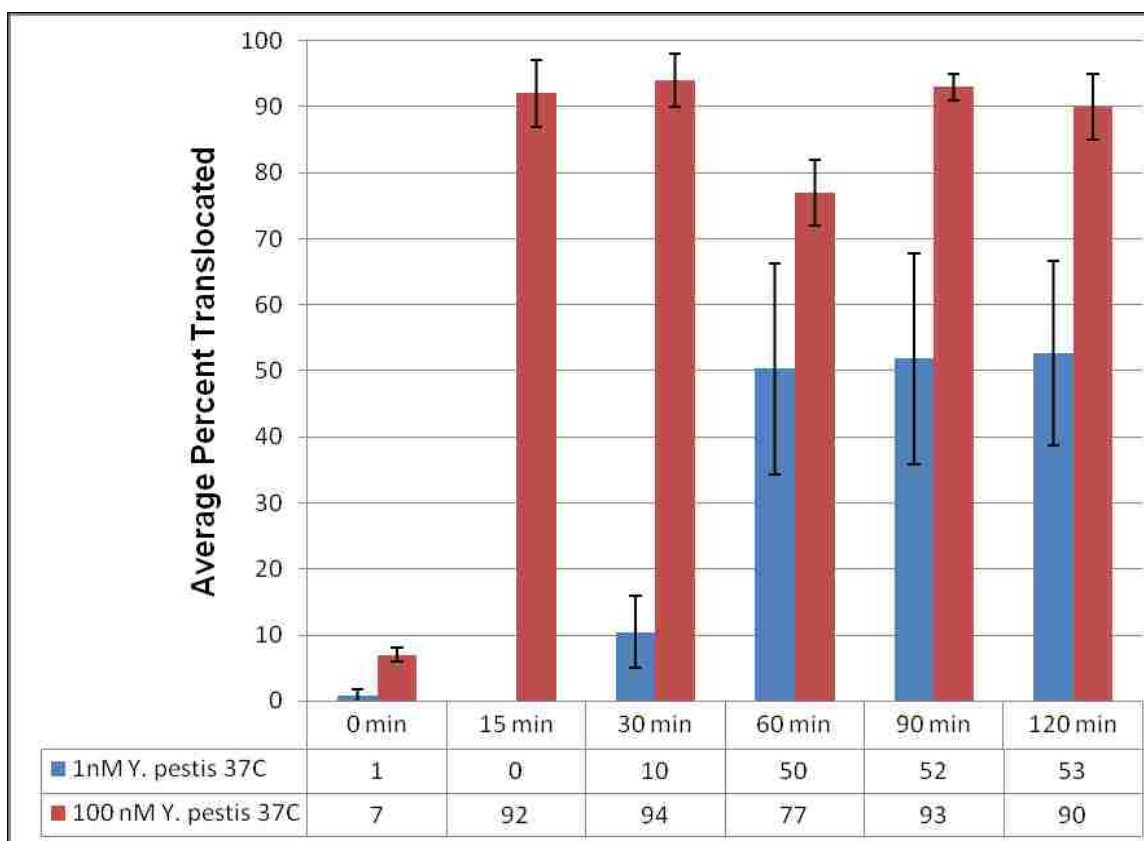


Figure 15. Average percentage of RAW 264.7 cells showing NF- $\kappa$ B translocation into the nucleus after exposure to *Y. pestis* 37°C LPS at 1nM and 100nM at the stated time intervals.

### 3.1.1.7 Summary

As can be seen in Figures 13, 14, and 15 above, and in the table below (table 1), the number of cells showing nuclear NF- $\kappa$ B increased upon stimulation with any LPS tested, then decreased at some point later in the assay. For all chemotype/concentration combinations except for 1nM *Y. pestis* 37°C LPS, this decrease occurred at 60 minutes, followed by another increase of NF- $\kappa$ B in the nucleus. The data for 1nM *Y. pestis* 37°C LPS show nuclear NF- $\kappa$ B increasing over time. By plotting the average of the 3 repetitions for each assay, one can see evidence for oscillation of NF- $\kappa$ B in and out of the nucleus (Figures 16 and 17). NF- $\kappa$ B can be seen going in, out, and back into the nucleus for all three chemotypes tested.

1nM on RAW 264.7						
	<i>E. coli</i> LPS		<i>Y. pestis</i> 21°C LPS		<i>Y. pestis</i> 37°C LPS	
Minutes (3 Reps)	Average % Translocated	±StDev	Average % Translocated	±StDev	Average % Translocated	±StDev
0	5	±2	3	±2	1	±1
15	94	±2	93	±8	0	±0
30	98	±3	98	±2	10	±5
60	84	±2	78	±7	50	±16
90	95	±1	97	±3	52	±16
120	93	±3	88	±9	53	±14
100nM on RAW 264.7						
	<i>E. coli</i> LPS		<i>Y. pestis</i> 21°C LPS		<i>Y. pestis</i> 37°C LPS	
Minutes (3 Reps)	Average % Translocated	±StDev	Average % Translocated	±StDev	Average % Translocated	±StDev
0	6	±1	7	±3	7	±1
15	90	±8	91	±10	92	±5
30	96	±2	86	±10	94	±4
60	69	±10	70	±14	77	±5
90	92	±6	95	±4	93	±2
120	93	±4	91	±2	90	±5

Table 1. Average percent of RAW 264.7 cells showing NF-κB translocation into the nucleus after exposure to at 1nM or 100nM LPS at the stated time intervals.

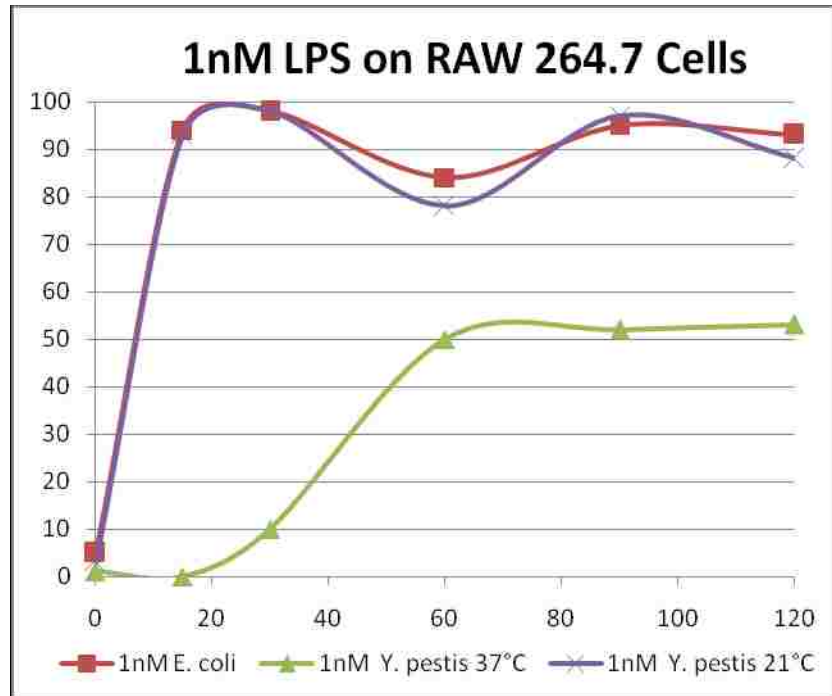


**Figure 16.** Plot of the average number of cells (of the 3 replicates) translocated at each time point for the 3 tested chemotypes at 1nM.

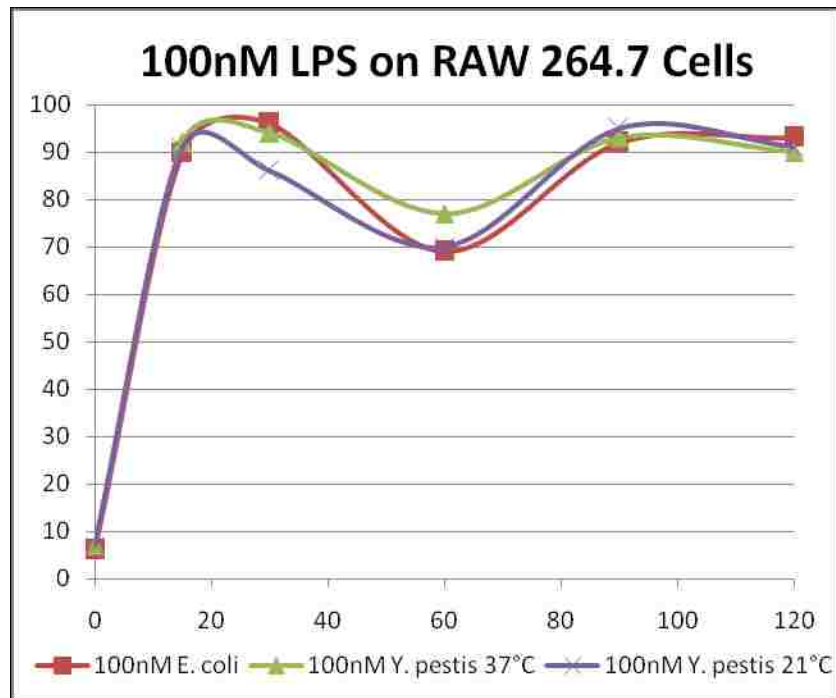


**Figure 17.** Plot of the average number of cells (of the 3 replicates) translocated at each time point for the 3 tested chemotypes at 100nM.



### **3.1.2 NF- $\kappa$ B Response due to LPS in RAW-RG16 Cells:**

#### **3.1.2.1 1nM *E. coli* LPS**

In RAW-RG16 cells expressing RelA fused to the green fluorescent protein EGFP, an average of 4% of cells showed nuclear translocation of NF- $\kappa$ B with no *E. coli* LPS present for the 3 repetitions (0 minutes). The standard deviation was 2%. After 15 minutes, an average of 60% of cells showed nuclear translocation of NF- $\kappa$ B in response to 1nM *E. coli* LPS, with a standard deviation of 9%. After 30 minutes of exposure to 1nM *E. coli* LPS, an average of 76% of cells showed nuclear translocation of NF- $\kappa$ B, with a standard deviation of 8%. An average of 43% of cells showed nuclear translocation of NF- $\kappa$ B in response to 1nM *E. coli* LPS after 60 minutes, with a standard deviation of 6%. An average of 65% of cells showed nuclear translocation of NF- $\kappa$ B in response to 1nM *E. coli* LPS after 90 minutes, with a standard deviation of 8%. At 120 minutes, an average of 80% of cells showed nuclear translocation of NF- $\kappa$ B in response to 1nM *E. coli* LPS, with a standard deviation of 6%. A table and plots of these results can be seen in Figure 18.

#### **3.1.2.2 100nM *E. coli* LPS**

In RAW-RG16 cells expressing RelA fused to the EGFP, an average of 1% of cells showed nuclear translocation of NF- $\kappa$ B with no *E. coli* LPS present for the 3 repetitions (0 minutes). The standard deviation was 1%. After 15 minutes, an average of 80% of cells showed nuclear translocation of NF- $\kappa$ B in response to 100nM *E. coli* LPS, with a standard deviation of 12%. After 30 minutes of exposure to 100nM *E. coli* LPS, an average of 81% of cells showed nuclear

translocation of NF- $\kappa$ B, with a standard deviation of 15%. An average of 65% of cells showed nuclear translocation of NF- $\kappa$ B in response to 100nM *E. coli* LPS after 60 minutes, with a standard deviation of 12%. An average of 86% of cells showed nuclear translocation of NF- $\kappa$ B in response to 100nM *E. coli* LPS after 90 minutes, with a standard deviation of 9%. At 120 minutes, an average of 86% of cells showed nuclear translocation of NF- $\kappa$ B in response to 100nM *E. coli* LPS, with a standard deviation of 11%. A table and plots of these results can be seen in Figure 18.

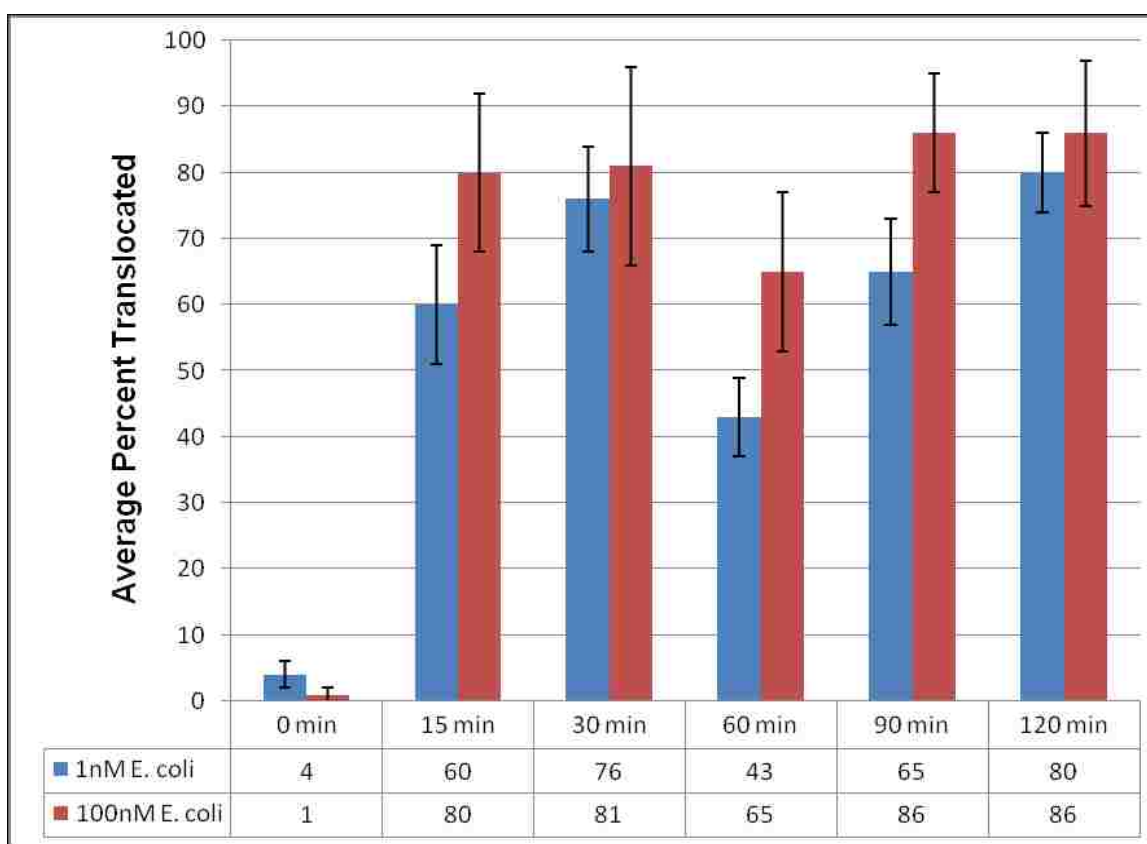


**Figure 18.** Average percentage of RAW-RG16 cells showing NF- $\kappa$ B translocation into the nucleus after exposure to *E. coli* LPS at 1nM and 100nM at the stated time intervals.

### 3.1.2.3 1nM *Y. pestis* 21°C LPS

In RAW-RG16 cells expressing RelA fused to EGFP, an average of 1% of cells showed nuclear translocation of NF- $\kappa$ B with no *Y. pestis* 21°C LPS present

for the 3 repetitions (0 minutes). The standard deviation was 2%. After 15 minutes, an average of 90% of cells showed nuclear translocation of NF- $\kappa$ B in response to 1nM *Y. pestis* 21°C LPS, with a standard deviation of 9%. After 30 minutes of exposure to 1nM *Y. pestis* 21°C LPS, an average of 93% of cells showed nuclear translocation of NF- $\kappa$ B, with a standard deviation of 4%. An average of 53% of cells showed nuclear translocation of NF- $\kappa$ B in response to 1nM *Y. pestis* 21°C LPS after 60 minutes, with a standard deviation of 9%. An average of 89% of cells showed nuclear translocation of NF- $\kappa$ B in response to 1nM *Y. pestis* 21°C LPS after 90 minutes, with a standard deviation of 8%. At 120 minutes, an average of 72% of cells showed nuclear translocation of NF- $\kappa$ B in response to 1nM *Y. pestis* 21°C LPS, with a standard deviation of 6%. A table and plots of these results can be seen in Figure 19.

#### **3.1.2.4 100nM *Y. pestis* 21°C LPS**

In RAW-RG16 cells expressing RelA fused to EGFP, an average of 3% of cells showed nuclear translocation of NF- $\kappa$ B with no *Y. pestis* 21°C LPS present for the 3 repetitions (0 minutes). The standard deviation was 3%. After 15 minutes, an average of 80% of cells showed nuclear translocation of NF- $\kappa$ B in response to 100nM *Y. pestis* 21°C LPS, with a standard deviation of 7%. After 30 minutes of exposure to 100nM *Y. pestis* 21°C LPS, an average of 49% of cells showed nuclear translocation of NF- $\kappa$ B, with a standard deviation of 7%. An average of 61% of cells showed nuclear translocation of NF- $\kappa$ B in response to 100nM *Y. pestis* 21°C LPS after 60 minutes, with a standard deviation of 9%. An average of 83% of cells showed nuclear translocation of NF- $\kappa$ B in response to

100nM *Y. pestis* 21°C LPS after 90 minutes, with a standard deviation of 7%. At 120 minutes, an average of 58% of cells showed nuclear translocation of NF-κB in response to 100nM *Y. pestis* 21°C LPS, with a standard deviation of 12%. A table and plots of these results can be seen in Figure 19.

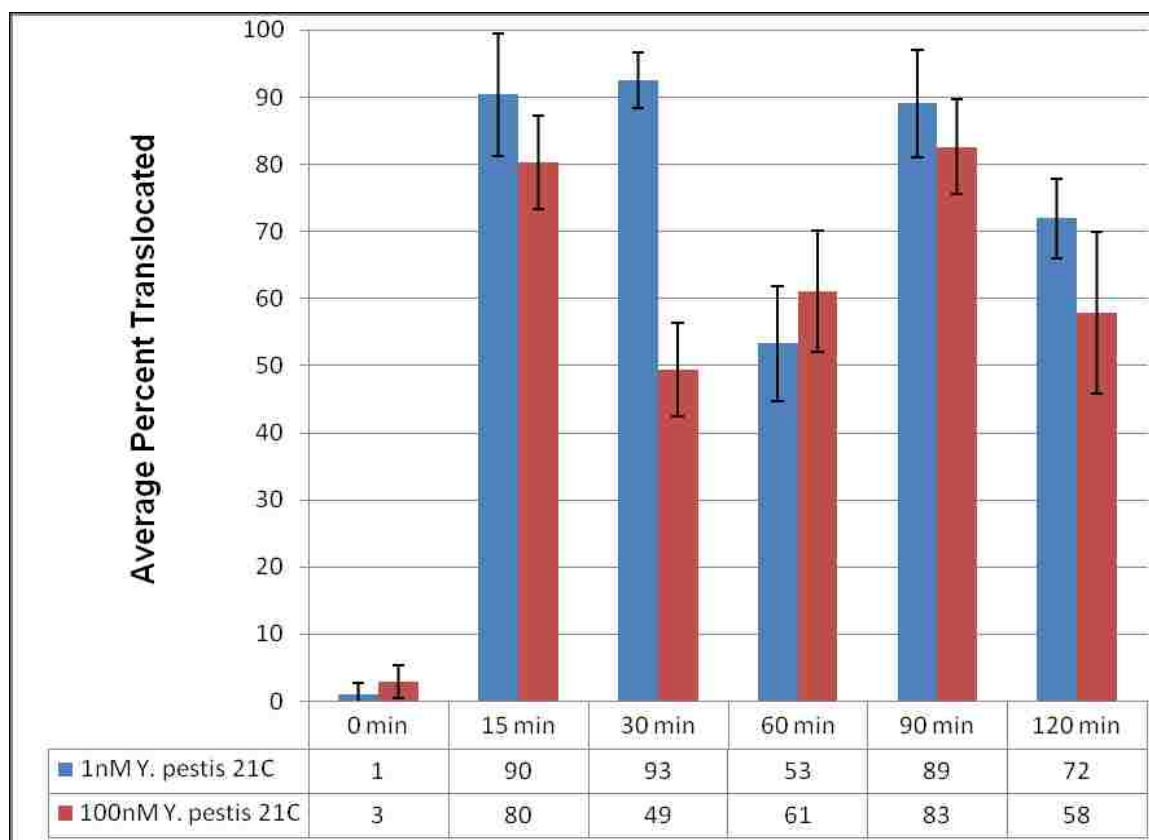


Figure 19. Average percentage of RAW-RG16 cells showing NF-κB translocation into the nucleus after exposure to *Y. pestis* 21° LPS at 1nM and 100nM at the stated time intervals.

### 3.1.2.5 1nM *Y. pestis* 37°C LPS

In RAW-RG16 cells expressing RelA fused to EGFP, an average of 5% of cells showed nuclear translocation of NF-κB with no *Y. pestis* 37°C LPS present for the 3 repetitions (0 minutes). The standard deviation was 3%. After 15 minutes, an average of 14% of cells showed translocation of NF-κB in response to 1nM *Y. pestis* 37°C LPS, with a standard deviation of 1%. After 30 minutes of exposure to 1nM *Y. pestis* 37°C LPS, an average of 59% of cells showed nuclear

translocation of NF- $\kappa$ B, with a standard deviation of 3%. An average of 75% of cells showed nuclear translocation of NF- $\kappa$ B in response to 1nM *Y. pestis* 37°C LPS after 60 minutes, with a standard deviation of 3%. An average of 82% of cells showed nuclear translocation of NF- $\kappa$ B in response to 1nM *Y. pestis* 37°C LPS after 90 minutes, with a standard deviation of 3%. At 120 minutes, an average of 63% of cells showed nuclear translocation of NF- $\kappa$ B in response to 1nM *Y. pestis* 37°C LPS, with a standard deviation of 8%. A table and plots of these results can be seen in Figure 20.

### **3.1.2.6 100nM *Y. pestis* 37°C LPS**

In RAW-RG16 cells expressing RelA fused to EGFP, an average of 1% of cells showed nuclear translocation of NF- $\kappa$ B with no *Y. pestis* 37°C LPS present for the 3 repetitions (0 minutes). The standard deviation was 2%. After 15 minutes, an average of 81% of cells showed nuclear translocation of NF- $\kappa$ B in response to 100nM *Y. pestis* 37°C LPS, with a standard deviation of 5%. After 30 minutes of exposure to 100nM *Y. pestis* 37°C LPS, an average of 83% of cells showed nuclear translocation of NF- $\kappa$ B, with a standard deviation of 5%. An average of 71% of cells showed nuclear translocation of NF- $\kappa$ B in response to 100nM *Y. pestis* 37°C LPS after 60 minutes, with a standard deviation of 8%. An average of 85% of cells showed nuclear translocation of NF- $\kappa$ B in response to 100nM *Y. pestis* 37°C LPS after 90 minutes, with a standard deviation of 5%. At 120 minutes, an average of 63% of cells showed nuclear translocation of NF- $\kappa$ B in response to 100nM *Y. pestis* 37°C LPS, with a standard deviation of 10%. A table and plots of these results can be seen in Figure 20.

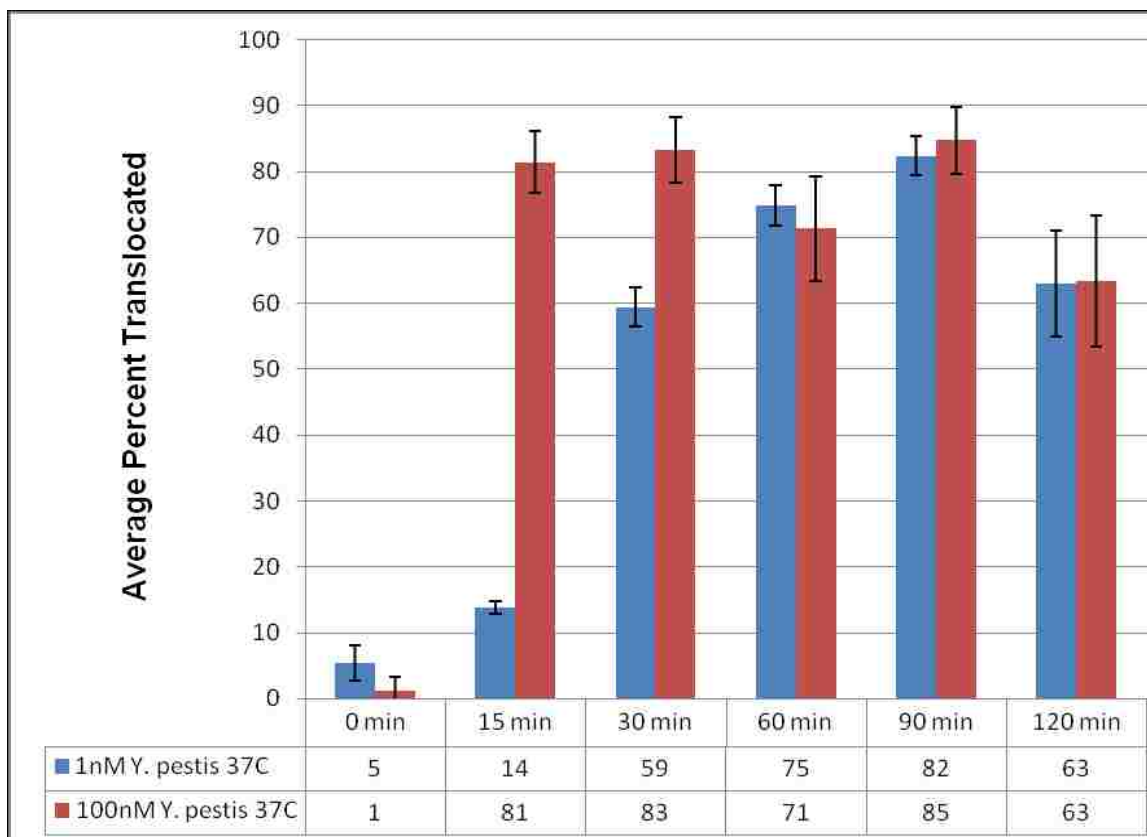


**Figure 20.** Average percentage of RAW-RG16 cells showing NF- $\kappa$ B translocation into the nucleus after exposure to *Y. pestis* 37° LPS at 1nM and 100nM at the stated time intervals.

### 3.1.2.7 Summary

As can be seen in Figures 18, 19, and 20 above, and in the table below (table 2), the number of cells showing nuclear localization of NF- $\kappa$ B increased upon stimulation with any LPS tested, then decreased again at some point later in the assay. For *E. coli* and *Y. pestis* 21°C LPS at 1nM, and *E. coli* and *Y. pestis* 37°C LPS at 100nM this decrease occurred at the 60 minute time point. For *Y. pestis* 21°C LPS, this occurred at 60 minutes for 1nM and 30 minutes for 100nM. For 1nM *Y. pestis* 37°C LPS, the decrease occurred at 120 minutes, after a peak at 90 minutes. For 100nM *Y. pestis* 21°C LPS, a decrease was seen at 30 minutes. By plotting the average of the 3 repetitions for each

concentration of each LPS chemotype, one can see evidence for oscillation of NF- $\kappa$ B in and out of the nucleus (Figures 21 and 22).

1nM on RAW-RG16						
	<i>E. coli</i> LPS		<i>Y. pestis</i> 21°C LPS		<i>Y. pestis</i> 37°C LPS	
Minutes (3 Reps)	Percent Translocated	Average $\pm$ StDev	Percent Translocated	Average $\pm$ StDev	Percent Translocated	Average $\pm$ StDev
0	4	$\pm$ 2	1	$\pm$ 2	5	$\pm$ 3
15	60	$\pm$ 9	90	$\pm$ 9	14	$\pm$ 1
30	76	$\pm$ 8	93	$\pm$ 4	59	$\pm$ 3
60	43	$\pm$ 6	53	$\pm$ 9	75	$\pm$ 3
90	65	$\pm$ 8	89	$\pm$ 8	82	$\pm$ 3
120	80	$\pm$ 6	72	$\pm$ 6	63	$\pm$ 8
100nM on RAW-RG16						
	<i>E. coli</i> LPS		<i>Y. pestis</i> 21°C LPS		<i>Y. pestis</i> 37°C LPS	
Minutes (3 Reps)	Percent Translocated	Average $\pm$ StDev	Percent Translocated	Average $\pm$ StDev	Percent Translocated	Average $\pm$ StDev
0	1	$\pm$ 1	3	$\pm$ 3	1	$\pm$ 2
15	80	$\pm$ 12	80	$\pm$ 7	81	$\pm$ 5
30	81	$\pm$ 15	49	$\pm$ 7	83	$\pm$ 5
60	65	$\pm$ 12	61	$\pm$ 9	71	$\pm$ 8
90	86	$\pm$ 9	83	$\pm$ 7	85	$\pm$ 5
120	86	$\pm$ 11	58	$\pm$ 12	63	$\pm$ 10

Table 2. Average percent of RAW-RG16 cells showing NF- $\kappa$ B translocation into the nucleus after exposure to at 1nM or 100nM LPS at the stated time intervals.

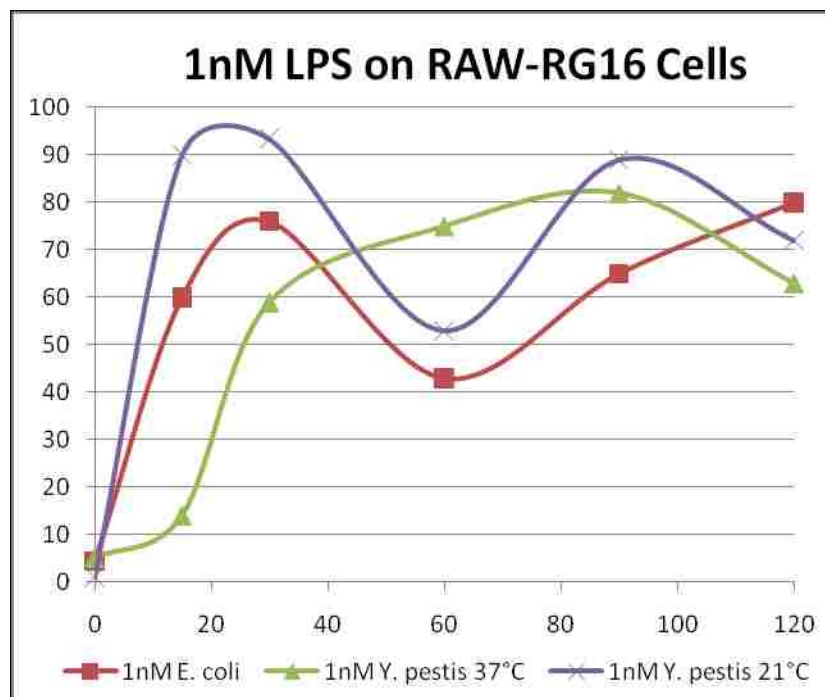


**Figure 21. Plot of the average number of cells (of the 3 replicates) translocated at each time point for the 3 tested chemotypes at 1nM.**

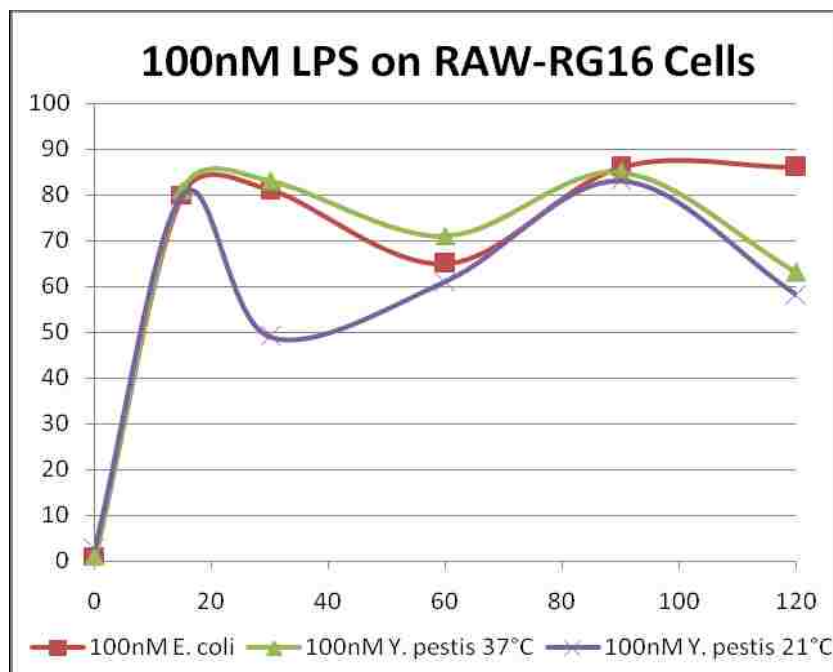


**Figure 22. Plot of the average number of cells (of the 3 replicates) translocated at each time point for the 3 tested chemotypes at 100nM.**

By comparing the figures for both the RAW 264.7 data and the RAW-RG16 data, it is clear that the transfected RelA-GFP behaves like the wild-type



NF- $\kappa$ B. RelA-GFP can be seen oscillating in and out of the nucleus for all three chemotypes tested, with a time scale similar to that of the wild-type NF- $\kappa$ B.

### **3.2 Live-Cell Microscopy**

In order to characterize NF- $\kappa$ B oscillations in RelA-GFP transfected macrophages in response to *E. coli* and *Y. pestis* LPS, a series of live microscopy experiments were carried out. Briefly, RAW-RG16 cells were imaged for one hour in complete medium, and if no NF- $\kappa$ B translocation was observed, LPS would be added. Cells were then imaged for another 4 hours and monitored for NF- $\kappa$ B translocation and/or oscillation. Three different chemotypes of LPS were tested (*E. coli*, *Y. pestis* 21°C, and *Y. pestis* 37°C) at two different concentrations (1nM and 100nM), and all experiments were carried out in triplicate.

#### **3.2.1 1nM *E. coli* LPS**

In RAW-RG16 cells expressing RelA fused to EGFP, an average of 100% of cells showed nuclear translocation of NF- $\kappa$ B when exposed to 1nM *E. coli* LPS over a 4 hour imaging period. There were no cells in any of the three repetitions where NF- $\kappa$ B remained exclusively in the cytoplasm. In cells that showed translocation of NF- $\kappa$ B into the nucleus, a certain number (47% on average) showed translocation of NF- $\kappa$ B back out into the cytoplasm during the 4 hour period, where it stayed for the remainder of the assay. A small percentage (5% on average) of cells showed translocation of NF- $\kappa$ B into the nucleus and no translocation back out (the NF- $\kappa$ B remained in the nucleus for the rest of the 4

hours). The remaining 48% of cells (on average) showed oscillation of NF- $\kappa$ B in and out of the nucleus throughout the 4 hour assay.

### **3.2.2 100nM *E. coli* LPS**

In RAW-RG16 cells expressing RelA fused to EGFP, an average of 100% of cells showed nuclear translocation of NF- $\kappa$ B when exposed to 100nM *E. coli* LPS over a 4 hour imaging period. There were no cells in any of the three repetitions where NF- $\kappa$ B remained exclusively in the cytoplasm. In cells that showed translocation of NF- $\kappa$ B into the nucleus, a certain number (14% on average) showed translocation of NF- $\kappa$ B back out into the cytoplasm during the 4 hour period, where it stayed for the remainder of the assay. The remaining 86% of cells (on average) showed oscillation of NF- $\kappa$ B in and out of the nucleus throughout the 4 hour assay.

### **3.2.3 1nM *Y. pestis* 21°C LPS**

In RAW-RG16 cells expressing RelA fused to EGFP, an average of 97% of cells showed nuclear translocation of NF- $\kappa$ B when exposed to 1nM *Y. pestis* 21°C LPS over a 4 hour period. There were very few cells in which NF- $\kappa$ B remained exclusively in the cytoplasm (3% on average). In cells that showed translocation of NF- $\kappa$ B into the nucleus, an average of 31% showed translocation of NF- $\kappa$ B back out into the cytoplasm during the 4 hour period, where it stayed for the remainder of the assay. The remaining 66% of cells (on average) showed oscillation of NF- $\kappa$ B in and out of the nucleus throughout the 4 hour assay.

### **3.2.4 100nM *Y. pestis* 21°C LPS**

In RAW-RG16 cells expressing RelA fused to EGFP, an average of 100% of cells showed nuclear translocation of NF- $\kappa$ B when exposed to 100nM *Y. pestis* 21°C LPS over a 4 hour imaging period. There were no cells in any of the three repetitions where NF- $\kappa$ B remained exclusively in the cytoplasm. In cells that showed translocation of NF- $\kappa$ B into the nucleus, a certain number (57% on average) showed translocation of NF- $\kappa$ B back out into the cytoplasm during the 4 hour period, where it stayed for the remainder of the assay. A small percentage (9% on average) of cells showed translocation of NF- $\kappa$ B into the nucleus and no translocation back out (the NF- $\kappa$ B remained in the nucleus for the rest of the 4 hours). The remaining 34% of cells (on average) showed oscillation of NF- $\kappa$ B in and out of the nucleus throughout the 4 hour assay.

### **3.2.5 1nM *Y. pestis* 37°C LPS**

In RAW-RG16 cells expressing RelA fused to EGFP, an average of 97% of cells showed nuclear translocation of NF- $\kappa$ B when exposed to 1nM *Y. pestis* 37°C LPS over a 4 hour imaging period. There were very few cells in which NF- $\kappa$ B remained exclusively in the cytoplasm (3% on average). In cells that showed translocation of NF- $\kappa$ B into the nucleus, a certain number (46% on average) showed translocation of NF- $\kappa$ B back out into the cytoplasm during the 4 hour period, where it stayed for the remainder of the assay. A small percentage (6% on average) of cells showed translocation of NF- $\kappa$ B into the nucleus and no translocation back out (the NF- $\kappa$ B remained in the nucleus for the rest of the 4

hours). The remaining 45% of cells (on average) showed oscillation of NF- $\kappa$ B in and out of the nucleus throughout the 4 hour assay.

### **3.2.6 100nM *Y. pestis* 37°C LPS**

In RAW-RG16 cells expressing RelA fused to EGFP, an average of 99% of cells showed nuclear translocation of NF- $\kappa$ B when exposed to 100nM *Y. pestis* 37°C LPS over a 4 hour imaging period. There were very few cells in which NF- $\kappa$ B remained exclusively in the cytoplasm (1% on average). In cells that showed translocation of NF- $\kappa$ B into the nucleus, a certain number (46% on average) showed translocation of NF- $\kappa$ B back out into the cytoplasm during the 4 hour period, where it stayed for the remainder of the assay. A small percentage (13% on average) of cells showed translocation of NF- $\kappa$ B into the nucleus and no translocation back out (the NF- $\kappa$ B remained in the nucleus for the rest of the 4 hours). The remaining 40% of cells (on average) showed oscillation of NF- $\kappa$ B in and out of the nucleus throughout the 4 hour assay.

### **3.3 Live Microscopy Data and Analysis of Oscillatory Behavior**

The ratio of mean nuclear intensity to mean cytoplasmic intensity was calculated for each cell and plots were generated for each cell over the entire 120 frames of an assay. The plots show intensity over time and were generated for all 18 datasets. Plots for all of the 18 datasets are displayed below in Figure 23 (each of the 3 repetitions of the 6 different concentration/chemotype combinations were overlaid to allow for easier presentation).

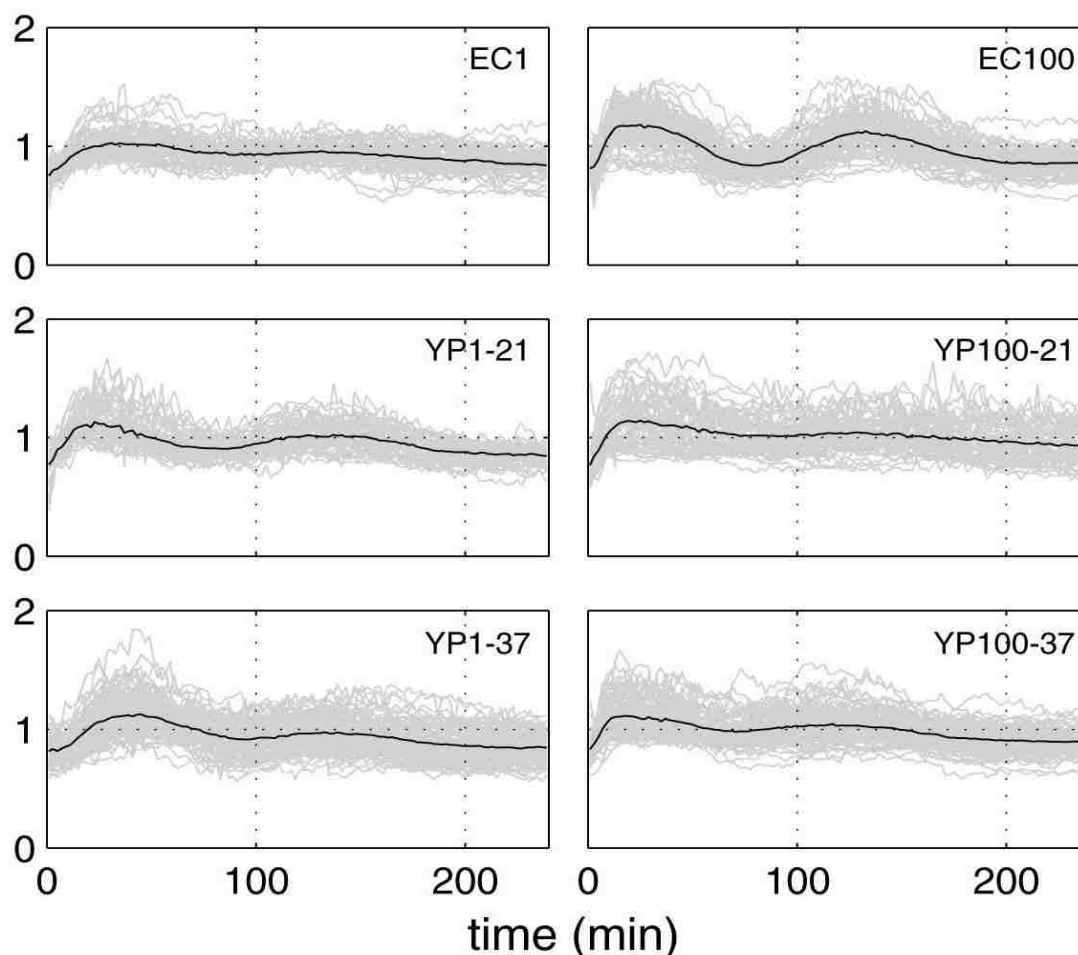


**Figure 23.** Intensity plots from Matlab® for all 18 datasets, with plots for each cell from each unique chemotype/concentration combination overlaid. The Y-axis shows the nuclear to cytoplasmic intensity ratio and the X-axis shows time (in minutes).

### 3.4 Summary

RAW-RG16 cells showed translocation of NF- $\kappa$ B in and out of the nucleus when exposed to any of the 6 unique chemotype/concentration combinations. Not every cell in each assay showed the same behavior, and the relative percentage of any behavior differed between chemotypes, but the large majority of cells in each assay showed either translocation of NF- $\kappa$ B in then out of the nucleus, or multiple nuclear oscillations of NF- $\kappa$ B. Control assays where no LPS was added showed no such translocations or oscillations. Plots for each cell can be found in Appendix A.

## Chapter 4. Discussion & Conclusions

## 4.1 Discussion

In order to study NF- $\kappa$ B oscillations in live macrophages in real-time, a fluorescent NF- $\kappa$ B construct (RelA-GFP) was generated. In the first series of immunocytochemical experiments using both wild-type RAW cells and in RAW-RG16 cells, it was verified that this fluorescent construct did localize like the wild-type NF- $\kappa$ B transcription factor, and could therefore be used as an indicator of wild-type NF- $\kappa$ B response.

### 4.1.1 Immunocytochemistry

#### 4.1.1.1 NF- $\kappa$ B Response due to LPS in RAW 264.7 Cells

In these experiments, RAW 264.7 cells were exposed to three different types of LPS (*E. coli*, *Y. pestis* 37°C, and *Y. pestis* 21°C), each at two different concentrations (1nM and 100nM). After staining and visualization, the localization of NF- $\kappa$ B in each cell was measured for every time point.

As can be seen in Figures 16 and 17 and Table 1, there are nuclear to cytoplasmic oscillations of NF- $\kappa$ B in RAW 264.7 cells exposed to LPS. The oscillations can be seen for all three LPS chemotypes tested. The only exception to this, i.e. cells showing a lack of NF- $\kappa$ B oscillations, but initial translocation, was seen in cells exposed to 1nM *Y. pestis* 37°C LPS. For the cells displaying oscillations in response to LPS-challenges, a total of two oscillations of NF- $\kappa$ B within 2 hours were observed for at least one concentration.

#### 4.1.1.2 NF- $\kappa$ B Response due to LPS in RAW-RG16 Cells

Once it was established that NF- $\kappa$ B oscillations occurred in wild-type RAW 264.7 cells exposed to LPS, the next step was to test whether this phenomenon also occurred in cells transfected with a fluorescent RelA construct. The use of fluorescently labeled RelA was necessary to be able to follow NF- $\kappa$ B translocation/oscillation during real-time microscopy. Just as in the experiments with wild-type cells, RAW-RG16 cells were exposed to three different types of LPS (*E. coli*, *Y. pestis* 37°C, and *Y. pestis* 21°C), each at two different concentrations (1nM and 100nM). The localization of NF- $\kappa$ B in each cell was determined (using fluorescence microscopy) for every time point and graphed.

As Figures 21 and 22 and Table 2 clearly show, there are nuclear to cytoplasmic oscillations of NF- $\kappa$ B in RAW-RG16 cells exposed to LPS. This evidence is present for all three LPS chemotypes tested, and for both concentrations tested. In all six cases, a number of cells show a single nuclear NF- $\kappa$ B increase with a later decrease. In 4 out of the 6 tests, a second increase and subsequent decrease can be seen. For 1nM *E. coli* LPS, there is a second increase, but not a subsequent decrease. For 1nM *Y. pestis* 37°C LPS, there is only one increase and decrease. A total of two oscillations of nuclear NF- $\kappa$ B in 2 hours were present for all LPS types tested for at least one concentration.

#### 4.1.1.3 Comparison of NF- $\kappa$ B Response in RAW 264.7 vs. RAW-RG16 Cells

By comparing the data from both the wild-type RAW 264.7 and the transfected RAW-RG16 experiments, one can see similar patterns (see Figures 24 and 25). At 1nM, both *E. coli* and *Y. pestis* 21°C caused NF- $\kappa$ B to oscillate in



and out of the nucleus twice in both wild-type and transfected RAW cells. At 100nM, *E. coli*, *Y. pestis* 37°C, and *Y. pestis* 21°C LPS all caused NF-κB to oscillate in and out of the nucleus twice in both wild-type and transfected RAW cells. The only exception to the pattern of two oscillations can be found with the use of 1nM *Y. pestis* 37°C LPS, which induced only a single NF-κB translocation in then out of the nucleus. It is important to note that this behavior is present in both the wild-type and transfected cell line experiments. Although it is not fully understood why this concentration of this chemotype only induced a single translocation, this behavior is probably not an outlier, as it was present in all three repetitions using both cell types. It is possible that there may have been some problem with the dilution of the LPS, or with the prep used that caused these results, as real-time testing using this LPS did not show the same oscillatory pattern.

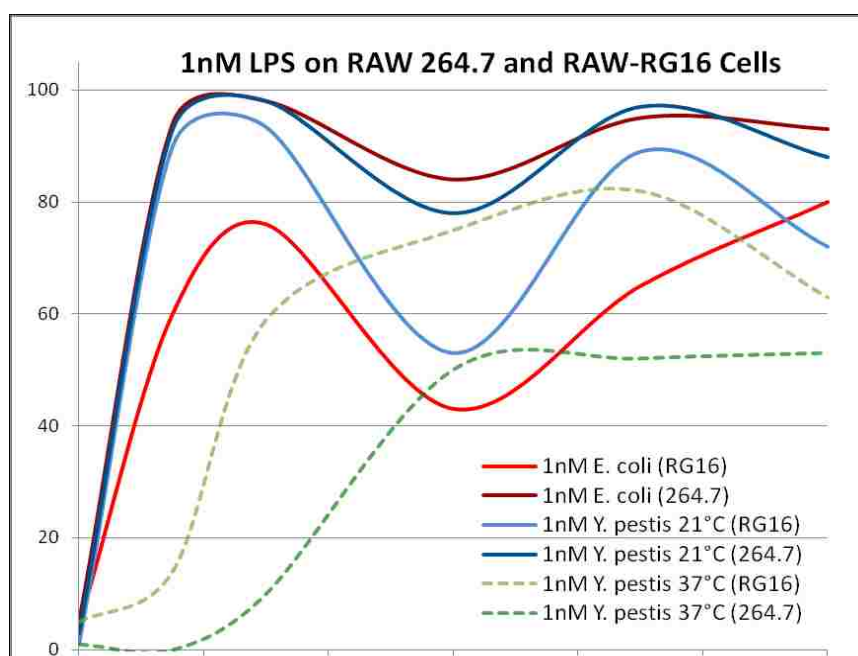


**Figure 24. Comparison of the average number of wild-type RAW 264.7 cells versus transfected RAW-RG16 cells showing nuclear NF-κB in response to 1nM LPS stimulation.**

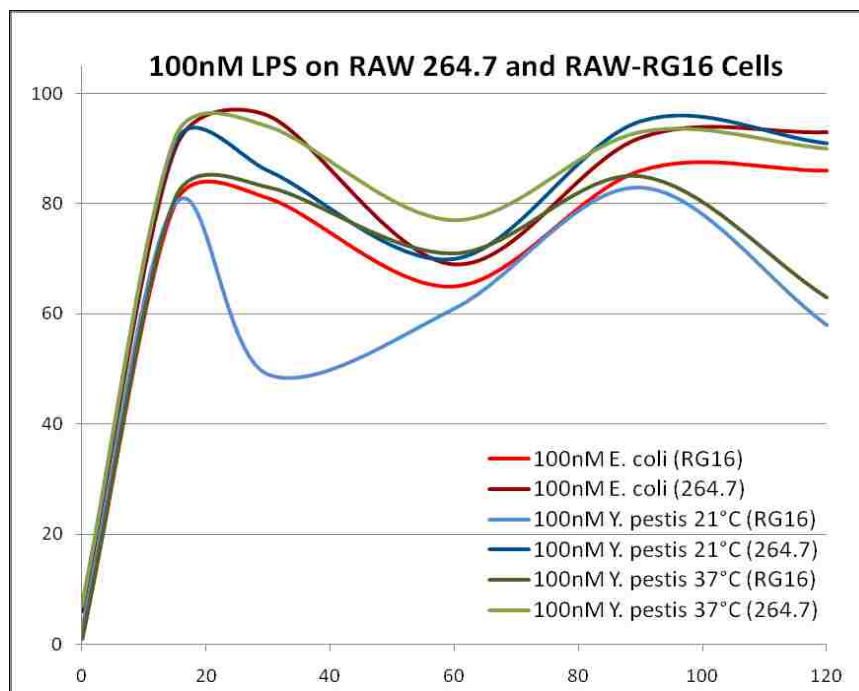


**Figure 25. Comparison of the average number of wild-type RAW 264.7 cells versus transfected RAW-RG16 cells showing nuclear NF-κB in response to 100nM LPS stimulation.**

One significant drawback to immunocytochemical experiments is the inability to track the oscillations in real-time and to track the oscillations at the level of individual cells. The presence of oscillations can only be assumed for a population of cells, calculated by the average number of cells with NF-κB in the nucleus at a given time point. This has been a drawback for all population-based methods such as those employed in previous oscillation studies using EMSA. The best method to visualize and analyze oscillations in a single cell is to perform live-cell microscopy on cells with fluorescently tagged NF-κB proteins.

#### 4.1.2 Live-Cell Microscopy

Once the presence of oscillations was established in wild-type and transfected RAW cells, a series of live-cell microscopy experiments were carried out in order to characterize these oscillations and look for any significant

differences in the response to different chemotypes. Just as in the immunocytochemical experiments, cells were exposed to the three different LPS chemotypes at the two different concentrations and imaged for 4 hours. These experiments showed that oscillations occur in live imaging experiments, and that they continue for at least the 4 hours that imaging occurred (which is longer than the time period examined in immunocytochemical experiments).

It was possible to elucidate differences in frequency, periodicity, and amplitude, but amplitude data are in general difficult to extract and normalize, due to relative fluorescence of individual cells and are therefore here only discussed qualitatively. CellProfiler™ software was able to correct for uneven illumination and background effects and export data on the mean intensity of each nucleus and corresponding cytoplasm. These data were used to plot the ratio of nuclear to cytoplasmic intensity in Matlab®. By using the ratio of nuclear to cytoplasmic intensity, any differences in the expression of RelA-GFP between cells would be corrected. These ratio plots were manually analyzed and clustered. Analysis uncovered different patterns in the oscillation of NF- $\kappa$ B depending on the chemotype/concentration to which the cells were exposed.

#### **4.1.2.1 *E. coli* LPS**

Exposure of RAW-RG16 cells to 1nM and 100nM *E.coli* LPS resulted in nuclear translocation of NF- $\kappa$ B in every cell in all three repetitions. In the majority of cells, NF- $\kappa$ B then translocated back out of the nucleus within the first 100 minutes. Using 1nM LPS, approximately half of the cells continued to oscillate, while the other half showed only one translocation in and out. Using 100nM LPS,

almost all of the cells showed continued oscillation for the entire 4 hours. The increased concentration of LPS appeared to increase the intensity of the oscillations; however both 1nM and 100nM showed damped oscillations over time (i.e. the amplitude appeared to decrease in each oscillation). Oscillations of NF- $\kappa$ B appeared more synchronous using 100nM LPS, as most of the cells showed 2 peaks at the same time points during the assay, and there appeared to be less variation in the amplitude between cells. Using 1nM, nearly half of all the cells showed only one peak, and in the other half of cells showing 2 peaks, the timing of the peaks varied. The amplitudes of the peaks at 1nM varied widely.

#### **4.1.2.2 *Y. pestis* 21°C LPS**

At 21°C, the temperature at which the insect vector (the flea) that spreads *Y. pestis* resides in nature, the LPS produced contains 6 acyl groups, making it very similar in structure to *E. coli* LPS (Rebeil et al., 2004). By exposing RAW cells to *Y. pestis* 21°C LPS, a direct comparison of the oscillations induced by these two chemotypes was possible. Like *E. coli* LPS, both 1nM and 100nM *Y. pestis* 21°C LPS caused NF- $\kappa$ B to translocate into the nucleus in almost every cell in all repetitions (a very small fraction of cells [3%] never translocated at 1nM). 1nM LPS caused about 2/3 of the cells to continue to oscillate twice during the 4 hours, while 100nM caused only about 1/3 to oscillate twice (the other 2/3 only translocated in and out once). This is opposite of the effect seen by increasing the concentration of *E. coli* LPS. The oscillations for both concentrations appeared damped over time, similar to *E. coli* LPS, and there was a lot of variation in the amplitude of the peaks. There was little synchronicity

between cells that did oscillate using either concentration, and the timing of the second peak varied widely.

#### **4.1.2.3 *Y. pestis* 37°C LPS**

At 37°C, the temperature at which *Y. pestis* resides following human infection, the LPS produced contains only 4 acyl groups, making it structurally different to the LPS produced at 21°C and to *E. coli* LPS. This tetraacyl LPS is known to cause an altered immune response and results in lower TNF $\alpha$  secretion in macrophages (Rebeil et al., 2004). Comparing the effect that this LPS has on NF- $\kappa$ B translocation and oscillation, it may be possible to elucidate how this altered response occurs. Like the other two LPS types tested, *Y. pestis* 37°C LPS caused translocation at least once in almost all of the cells. At both 1nM and 100nM, almost half of the cells showed only a single translocation in and out, while around 40% showed oscillations with 2 peaks during the 4 hours. Oscillations due to this LPS were not synchronous, as the timing of the second peak varied widely at both concentrations. At both concentrations, there was a lot of variation in the intensity of the translocations, with some cells showing a rapid and complete transfer to/from the nucleus and others showing a more muted response.

Upon initial characterization, there appeared to be little difference between the 21°C and 37°C *Y. pestis* LPS, as both displayed significant heterogeneity in their responses. Neither LPS caused synchronous oscillations, with both showing large variation in the timing of the oscillation peaks. One would expect that the 21°C LPS would induce a reaction similar to that caused by *E. coli* LPS, but this

was not the case either, as their oscillatory patterns were very different. At this point a more advanced method of analysis was required to find any similarities or differences, so the data were put into clusters to see if any patterns emerged.

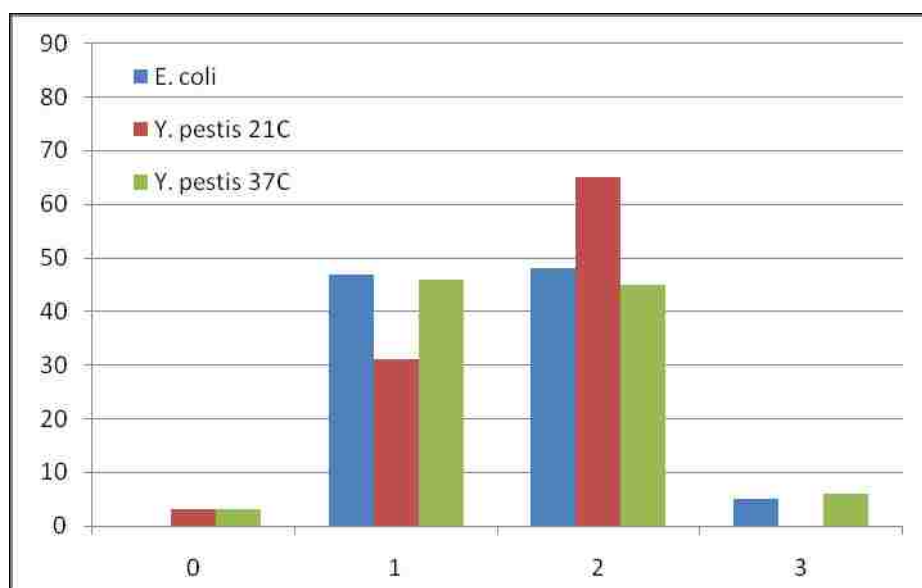
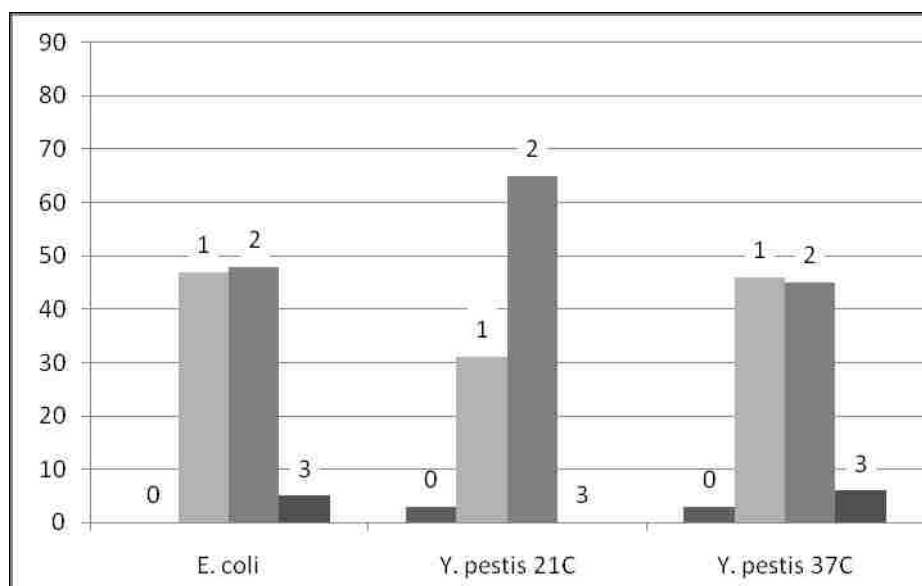
#### **4.1.3 Oscillatory Behavior Clustering:**

The decision of how to cluster the oscillation data was based upon a manual analysis of the movies and the plots generated. Initial analysis of the data showed several distinct patterns, including those cells that did not translocate, some that oscillated once, some twice, and some three times. There were also different intensities of oscillation, with some cells showing complete transfer of RelA-GFP to and from the nucleus, and others showing only a portion of the RelA-GFP translocating in. The timing of the oscillatory peaks was also different between cells. Because of the difficulties in defining some of these categories, and the large quantity of data to be analyzed, a simpler way to cluster the data was devised. It was assumed that any similarities in oscillatory behavior between chemotypes would be revealed using this method, and could be probed further in the future by dividing up these clusters into smaller ones. The different oscillatory behaviors were grouped into 4 types, and for each experiment, the number of cells displaying each behavior were counted. The clusters decided upon were the following: type 0 - cells that showed no RelA-GFP translocation into the nucleus, type 1 - cells that showed translocation in, then back out of the nucleus, type 2 - cells that showed oscillation in and out of the nucleus more than once, and type 3 - cells that showed RelA-GFP translocate into the nucleus and not back out. A table of the clustering results can be found here in Table 3.

1nM on RAW-RG16						
	<i>E. coli</i>		<i>Y. pestis 21°C</i>		<i>Y. pestis 37°C</i>	
Translocation Type	Average Percent	±StDev	Average Percent	±StDev	Average Percent	±StDev
0	0	±0	3	±6	3	±3
1	47	±16	31	±16	46	±12
2	48	±14	65	±11	45	±193
3	5	±4	0	±0	6	±10
100nM on RAW-RG16						
	<i>E. coli</i>		<i>Y. pestis 21°C</i>		<i>Y. pestis 37°C</i>	
Translocation Type	Average Percent	±StDev	Average Percent	±StDev	Average Percent	±StDev
0	0	±0	0	±0	1	±2
1	14	±14	57	±35	46	±27
2	86	±14	33	±41	40	±36
3	0	±0	9	±16	13	±8

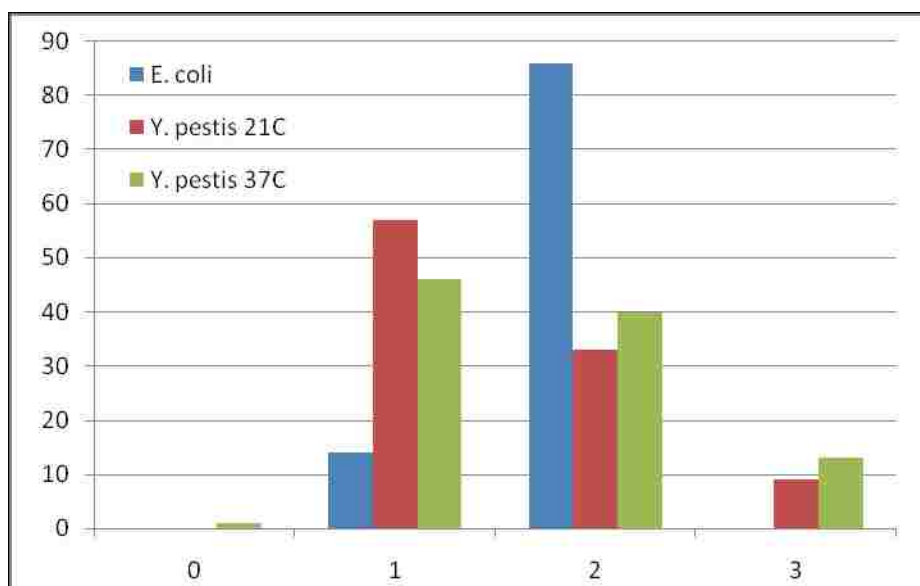
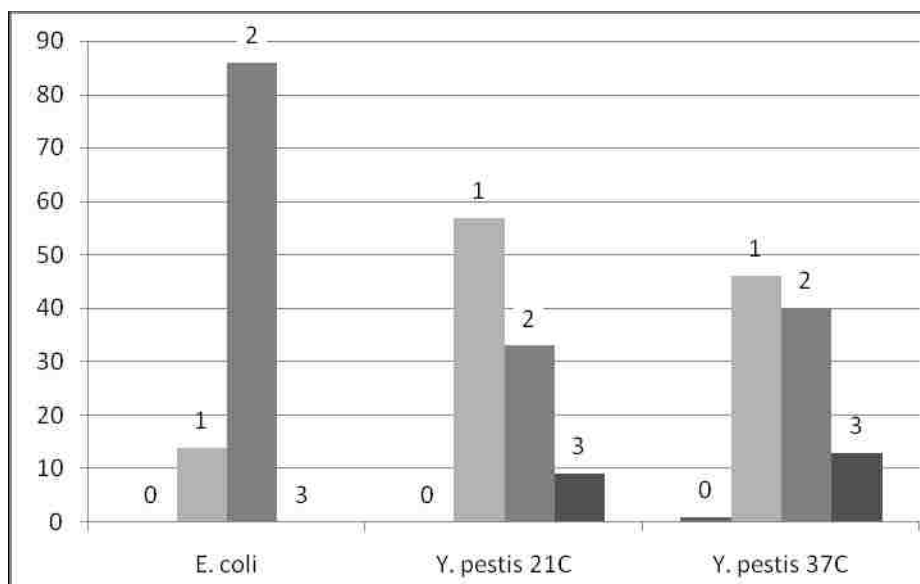
**Table 3. Percentage of RAW-RG16 cells showing particular NF-κB localization behaviors after exposure to the stated LPS chemotypes at 1nM and 100nM, at the stated time intervals. Types are as follows: no translocation into the nucleus (type 0), translocation in, then back out of the nucleus (type 1), oscillation in and out of the nucleus more than once (type 2), or translocation into the nucleus and not back out (type 3).**

To improve our visualization of patterns and/or differences in oscillatory behavior between chemotypes, the data from table 3 were used to generate several bar charts. These charts are organized by chemotype, concentration, and oscillation behavior type, and can be seen in figures 26-29 below:



Figures 26 and 27. Comparison of NF- $\kappa$ B oscillation types stimulated by 1nM *E. coli*, *Y. pestis 37°C*, or *Y. pestis 21°C* LPS. Bars represent the average number of cells out of three repetitions that displayed one of four oscillation types. Oscillation types are as follows: no translocation into the nucleus (type 0), translocation in, then back out of the nucleus (type 1), oscillation in and out of the nucleus more than once (type 2), or translocation into the nucleus and not back out (type 3). Figure 26 shows the data grouped by organism, while Figure 27 shows the data grouped by oscillation type.





**Figures 28 and 29. Comparison of NF- $\kappa$ B oscillation types stimulated by 100nM *E. coli*, *Y. pestis 37°C*, or *Y. pestis 21°C* LPS. Bars represent the average number of cells out of three repetitions that displayed one of four oscillation types. Oscillation types are as follows: no translocation into the nucleus (type 0), translocation in, then back out of the nucleus (type 1), oscillation in and out of the nucleus more than once (type 2), or translocation into the nucleus and not back out (type 3). Figure 28 shows the data grouped by organism, while Figure 29 shows the data grouped by oscillation type.**

Clustering the oscillation data into the four groups highlighted a key feature - all six chemotype/concentration combinations caused most of the cells to oscillate at least once, and many two or three times. Cells rarely failed to

oscillate or to translocate and have RelA-GFP remain in the nucleus. Another important observation is that there do not appear to be any major differences in this pattern between chemotypes. The 100nM *E. coli* data stand out as a larger majority oscillated multiple times. Although our hypothesis was that the oscillatory behavior of *E. coli* LPS and *Y. pestis* 21°C LPS would be similar based on the similarity of the LPS structure, and that of *Y. pestis* 37°C LPS would be very different, no such oscillatory differences were observed.

Comparing the data based on concentration, it was not possible to establish a clear difference between the 1nM and 100nM concentrations, but some differences were observed. For example, *E. coli* LPS caused 86% of the cells to display more than one oscillation at 100nM compared to only 48% at 1nM *E. coli* LPS. Although there are marked differences between the 1nM and 100nM data, no definitive statements can be made about the effect that increased concentration has on oscillation behavior. In the case of *E. coli* LPS, the increase appeared to make the oscillations more synchronous, although this was difficult to replicate in every assay. For *Y. pestis* 21°C LPS, the increased concentration caused more cells to oscillate only once. For *Y. pestis* 37°C LPS, there was very little change in the oscillatory behavior due to the increased concentration of LPS added. These concentrations were selected based on previous publications (Du et al., 1999), with 1nM LPS being considered significantly closer to physiological conditions (100nM concentrations are probably too high to be physiologically relevant, but were used to elucidate a

positive control response). To date, there is virtually no literature available discussing physiological LPS concentrations.

Although no appreciable differences in oscillatory behavior between the different LPS species and concentrations were seen, it is conclusive that all LPS were able to elucidate oscillations. This in itself is a novel finding for the cell system studied. The fact that there are no distinct patterns between the different forms of LPS indicates that LPS, independent of species origin, is capable of stimulating the immune system through TLR4-signalling events. This finding goes somewhat against the theory that *Y. pestis* is a successful gram-negative bacterium capable of avoiding host TLR4-response once it has adapted to the host temperature. This study suggests that *Y. pestis* has different mechanisms to survive the innate immune response. Another important factor to consider is the fact that RAW-RG16 cells are overexpressing NF- $\kappa$ B as compared to wild-type cells, which may lead to a less synchronous response (Nelson et al., 2005), although the use of the  $\beta$ -actin promoter was designed to reduce overexpression. While this is an important factor, the cells used here were tested in staining experiments showing that both the wild-type RelA (red immunostaining) and the transfected (green) RelA, were translocating concomitantly (data not shown). This suggests that the overexpression may not have an as big effect as anticipated.

## 4.2 Conclusions

This work is the first study undertaken that shows, in real-time, NF- $\kappa$ B oscillating in and out of the nucleus in response to LPS in macrophages. All

previous studies have been done on whole cell populations or on other cell types. Oscillations of NF- $\kappa$ B due to LPS were thought not to occur (Covert et al., 2005), but that has been proven false here and in one other published study (Klinke et al., 2008). This is also one of the first studies to be carried out using RAW macrophage cells, which is important as macrophages are highly specialized cells, and other cell lines may not constitute an appropriate model for them.

NF- $\kappa$ B is studied extensively for one important reason, that it is important in so many cellular responses. The one great question that remains is how does NF- $\kappa$ B cause so many distinct responses due to different stimuli when the number of pathways for its stimulation are limited? One competing answer to this question is that these distinct responses are due to differential temporal regulation. This study helps to answer this question by using three different stimuli that are known to cause distinct immune responses in humans and determining how they change the dynamics of NF- $\kappa$ B oscillation. The data here show that while the responses to the different stimuli do lead to different oscillatory dynamics, they do not show any easily discernable patterns, and these dynamics vary widely for each experiment conducted. This leads to the conclusion that the oscillatory dynamics may not play as large of a role as initially thought, i.e. that the temporal profile of NF- $\kappa$ B may not be stimulus specific (at least at the chemotype level). It is important to recognize, however, that these experiments did not examine gene expression due to NF- $\kappa$ B oscillation, and are therefore limited. They suggest that the dynamics are most likely less important, and that they require further study, preferentially at a true single cell level, where

cells are cut off from the secondary secretion of inflammatory markers in response to LPS induced TLR4 signaling events. It is also possible that stimulus-specific oscillation patterns only emerge when using different concentrations or completely different stimulus types (like TNF $\alpha$  vs. LPS), rather than related stimulus types (like two LPS chemotypes).

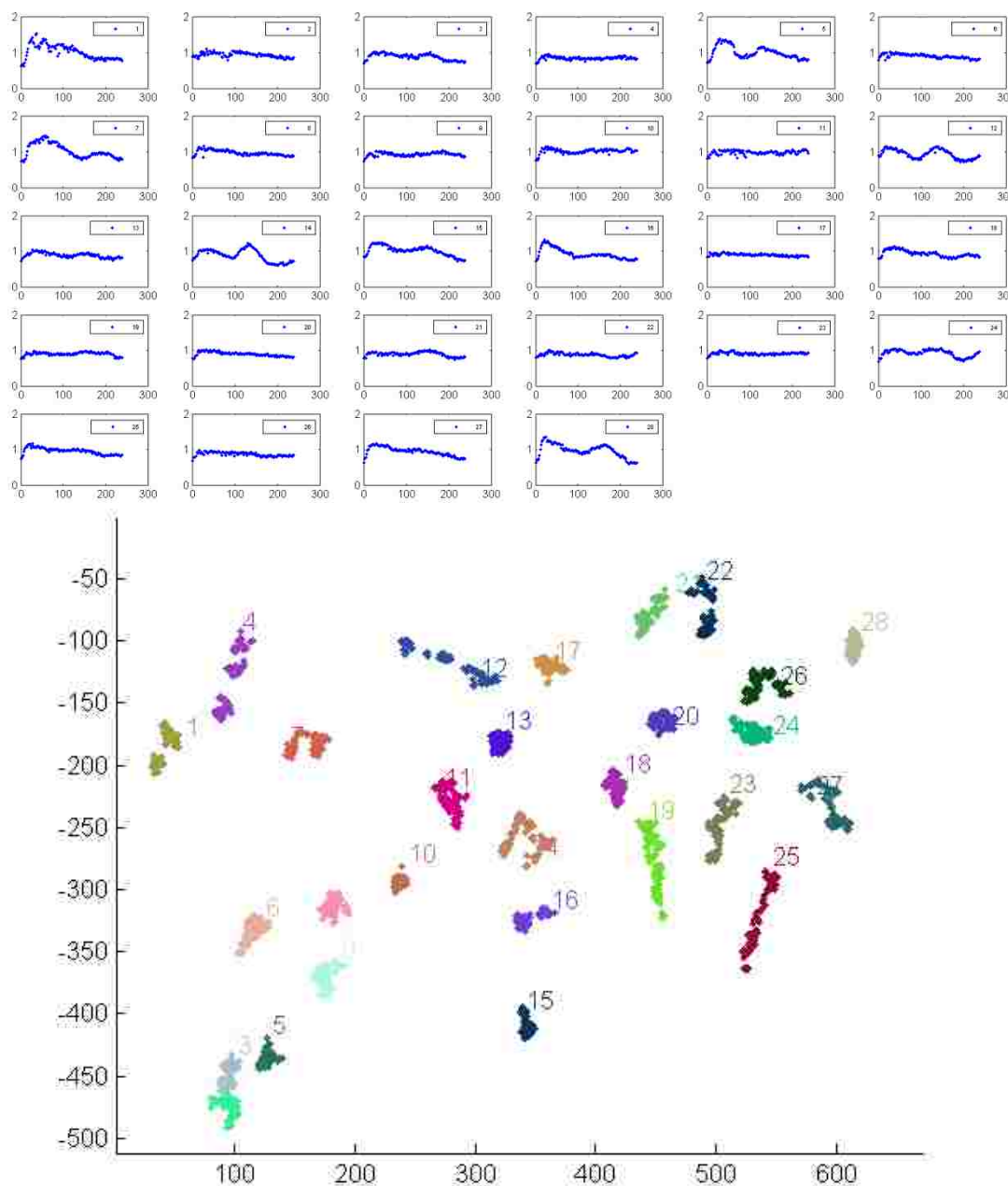
It is clear from this study and others that the NF- $\kappa$ B signaling cascade is an incredibly complex system with many parameters, and that any model of the system must be able to incorporate the high level of heterogeneity seen in experiments. By oversimplifying the system, one may fail to fully understand it, which may inhibit the ability to make relevant therapeutic discoveries possible.

Appendices.

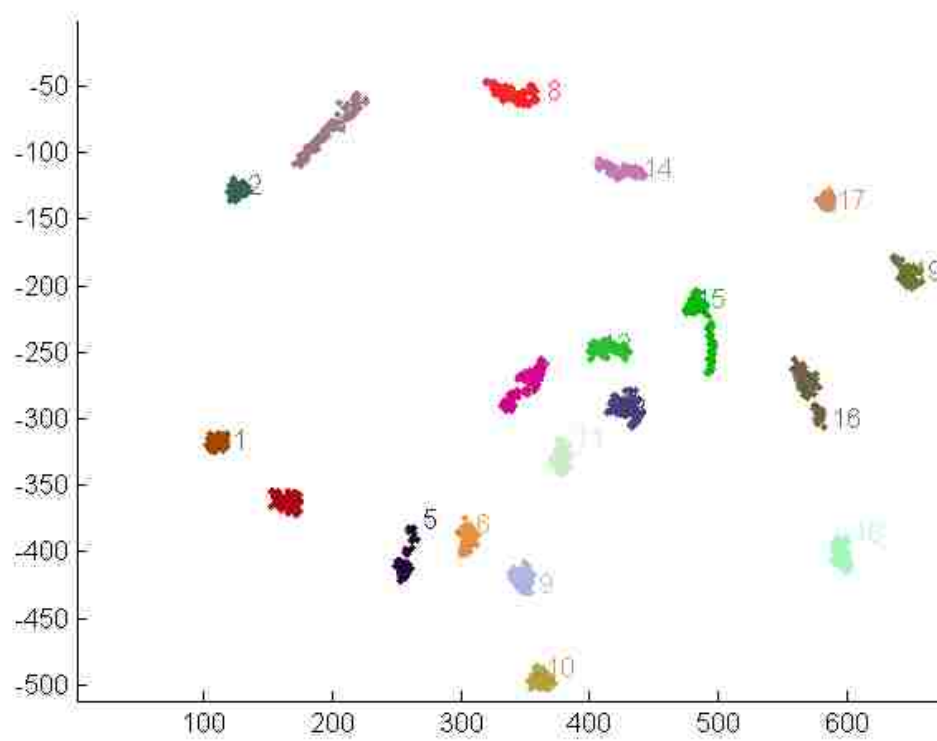
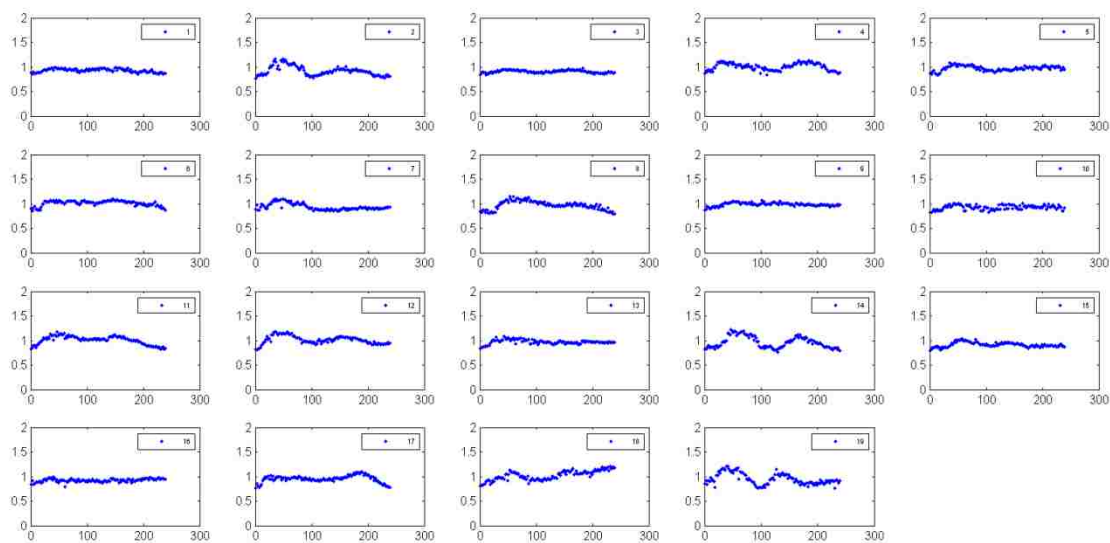
---

## Appendix A. Oscillation Data Plots

The following figures display the nuclear to cytoplasmic intensity ratio data for each individual cell analyzed in each dataset captured. Each set of plots is accompanied by its corresponding cell position plot (which can be used to find the exact cell being analyzed in each movie). The number of cells varies for each experiment, so the number of plots in each figure do as well. The plots are numbered starting at the upper left and going to the right, then proceeding to the next row (like a book).

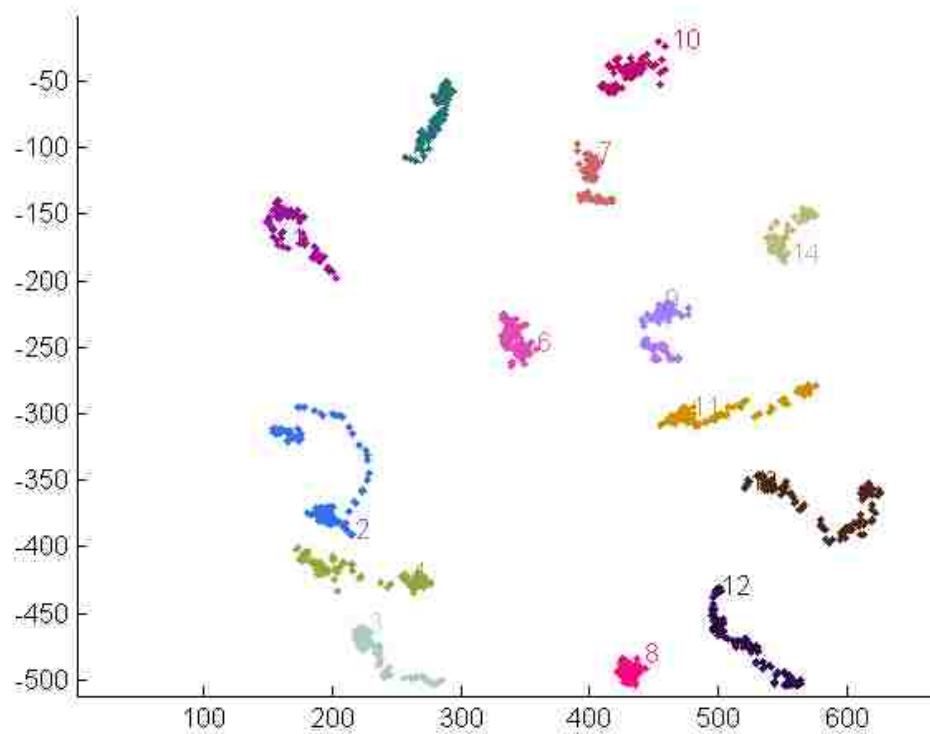
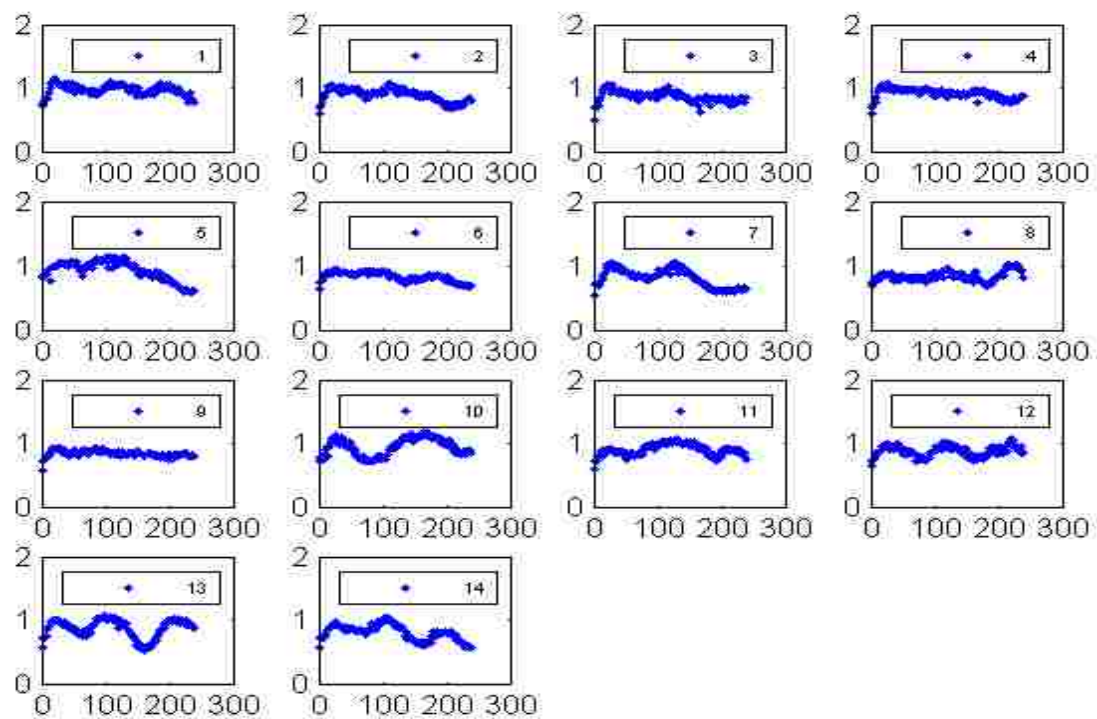


1nM *E. coli* LPS- 12/12/2007

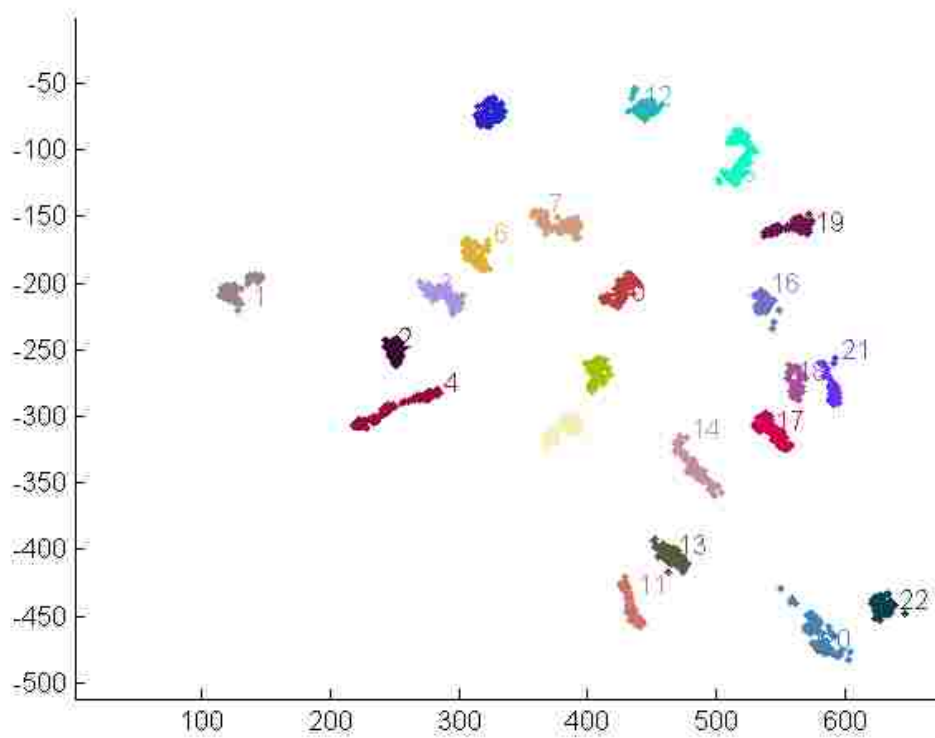
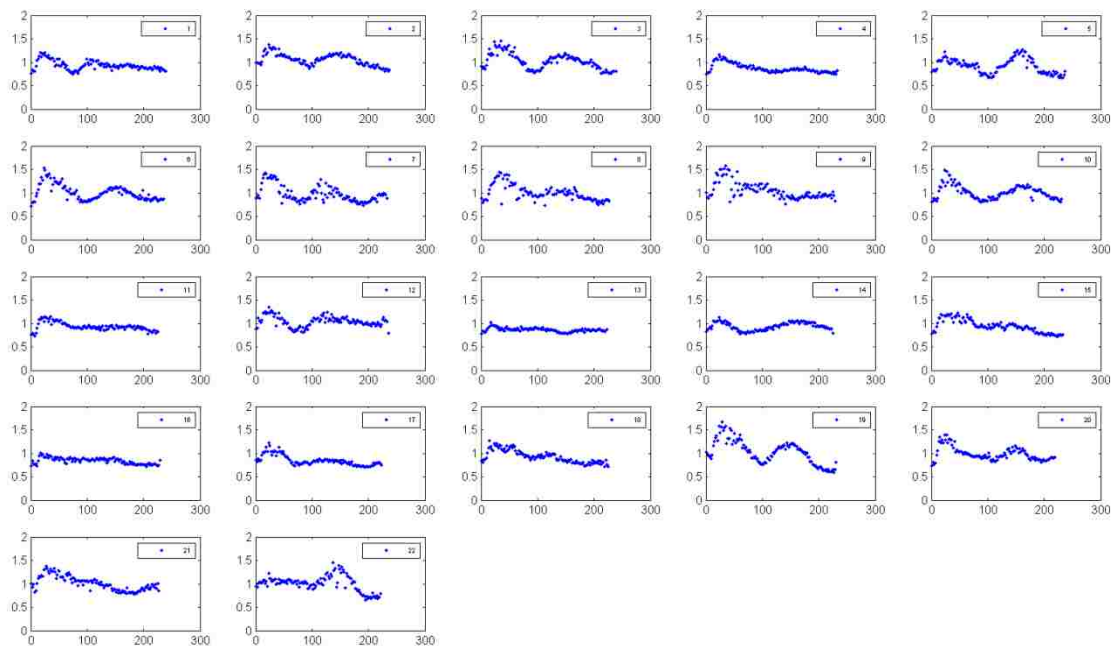


1nM *E. coli* LPS- 2/27/2008

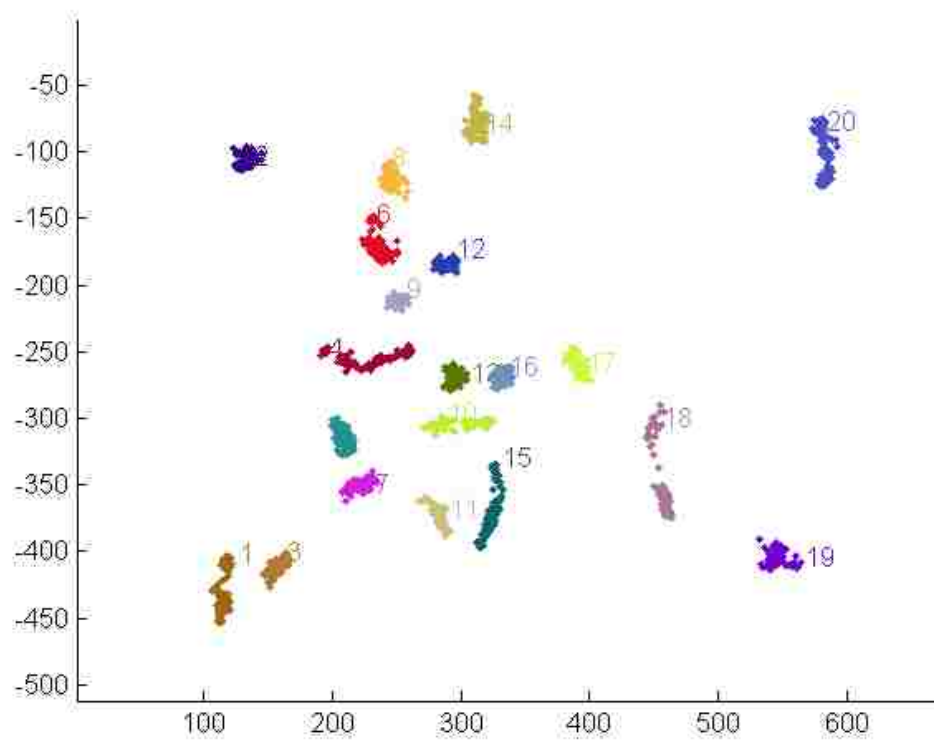
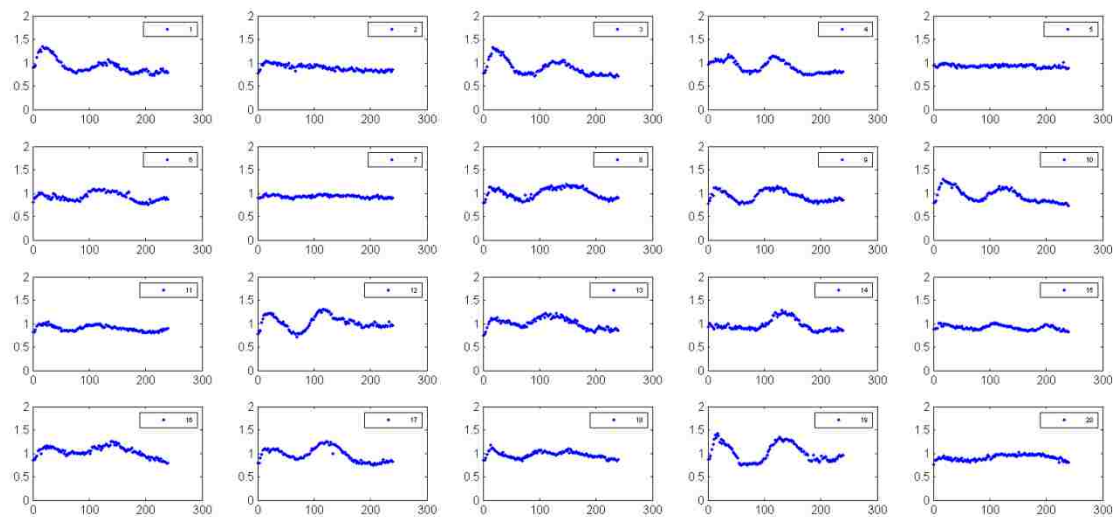




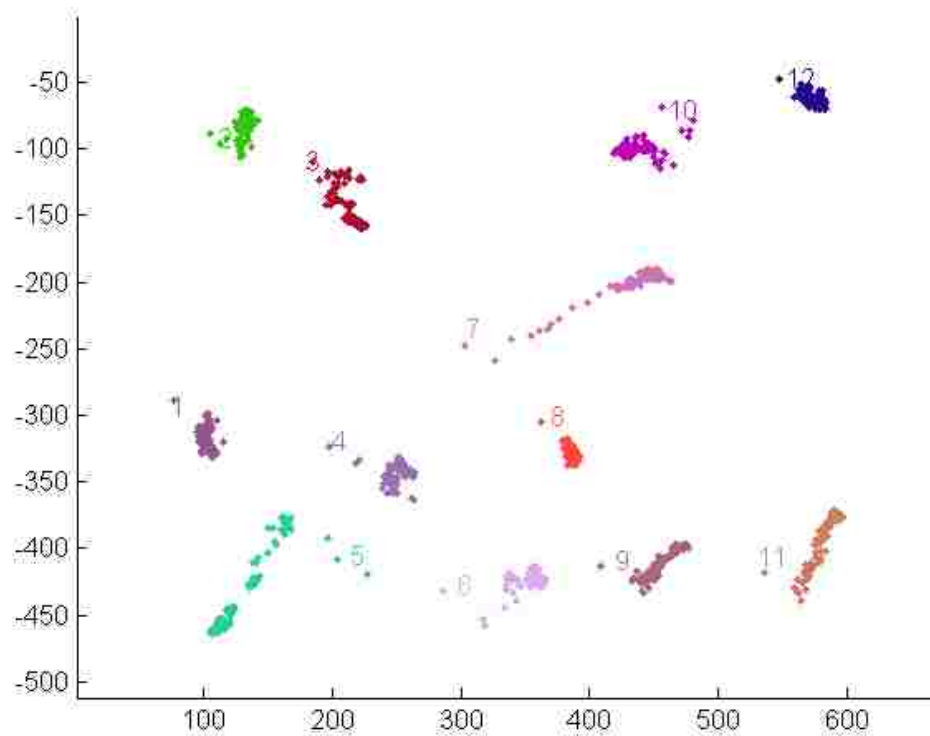
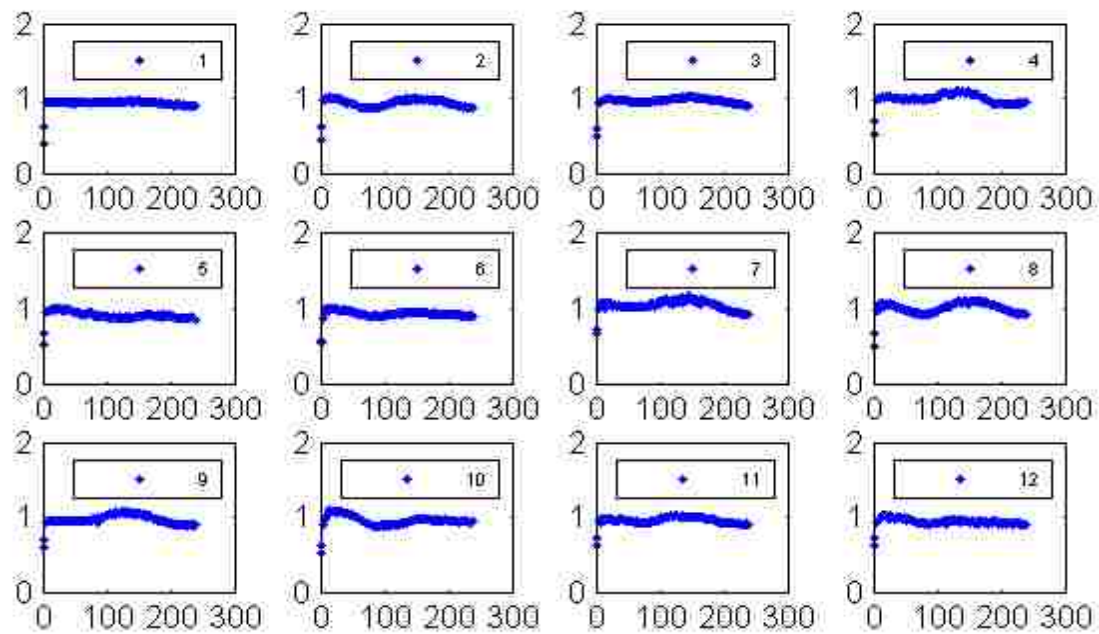
1nM *E. coli* LPS - 7/21/2008



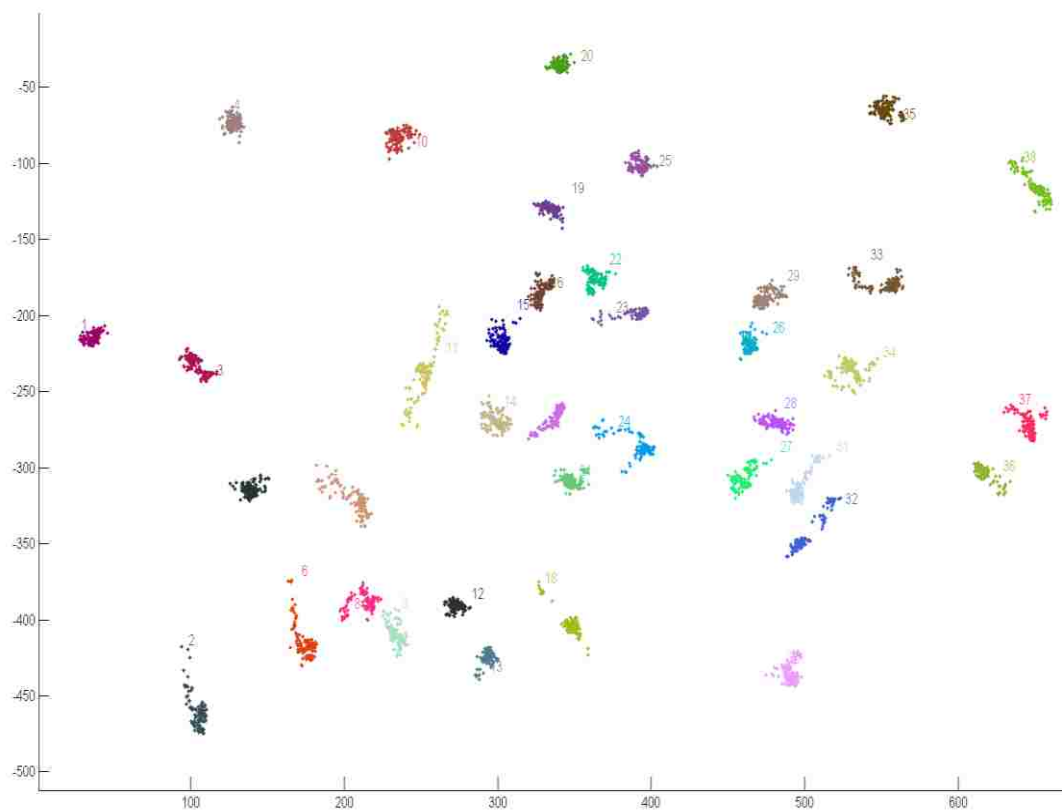
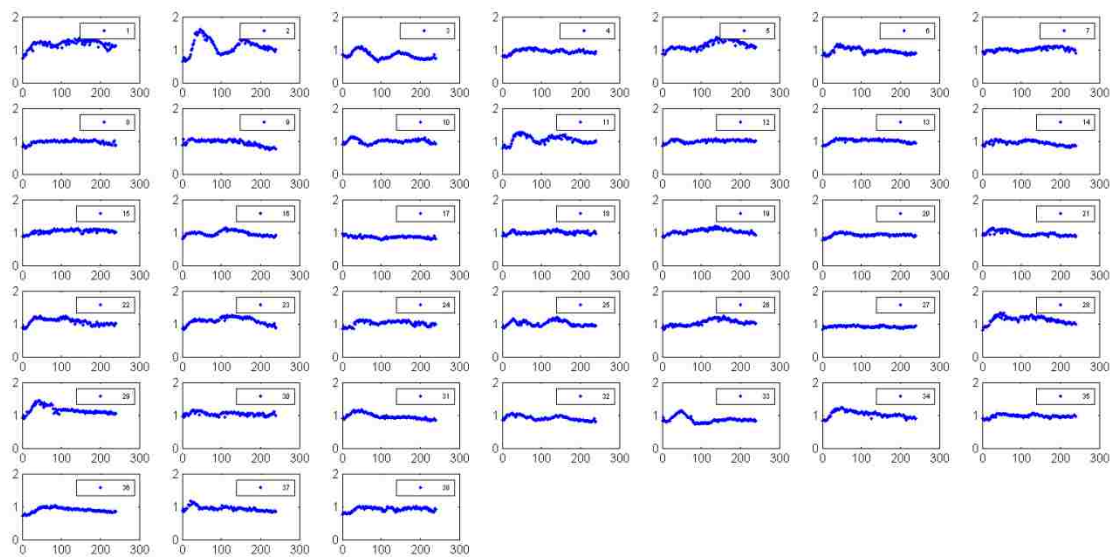
1nM *Y. pestis* 21°C LPS - 11/28/2007



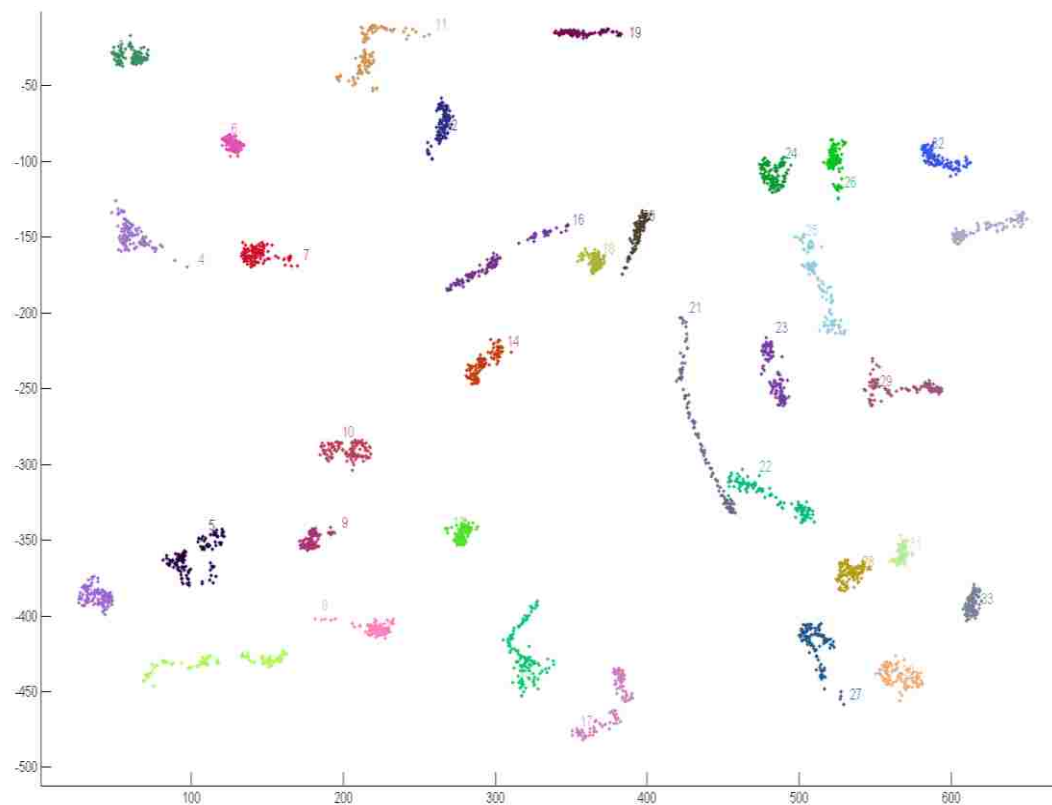
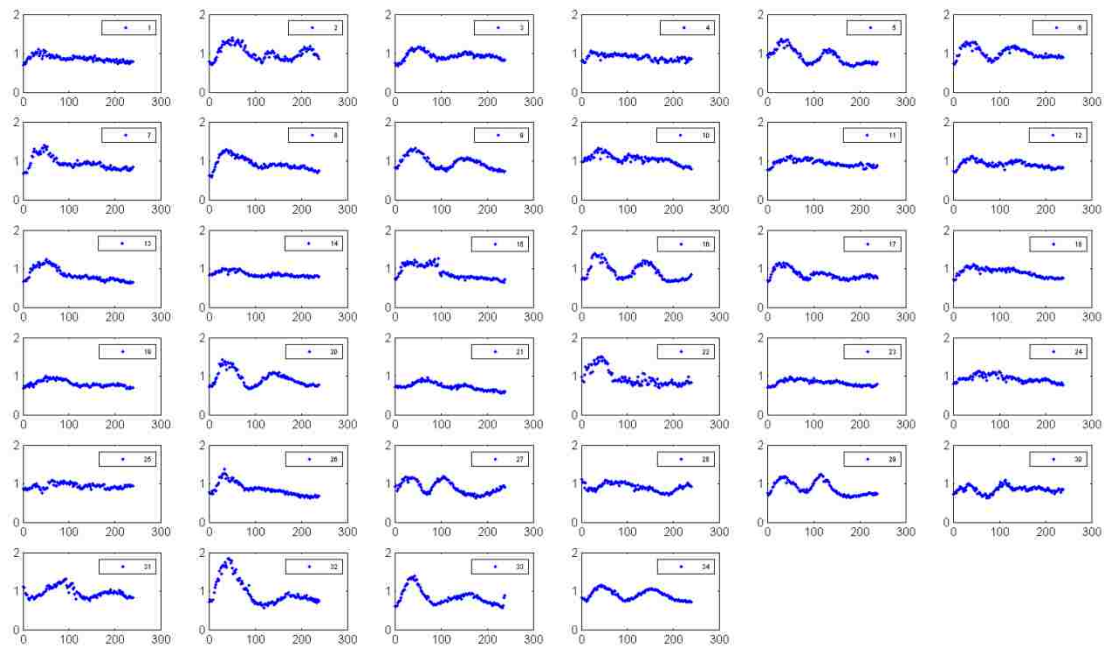
1nM *Y. pestis* 21°C LPS - 11/30/2007



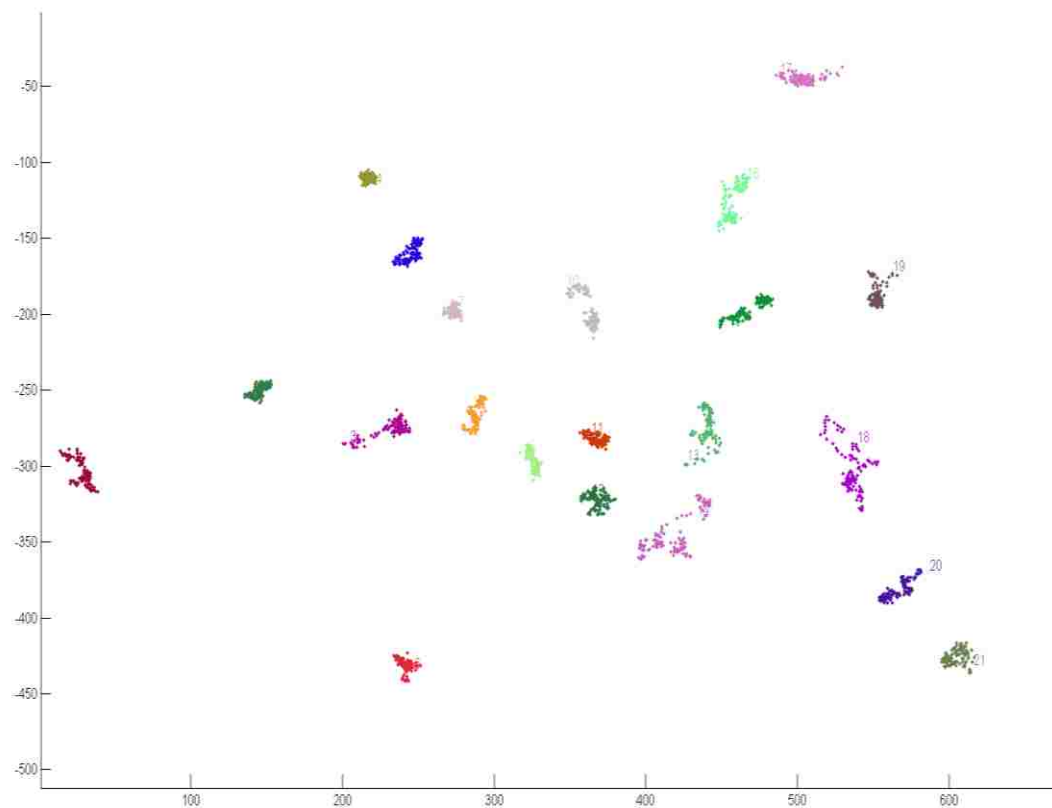
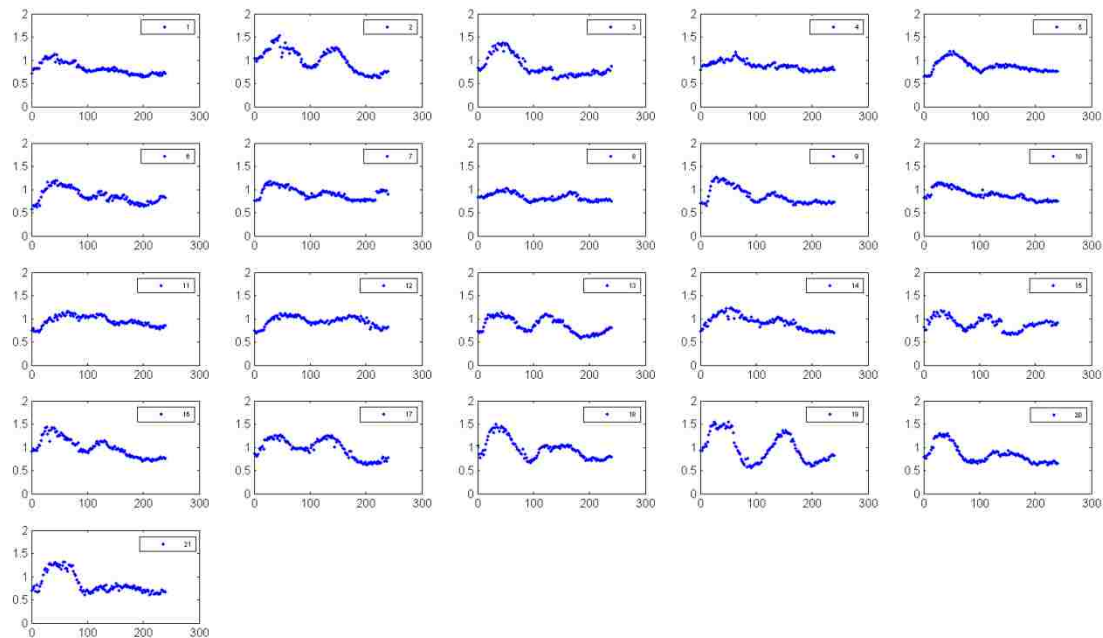
1nM *Y. pestis* 21°C LPS - 9/12/2008



1nM *Y. pestis* 37°C LPS - 11/09/2007

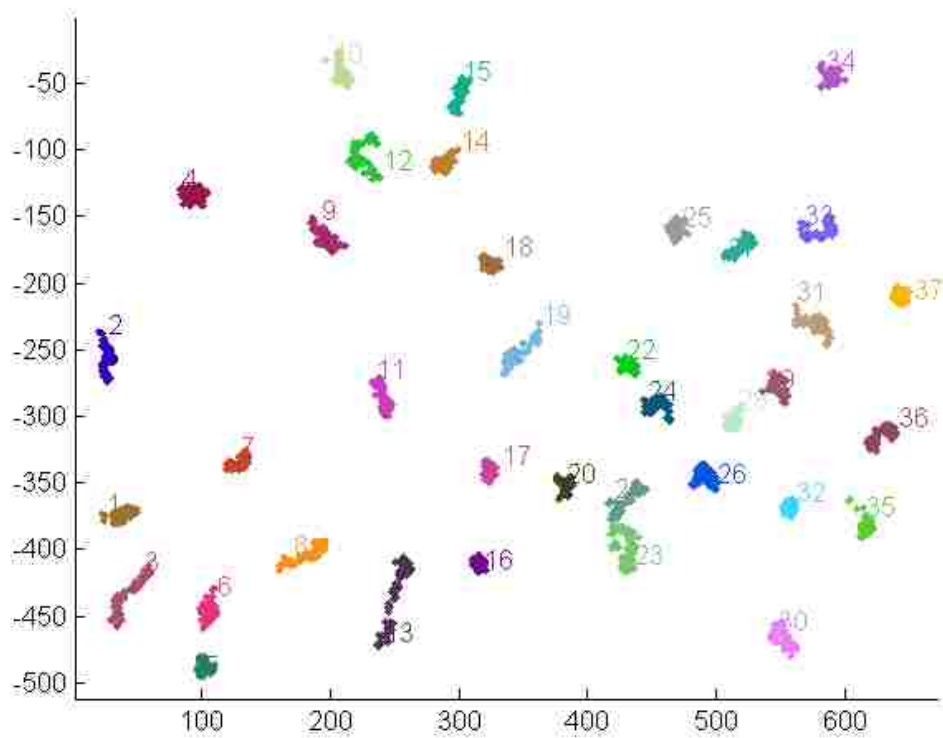
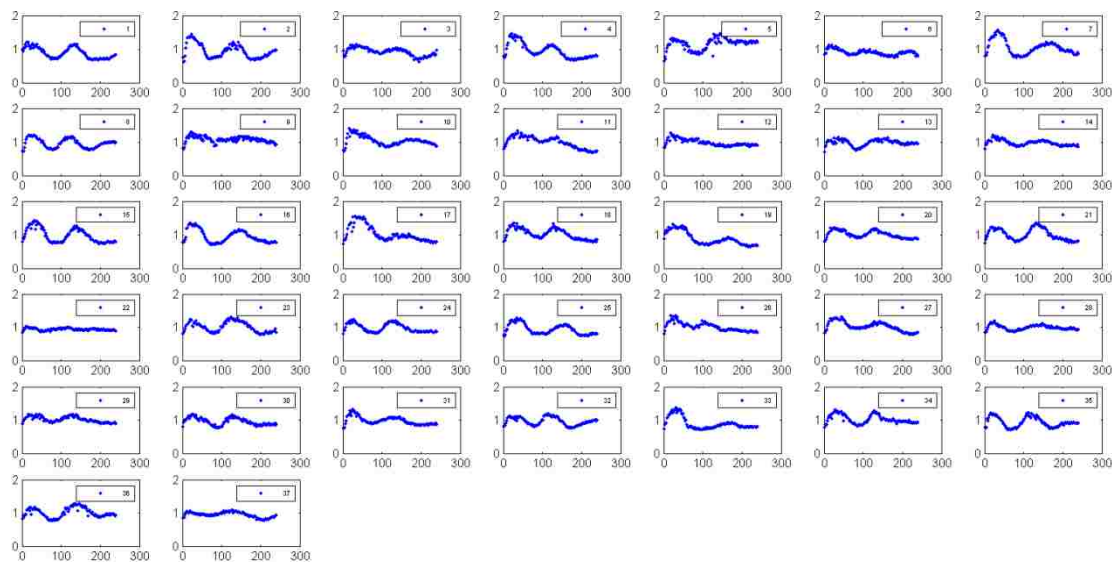


1nM *Y. pestis* 37°C LPS - 11/13/2007



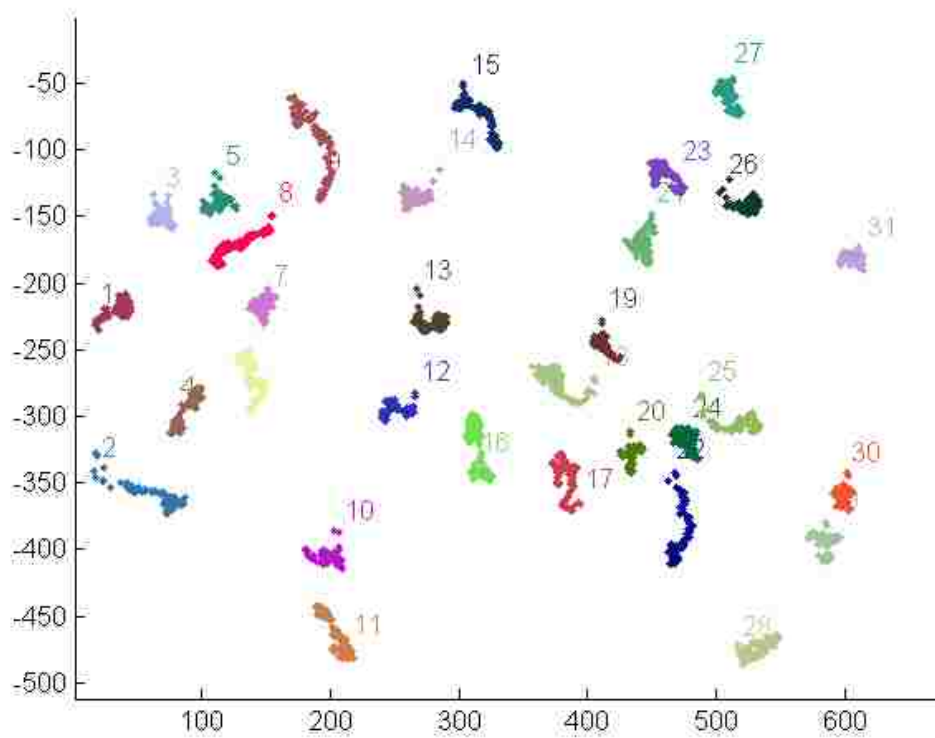
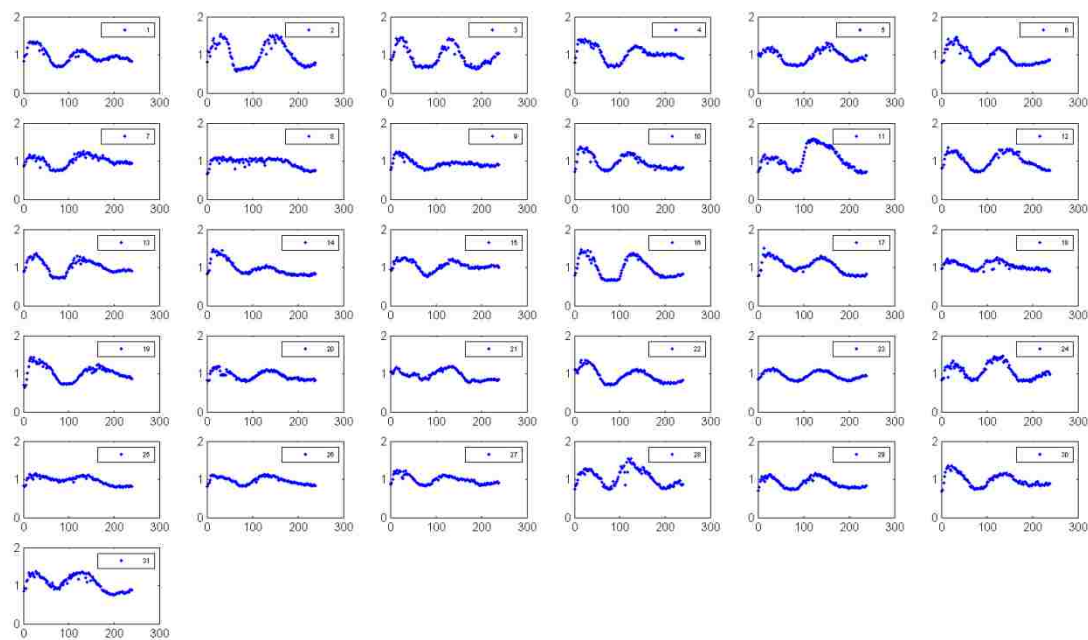
1nM *Y. pestis* 37°C LPS – 11/15/2007



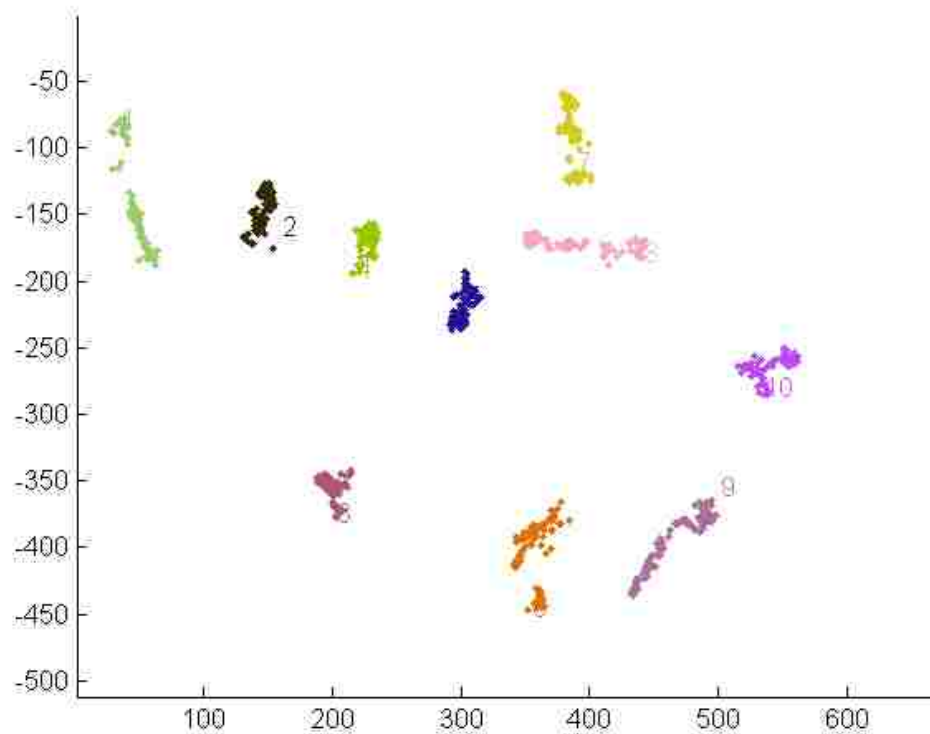
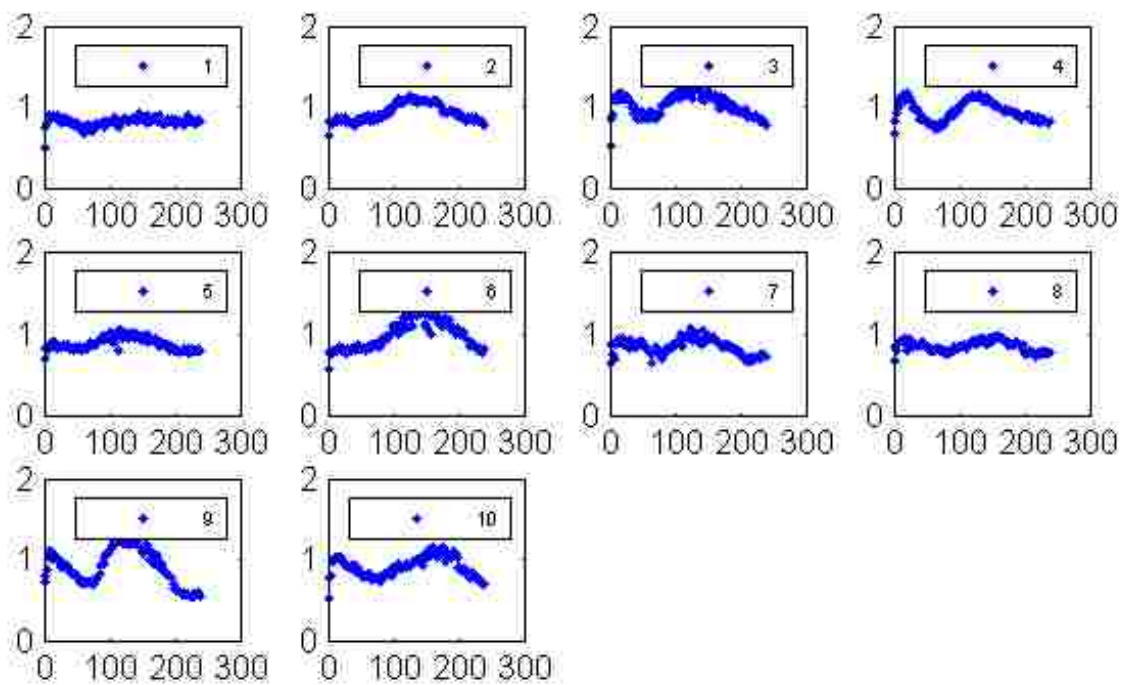


100nM *E. coli* LPS - 11/7/2007

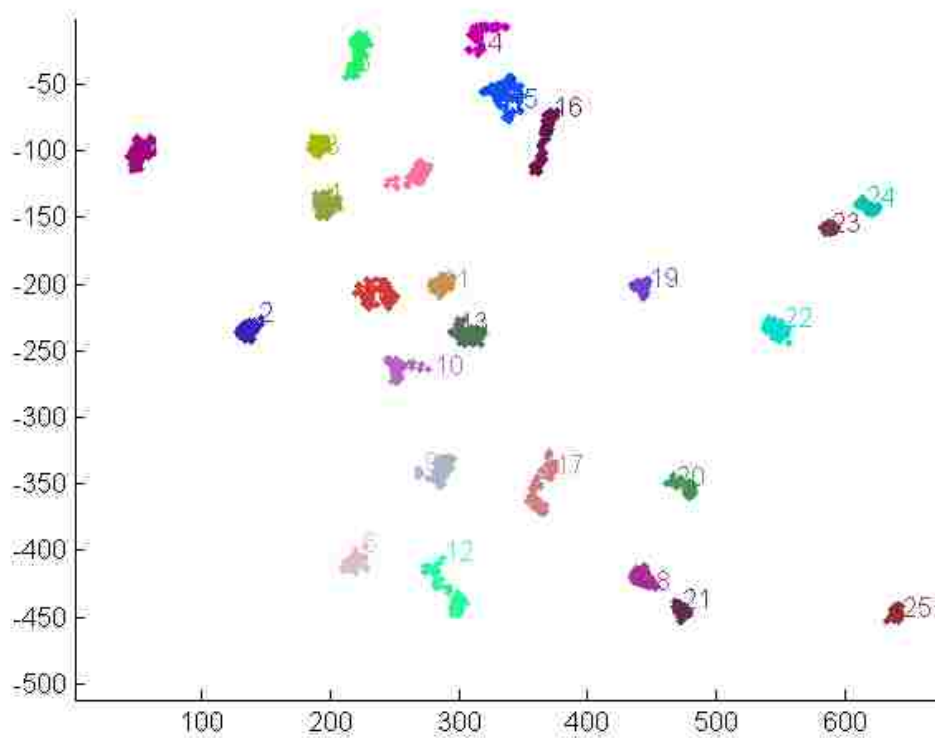
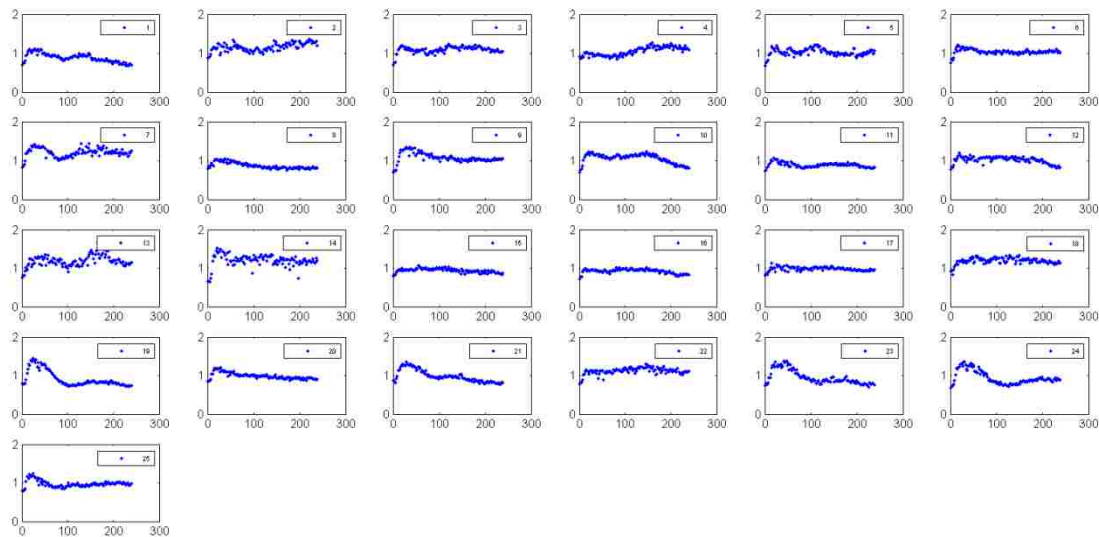




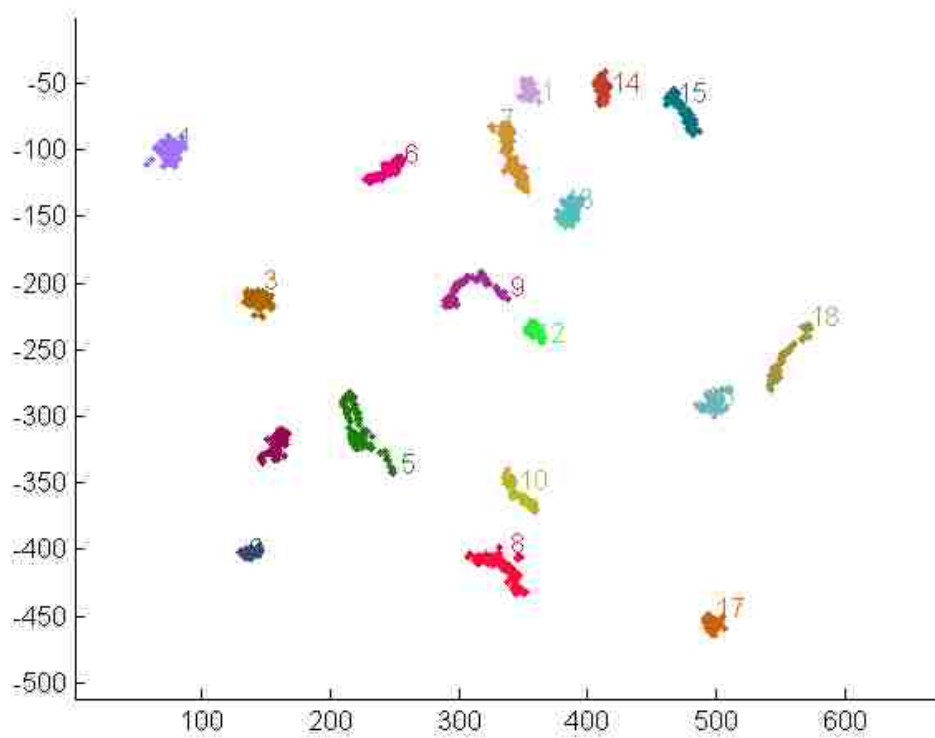
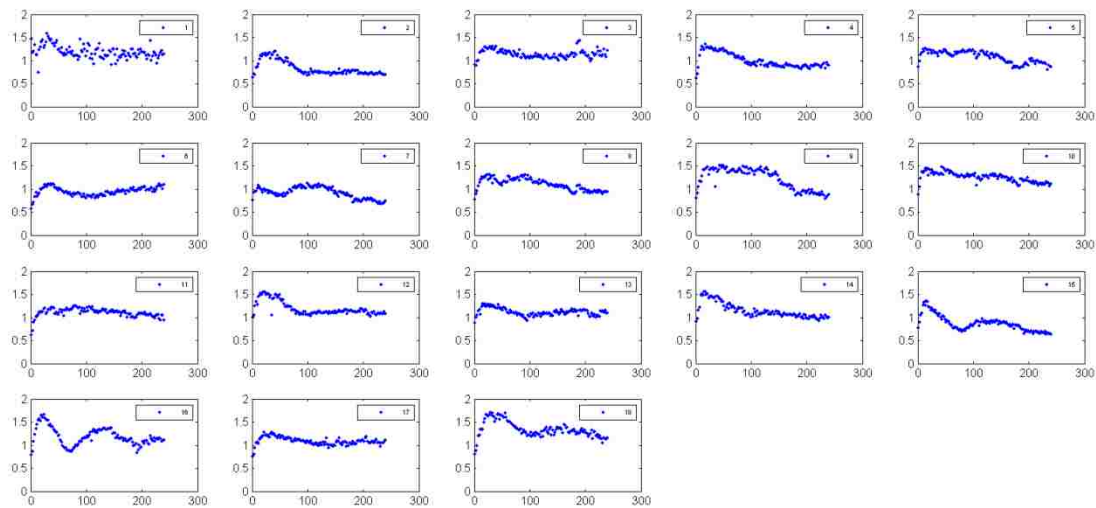
100nM *E. coli* LPS - 11/08/2007



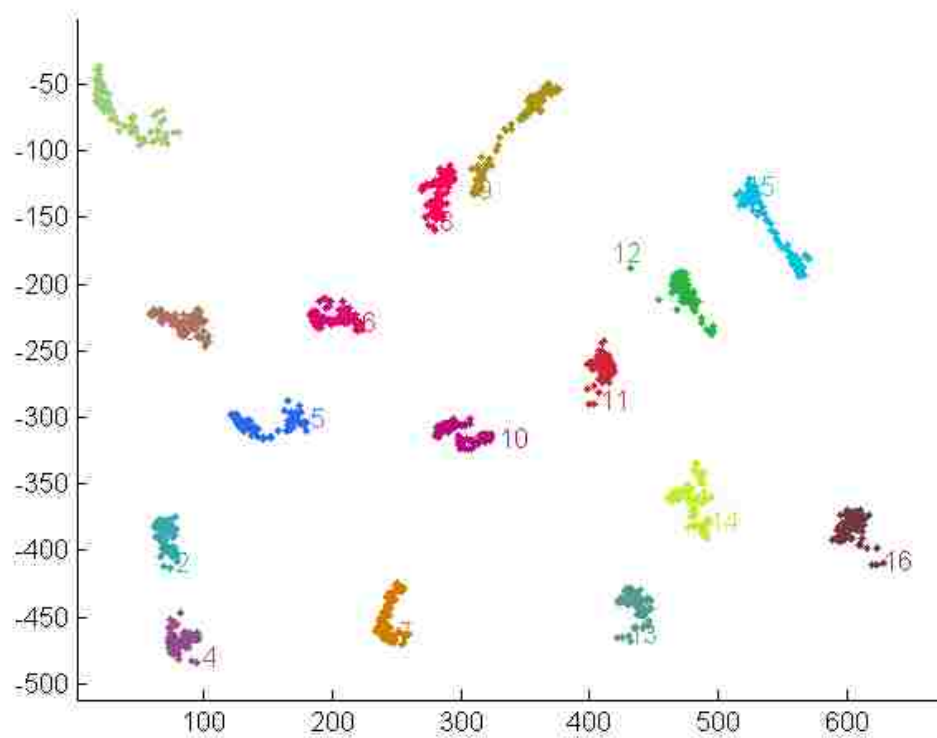
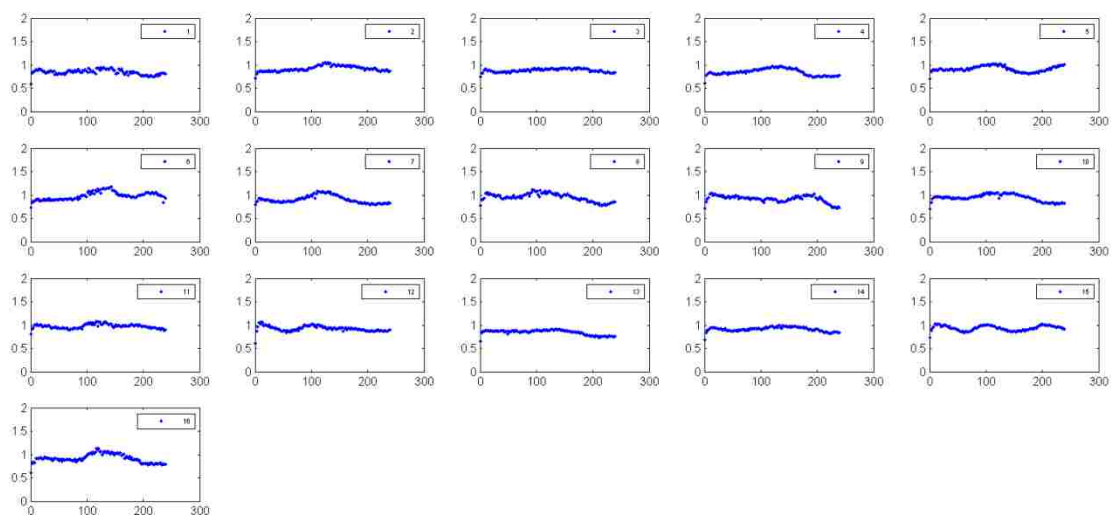
100nM *E. coli* LPS - 9/18/2008



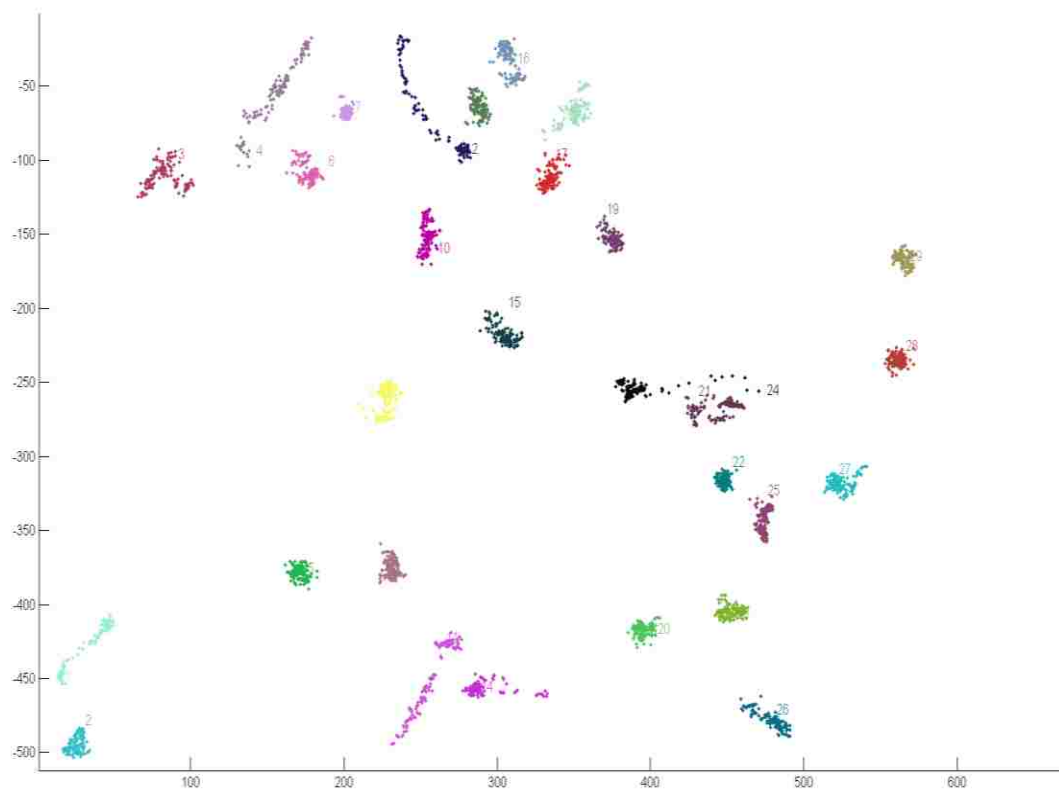
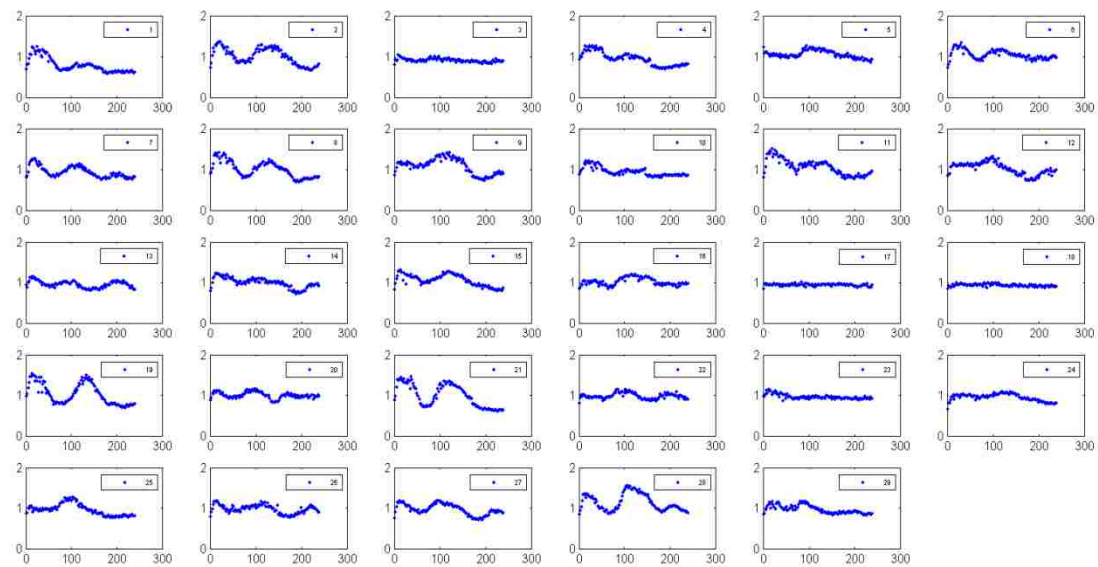
100nM *Y. pestis* 21°C LPS - 11/29/2007



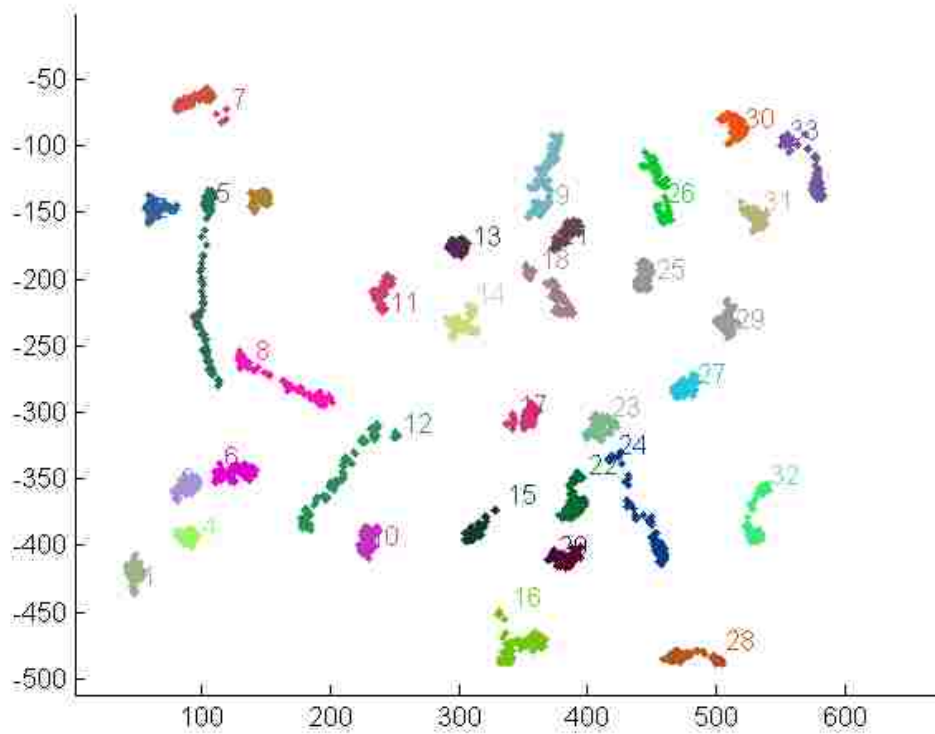
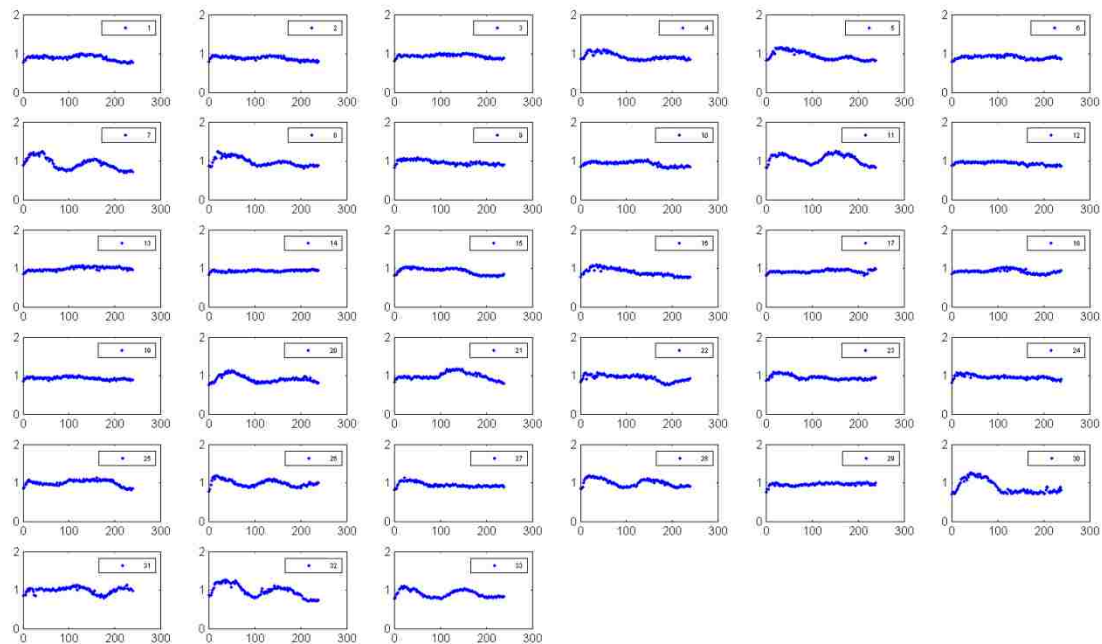
100nM *Y. pestis* 21°C LPS - 12/7/2007



100nM *Y. pestis* 21°C LPS -9/17/2008

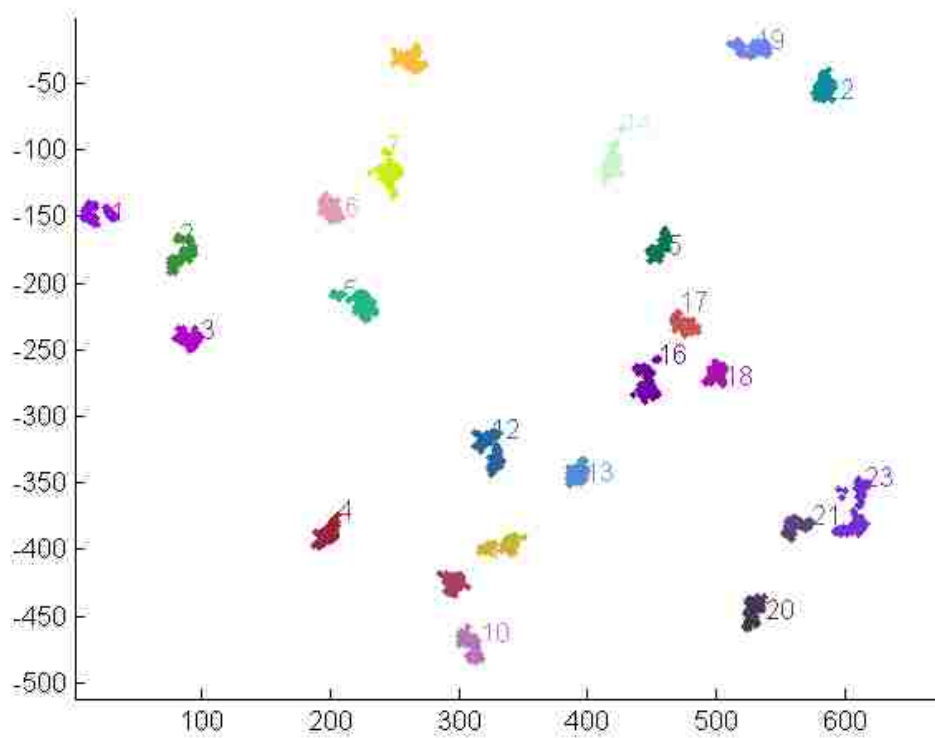
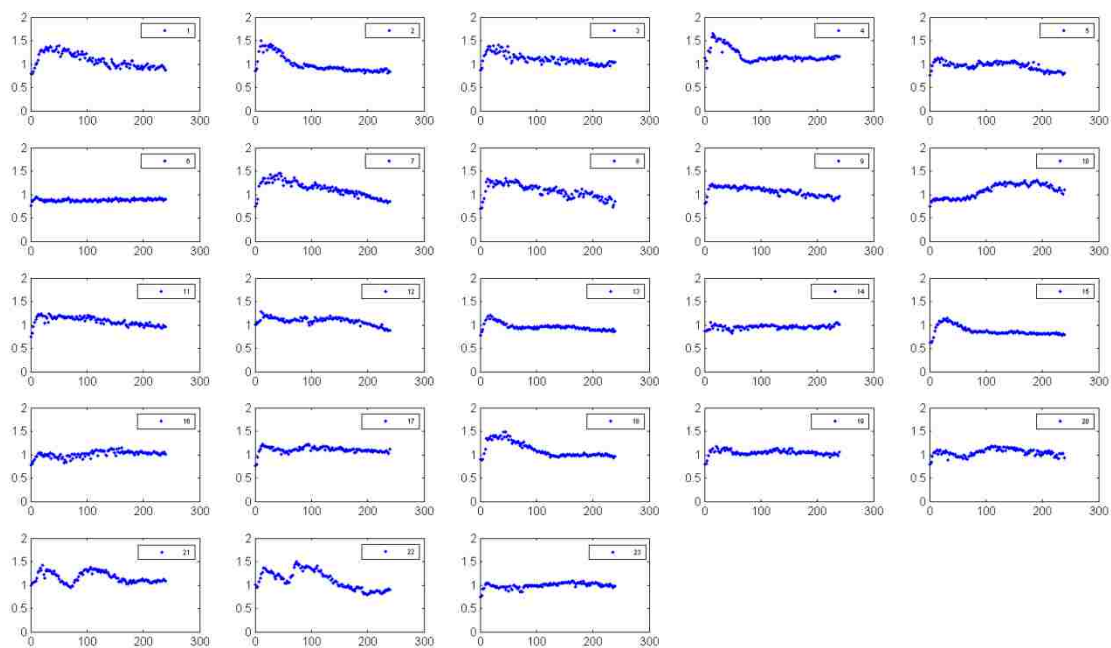


100nM *Y. pestis* 37°C LPS – 11/20/2007



100nM *Y. pestis* 37°C LPS - 11/21/2007





100nM *Y. pestis* 37°C LPS - 12/4/2007



## Appendix B. Matlab and CellProfiler Scripts

The following are the Matlab scripts used to process the raw data for input into CellProfiler and to further process and visualize the outputs of CellProfiler.

```

%-----
% Calculate background by averaging all the movie images
%
% Igal Brenner, 3-2008
%-----
clear all

% Put here the part of the file name that is not changing by a running number
% ex: for "10-19-07 1nM ecoli062.tif" write: 10-19-07 1nM ecoli
file_prefix = '9-18-08 100nM ecoli LPS';

%maximum expected index. The program checks for existence also, so no
%harm in exceeding
max_index = 119;

% just check that the first file in the series exists
fid = fopen([file_prefix '000.tif'],'r');fclose('all');
if fid>2
    temp= imread([file_prefix '000.tif']);

    %create an empty array for the running average
    av_t = zeros(size(temp,1), size(temp,2));
    %start file reading loop
    for i=0:1
        for j=0:9
            for k=0:9
                if i*100+j*10+k<=max_index
                    file_number = ( strcat(int2str(i) , int2str(j) ,
int2str(k) ) );

                    %skip here any indices:
                    if file_number=='000'
                    else
                        %check for file existence
                        fname = strcat(file_prefix, file_number, '.tif');
                        fid = fopen(fname,'r');fclose('all');
                        if fid>=3
                            display( ['Reading file ' fname]);
                            t=imread( strcat(file_prefix, file_number,
'.tif'));

                            av_t = av_t + double(t(:,:,2));
                        else
                            beep;display(['File ' fname ' does not exist']);
                            %return;
                        end
                    end %if
                end %if
            end %k
        end % j
    end %i

    av_t_norm = av_t/(max(max(av_t)))*255;
    temp= uint8(av_t_norm);
    imwrite(temp,'back.tif','tiff');
    imagesc(av_t);
else
    beep;display(['File ' file_prefix '000.tif does not exist']);
end

```

```

%-----
%-          Analyze Cellprofiler output and rearrange the data if
%-          the cell positions was shuffled.
%-          Igal Brener, 4-2-09
%-----

close all;clear all

%-- the files need to be in Excel format: careful because cellprofiler
% saves them in text format and it calls them Excel. To the files have to be
% resaved

%% EDIT %%
ynuc=xlsread('9-17-08DefaultOUT.mat_ShrunkenNuclei.xls');
ycyt=xlsread('9-17-08DefaultOUT.mat_Cytoplasm.xls');

%% EDIT %%

% number of images collected
ni = 120;
%%

%%
%-----
%--   DON'T EDIT BELOW THIS  --
%-----

rand('state',900);

% number of cells imaged
if (floor( size (ynuc,1)/ni) - ( size (ynuc,1)/ni) ~=0 ) | (floor( size
(ycyt,1)/ni) - ( size (ycyt,1)/ni) ~=0)
    disp('Problem with data, number of frames * ncells NE file dimension');
    beep
    stop
else

    nc = ( size (ynuc,1)/ni) ;

    % in case we want to process less frames
    start_frame=1;
    stop_frame= ni; %ni;

    % 0 if we don't want to plot cell positions
    plot_flag = 1;

    % what is the time between frames
    time_per_frame=1;

    cell_ind = 1:nc;
    cell_pointer = cell_ind-1;
    %The index where x and y reside in the big cellprofiler matrix
    x = 1;
    y = 2;

    % the index for the quantity we want to extract
    Nuc_Int_Intensity_index = 5;
    Nuc_Mean_Intensity_index = 6;
    Cyt_Int_Intensity_index = 5;
    Cyt_Mean_Intensity_index = 6;

    Nuc_Int_Intensity_mat = zeros(ni,nc);
    Nuc_Mean_Intensity_mat = zeros(ni,nc);

```

```

Nuc_Int_Norm_Intensity_mat = zeros(ni,nc);
Nuc_Mean_Norm_Intensity_mat = zeros(ni,nc);

Cyt_Int_Intensity_mat = zeros(ni,nc);
Cyt_Mean_Intensity_mat = zeros(ni,nc);

Cyt_Int_Norm_Intensity_mat = zeros(ni,nc);
Cyt_Mean_Norm_Intensity_mat = zeros(ni,nc);
Nuc_by_Cyt_Norm_matrix = zeros(ni,nc);
big_cell_plot_ind = zeros(nc,ni);

% initialize the distance matrix inputs
x0 = ynuc(cell_ind,x)*ones(1,nc);
y0 = ynuc(cell_ind,y)*ones(1,nc);
index = 1:nc:ni*nc;
l = round(rand(nc,3)*100)./100;

% initialize the data matrices for the first point
jj=1;
ci = ((jj-1)*nc)+1:(jj*nc);
Nuc_Int_Intensity = ynuc(ci,Nuc_Int_Intensity_index); % y-variables for
this image frame
Nuc_Mean_Intensity = ynuc(ci,Nuc_Mean_Intensity_index); % y-variables for
this image frame
Nuc_Int_Intensity_mat(jj,:) = Nuc_Int_Intensity';
Nuc_Mean_Intensity_mat(jj,:) = Nuc_Mean_Intensity';

Cyt_Int_Intensity = ycyt(ci,Cyt_Int_Intensity_index); % y-variables for
this image frame
Cyt_Mean_Intensity = ycyt(ci,Cyt_Mean_Intensity_index); % y-variables for
this image frame
Cyt_Int_Intensity_mat(jj,:) = Cyt_Int_Intensity';
Cyt_Mean_Intensity_mat(jj,:) = Cyt_Mean_Intensity';

% plot the number index of the first point
if plot_flag>0
    figure(1)
    for ii = 1:nc
        text(x0(ii,1)+5,-y0(ii,1)+5,int2str(ii),'Color',l(ii,:))
    end
    hold on,axis([1 672 -512 -1]);
end

% plot cell position
cell_plot_ind = cell_ind;
disp('Plotting...')

%----- Main loop -----
for jj = start_frame+1:stop_frame,
    disp(jj)
    ci = ((jj-1)*nc)+1:(jj*nc);
    X = ynuc(ci,x); % x-variables for this image frame
    Y = ynuc(ci,y); % y-variables for this image frame
    Nuc_Int_Intensity = ynuc(ci,Nuc_Int_Intensity_index); % y-variables for
this image frame
    Nuc_Mean_Intensity = ynuc(ci,Nuc_Mean_Intensity_index); % y-variables
for this image frame
    Cyt_Int_Intensity = ycyt(ci,Cyt_Int_Intensity_index); % y-variables for
this image frame
    Cyt_Mean_Intensity = ycyt(ci,Cyt_Mean_Intensity_index); % y-variables
for this image frame

```

```

xn = X*ones(1,nc); % x-variable matrix
yn = Y*ones(1,nc); % y-variable matrix
% Compute the distance matrix
dm0 = sqrt((x0-xn').^2+(y0-yn').^2);
% find the index (di) of the minimum distance cells traveled (dd)
[dd,di] = min(dm0,[],1);
cell_tem_ind = di-cell_ind; % determine how cells swap positions
if sum(cell_tem_ind~=0)>1 % only concerned with pairs of index changes
    adjst_ind = cell_tem_ind; % position swap vector
else
    adjst_ind = zeros(1,nc);
end
% form the permutation matrix based on how cells swap
perm_mat = zeros(nc);
perm_mat(cell_ind + adjst_ind+nc*(cell_ind-1)) = 1;
% apply the permutation to the index of cells
X = perm_mat*X;
Y = perm_mat*Y;
Nuc_Int_Intensity = perm_mat*Nuc_Int_Intensity;
Nuc_Mean_Intensity = perm_mat*Nuc_Mean_Intensity;
Cyt_Int_Intensity = perm_mat*Cyt_Int_Intensity;
Cyt_Mean_Intensity = perm_mat*Cyt_Mean_Intensity;

if plot_flag>0
    figure(1)
    for ii=1:nc
        plot(X(ii),-Y(ii),'.','Color',l(ii,:));
    end
end
x0 = X*ones(1,nc); % x-variable matrix
y0 = Y*ones(1,nc); % y-variable matrix
big_cell_plot_ind(:,jj) = cell_plot_ind';
drawnow
Nuc_Int_Intensity_mat(jj,:) = Nuc_Int_Intensity';
Nuc_Mean_Intensity_mat(jj,:) = Nuc_Mean_Intensity';
Cyt_Int_Intensity_mat(jj,:) = Cyt_Int_Intensity';
Cyt_Mean_Intensity_mat(jj,:) = Cyt_Mean_Intensity';
end

%Normalize nuclear by cytoplasm
Nuc_by_Cyt_matrix = Nuc_Mean_Intensity_mat./Cyt_Mean_Intensity_mat;
Nuc_by_Cyt_Int_matrix = Nuc_Int_Intensity_mat./Cyt_Int_Intensity_mat;

for ii=1:nc
    Nuc_Mean_Norm_Intensity_mat(1:ni,ii) = Nuc_Mean_Intensity_mat(1:ni,ii)
/ max(Nuc_Mean_Intensity_mat(1:ni,ii) );
    Nuc_Int_Norm_Intensity_mat(1:ni,ii) = Nuc_Int_Intensity_mat(1:ni,ii) /
max(Nuc_Int_Intensity_mat(1:ni,ii) );
    Cyt_Mean_Norm_Intensity_mat(1:ni,ii) = Cyt_Mean_Intensity_mat(1:ni,ii)
/ max(Cyt_Mean_Intensity_mat(1:ni,ii) );
    Cyt_Int_Norm_Intensity_mat(1:ni,ii) = Cyt_Int_Intensity_mat(1:ni,ii) /
max(Cyt_Int_Intensity_mat(1:ni,ii) );
    Nuc_by_Cyt_Norm_matrix(1:ni,ii) = Nuc_by_Cyt_matrix(1:ni,ii) /
max(Nuc_by_Cyt_matrix(1:ni,ii) );
end

%---Save Nuclear stuff ---
temp=Nuc_Mean_Intensity_mat(1:end,:);save Nuc_Mean_Intensity.txt -ascii -
tabs -double temp
temp=Nuc_Mean_Norm_Intensity_mat(1:end,:) ; save
Nuc_Mean_Norm_Intensity.txt -ascii -tabs -double temp

```

```

temp=Nuc_Int_Intensity_mat(1:end,:);save Nuc_Int_Intensity.txt -ascii -tabs
-double temp
temp=Nuc_Int_Norm_Intensity_mat(1:end,:) ; save Nuc_Int_Norm_Intensity.txt
-ascii -tabs -double temp

%-- Save Cyto stuff ----
temp=Cyt_Mean_Intensity_mat(1:end,:);save Cyt_Mean_Intensity.txt -ascii -
tabs -double temp
temp=Cyt_Mean_Norm_Intensity_mat(1:end,:) ; save
Cyt_Mean_Norm_Intensity.txt -ascii -tabs -double temp

temp=Cyt_Int_Intensity_mat(1:end,:);save Cyt_Int_Intensity.txt -ascii -tabs
-double temp
temp=Cyt_Int_Norm_Intensity_mat(1:end,:) ; save Cyt_Int_Norm_Intensity.txt
-ascii -tabs -double temp

%-- Save Extra stuff ----
temp = Nuc_by_Cyt_Norm_matrix(1:end,:);save Nuc_by_Cyt_Norm_Intensity.txt -
ascii -tabs -double temp
temp = Nuc_by_Cyt_matrix (1:end,:);save Nuc_by_Cyt_Mean_Intensity.txt -
ascii -tabs -double temp
temp = Nuc_by_Cyt_Int_matrix (1:end,:);save Nuc_by_Cyt_Int_Intensity.txt -
ascii -tabs -double temp

Uber_plot_cellprofiler_results

disp('...done.')

end

```

```

%-----
%-          Plot Cellprofiler output
%-          Igal Brener, 4-2-09
%-----

%clc;
%close all
%clear all
%
% %-----
% figure
% single_cell_num = 12;
% %load 'Nuc_Mean_Norm_Intensity.txt'
% %y=Nuc_Mean_Norm_Intensity;
% load 'Nuc_Mean_Intensity.txt'
% y=Nuc_Mean_Intensity;
%
% N_cells = size(y,2);
% N_frames = size(y,1);
% plot_frame = [floor(sqrt(N_cells))+1, floor(sqrt(N_cells))+1 ];
%
% title('Nucleus')
% % Write here the cells to analyze
% for ii= 1:N_cells %
%     if (ii~=0) % && (ii~=28) && (ii~=24) && (ii~=1) && (i~=4) %skip
problematic cells
%         yy = y(:,ii);
%         yy = yy(:) - min(yy);
%         yy=yy(:);
%
%         t=1:2:N_frames*2;t=t(:);
%
%         subplot(plot_frame(1), plot_frame(2), ii);
%         plot(t,yy, '.');hold on;
%         axis([0 300 0 1]);
%         h = legend(int2str(ii));set(h, 'FontSize', 6);drawnow
%         hold off;
%     end;
% end;
%
% %-----
% figure
% %load 'Cyt_Mean_Norm_Intensity.txt'
% %y=Cyt_Mean_Norm_Intensity;
% load 'Cyt_Mean_Intensity.txt'
% y=Cyt_Mean_Intensity;
%
% N_cells = size(y,2);
% N_frames = size(y,1);
% plot_frame = [floor(sqrt(N_cells))+1, floor(sqrt(N_cells))+1 ];
%
% title('Cytoplasm')
% % Write here the cells to analyze
% for ii= 1:N_cells %
%     if (ii~=0) % && (ii~=28) && (ii~=24) && (ii~=1) && (i~=4) %skip
problematic cells
%         yy = y(:,ii);

```

```

%         yy = yy(:) - min(yy);
%         YY=YY(:);
%
%         t=1:2:N_frames*2;t=t(:);
%
%         subplot(plot_frame(1), plot_frame(2), ii);
%         plot(t,yy,'.');hold on;
%         axis([0 300 0 1]);
%         h = legend(int2str(ii));set(h, 'FontSize', 6);drawnow
%         hold off;
%     end;
% end;
%
%-----
% figure
% load 'Nuc_by_Cyt_Norm_Intensity.txt'
% y=Nuc_by_Cyt_Norm_Intensity;
%
% N_cells = size(y,2);
% N_frames = size(y,1);
% plot_frame = [floor(sqrt(N_cells))+1, floor(sqrt(N_cells))+1 ];
%
%
% title('Ratio')
% % Write here the cells to analyze
% for ii= 1:N_cells %
%     if (ii~=0) % && (ii~=28) && (ii~=24) && (ii~=1) && (ii~=4) %skip
% problematic cells
%         yy = y(:,ii);
%         YY = yy(:) - min(yy);
%         YY=YY(:);
%
%         t=1:2:N_frames*2;t=t(:);
%
%         subplot(plot_frame(1), plot_frame(2), ii);
%         plot(t,yy,'.');hold on;
%         axis([0 300 0 1]);
%         h = legend(int2str(ii));set(h, 'FontSize', 6);drawnow
%         hold off;
%     end;
% end;
%
%-----
% figure
% load 'Nuc_by_Cyt_Mean_Intensity.txt'
% y=Nuc_by_Cyt_Mean_Intensity;
%
% load 'Nuc_by_Cyt_Mean_Intensity.txt'
% y=Nuc_by_Cyt_Mean_Intensity;
%
% N_cells = size(y,2);
% N_frames = size(y,1);
% plot_frame = [floor(sqrt(N_cells))+1, floor(sqrt(N_cells))+1 ];
%
% title('Ratio')
% % Write here the cells to analyze

```

```

for ii= 1:N_cells %
    if (ii~=0) % && (ii~=28) && (ii~=24) && (ii~=1) && (ii~=4) %skip
problematic cells
        yy = y(:,ii);
        %yy = yy(:) - min(yy);
        YY=yy(:);

        t=1:2:N_frames*2;t=t(:);

        subplot(plot_frame(1), plot_frame(2), ii);
        plot(t,yy, '.');hold on;
        axis([0 300 0 2]);
        h = legend(int2str(ii));set(h, 'FontSize', 6);drawnow
        hold off;
    end;
end;

%-----
% figure
% load 'Nuc_by_Cyt_Int_Intensity.txt'
% y=Nuc_by_Cyt_Int_Intensity;
%
% %load 'Nuc_by_Cyt_Mean_Intensity.txt'
% %y=Nuc_by_Cyt_Mean_Intensity;
%
% N_cells = size(y,2);
% N_frames = size(y,1);
% plot_frame = [floor(sqrt(N_cells))+1, floor(sqrt(N_cells))+1 ];
%
% title('Ratio')
% % Write here the cells to analyze
% for ii= 1:N_cells %
%     if (ii~=0) % && (ii~=28) && (ii~=24) && (ii~=1) && (ii~=4) %skip
problematic cells
%         yy = y(:,ii);
%         %yy = yy(:) - min(yy);
%         YY=yy(:);
%
%         t=1:2:N_frames*2;t=t(:);
%
%         subplot(plot_frame(1), plot_frame(2), ii);
%         plot(t,yy, '.');hold on;
%         axis([0 300 0 .001]);
%         h = legend(int2str(ii));set(h, 'FontSize', 6);drawnow
%         hold off;
%     end;
% end;
%

```



## CellProfiler Pipeline:

The following is a text version of the pipeline file used in CellProfiler. This shows the names of all of the input files as well. This example uses the dataset from 2-27-08. The same file was used for every dataset with the appropriate substitutions made.

Saved Pipeline, in file lgal\_5-09\_-nucle+cyto-v5-exp-shrunk-PIPE.txt, Saved on 29-Jun-2010

Pixel Size: 1

Pipeline:

```

LoadSingleImage
LoadImages
ColorToGray
CorrectIllumination_Calculate
CorrectIllumination_Apply
LoadImages
ColorToGray
IdentifyPrimAutomatic
ExpandOrShrink
ExpandOrShrink
IdentifySecondary
IdentifyTertiarySubregion
MeasureObjectIntensity
ExportToExcel

```

### Module #1: LoadSingleImage revision - 4

This module loads one image for \*all\* cycles that will be processed. Typically, however, a different module (LoadImages) is used to load new sets of images during each cycle of processing. n/a

Enter the path name to the folder where the images to be loaded are located. Type period (.) for the default image folder, or type ampersand (&) for the default output folder. .\back

What image file do you want to load? Include the extension, like .tif 02-27-08 back.tif

What do you want to call that image? BackrAvg

What image file do you want to load? Include the extension, like .tif Do not use

What do you want to call that image? Do not use

What image file do you want to load? Include the extension, like .tif Do not use

What do you want to call that image? Do not use

What image file do you want to load? Include the extension, like .tif Do not use

What do you want to call that image? Do not use

### Module #2: LoadImages revision - 2

How do you want to load these files? Text-Exact match

Type the text that one type of image has in common (for TEXT options), or their position in each group (for ORDER option): 02-27-08 1nM ecoli

What do you want to call these images within CellProfiler? Orig

Type the text that one type of image has in common (for TEXT options), or their position in each group (for ORDER option). Type "Do not use" to ignore: Do not use

What do you want to call these images within CellProfiler? (Type "Do not use" to ignore) Do not use

Type the text that one type of image has in common (for TEXT options), or their position in each group (for ORDER option): Do not use

What do you want to call these images within CellProfiler? Do not use

Type the text that one type of image has in common (for TEXT options), or their position in each group (for ORDER option): Do not use

What do you want to call these images within CellProfiler? Do not use

If using ORDER, how many images are there in each group (i.e. each field of view)? 1  
 What type of files are you loading? individual images  
 Analyze all subfolders within the selected folder? No  
 Enter the path name to the folder where the images to be loaded are located. Type period (.)  
 for default image folder. .cells  
 Note - If the movies contain more than just one image type (e.g., brightfield, fluorescent, field-  
 of-view), add the GroupMovieFrames module. n/a  
 Module #3: ColorToGray revision - 1  
 What did you call the image to be converted to Gray? Orig  
 How do you want to convert the color image? Split  
 COMBINE options: n/a  
 What do you want to call the resulting grayscale image? OrigGray  
 Enter the relative contribution of the red channel 0  
 Enter the relative contribution of the green channel 1  
 Enter the relative contribution of the blue channel 0  
 SPLIT options: n/a  
 What do you want to call the image that was red? Type N to ignore red. N  
 What do you want to call the image that was green? Type N to ignore green. OrigGreen  
 What do you want to call the image that was blue? Type N to ignore blue. N

#### Module #4: CorrectIllumination\_Calculate revision - 7

What did you call the images to be used to calculate the illumination function? BackrAvg  
 What do you want to call the illumination function? IllumGreen  
 Do you want to calculate using regular intensities or background intensities? Regular  
 For REGULAR INTENSITY: If the incoming images are binary and you want to dilate each  
 object in the final averaged image, enter the radius (roughly equal to the original radius of the  
 objects). Otherwise, enter 0. 70  
 For BACKGROUND INTENSITY: Enter the block size, which should be large enough that  
 every square block of pixels is likely to contain some background pixels, where no objects are  
 located. 70  
 Do you want to rescale the illumination function so that the pixel intensities are all equal to or  
 greater than one (Y or N)? This is recommended if you plan to use the division option in  
 CorrectIllumination\_Apply so that the resulting images will be in the range 0 to 1. Yes  
 Enter Each to calculate an illumination function for Each image individually (in which case,  
 choose Pipeline mode in the next box) or All to calculate an illumination function based on All the  
 specified images to be corrected. See the help for details. Each  
 Are the images you want to use to calculate the illumination function to be loaded straight from  
 a Load Images module, or are they being produced by the pipeline? See the help for details.  
 Pipeline  
 Enter the smoothing method you would like to use, if any. No smoothing  
 For MEDIAN FILTER or GAUSSIAN FILTER, specify the approximate width of the artifacts to  
 be smoothed (in pixels), or leave the word "Automatic". Automatic  
 If you want override the above width of artifacts and set your own filter size (in pixels), please  
 specify it here. Otherwise leave "Do not use". Do not use  
 (For "All" mode only) What do you want to call the averaged image (prior to dilation or  
 smoothing)? (This is an image produced during the calculations - it is typically not needed for  
 downstream modules) Do not use  
 What do you want to call the image after dilation but prior to smoothing? (This is an image  
 produced during the calculations - it is typically not needed for downstream modules) Do not  
 use

#### Module #5: CorrectIllumination\_Apply revision - 3

What did you call the image to be corrected? OrigGreen  
 What do you want to call the corrected image? CorrGreen

What did you call the illumination correction function image to be used to carry out the correction (produced by another module or loaded as a .mat format image using Load Single Image)? IllumGreen

How do you want to apply the illumination correction function? Divide

If you chose division, Choose rescaling method. No rescaling

Module #6: LoadImages revision - 2

How do you want to load these files? Text-Exact match

Type the text that one type of image has in common (for TEXT options), or their position in each group (for ORDER option): black 02-27-08 1nM ecoli

What do you want to call these images within CellProfiler? OrigNuclMaskColor

Type the text that one type of image has in common (for TEXT options), or their position in each group (for ORDER option). Type "Do not use" to ignore: Do not use

What do you want to call these images within CellProfiler? (Type "Do not use" to ignore) Do not use

Type the text that one type of image has in common (for TEXT options), or their position in each group (for ORDER option): Do not use

What do you want to call these images within CellProfiler? Do not use

Type the text that one type of image has in common (for TEXT options), or their position in each group (for ORDER option): Do not use

What do you want to call these images within CellProfiler? Do not use

If using ORDER, how many images are there in each group (i.e. each field of view)? 3

What type of files are you loading? individual images

Analyze all subfolders within the selected folder? No

Enter the path name to the folder where the images to be loaded are located. Type period (.) for default image folder. \nuclei

Note - If the movies contain more than just one image type (e.g., brightfield, fluorescent, field-of-view), add the GroupMovieFrames module. n/a

Module #7: ColorToGray revision - 1

What did you call the image to be converted to Gray? OrigNuclMaskColor

How do you want to convert the color image? Combine

COMBINE options: n/a

What do you want to call the resulting grayscale image? OrigNuclMask

Enter the relative contribution of the red channel 1

Enter the relative contribution of the green channel 1

Enter the relative contribution of the blue channel 1

SPLIT options: n/a

What do you want to call the image that was red? Type N to ignore red. OrigRed

What do you want to call the image that was green? Type N to ignore green. OrigGreen

What do you want to call the image that was blue? Type N to ignore blue. OrigBlue

Module #8: IdentifyPrimAutomatic revision - 12

What did you call the images you want to process? OrigNuclMask

What do you want to call the objects identified by this module? Nuclei

Typical diameter of objects, in pixel units (Min,Max): 8,50

Discard objects outside the diameter range? Yes

Try to merge too small objects with nearby larger objects? No

Discard objects touching the border of the image? No

Select an automatic thresholding method or enter an absolute threshold in the range [0,1]. To choose a binary image, select "Other" and type its name. Choosing "All" will use the Otsu Global method to calculate a single threshold for the entire image group. The other methods calculate a threshold for each image individually. "Set interactively" will allow you to manually adjust the threshold during the first cycle to determine what will work well. 0.5

Threshold correction factor 1

Lower and upper bounds on threshold, in the range [0,1] 0,1

For MoG thresholding, what is the approximate fraction of image covered by objects? 0.1  
 Method to distinguish clumped objects (see help for details): Intensity  
 Method to draw dividing lines between clumped objects (see help for details): None  
 Size of smoothing filter, in pixel units (if you are distinguishing between clumped objects).  
 Enter 0 for low resolution images with small objects (~< 5 pixel diameter) to prevent any image smoothing. Automatic  
 Suppress local maxima within this distance, (a positive integer, in pixel units) (if you are distinguishing between clumped objects) Automatic  
 Speed up by using lower-resolution image to find local maxima? (if you are distinguishing between clumped objects) Yes  
 Enter the following information, separated by commas, if you would like to use the Laplacian of Gaussian method for identifying objects instead of using the above settings: Size of neighborhood(height,width),Sigma,Minimum Area,Size for Wiener Filter(height,width),Threshold  
 Do not use  
 What do you want to call the outlines of the identified objects (optional)? Do not use  
 Do you want to fill holes in identified objects? Yes  
 Do you want to run in test mode where each method for distinguishing clumped objects is compared? No

#### Module #9: ExpandOrShrink revision - 2

What did you call the objects that you want to expand or shrink? Nuclei  
 What do you want to call the expanded or shrunken objects? ShrunkenNuclei  
 Were the objects identified using an Identify Primary or Identify Secondary module (note: shrinking results are not perfect with Secondary objects)? Primary  
 Do you want to expand or shrink the objects? Shrink  
 Enter the number of pixels by which to expand or shrink the objects, or "Inf" to either shrink to a point or expand until almost touching, or 0 (the number zero) to simply add partial dividing lines between objects that are touching (experimental feature). 2  
 What do you want to call the outlines of the identified objects (optional)? Do not use

#### Module #10: ExpandOrShrink revision - 2

What did you call the objects that you want to expand or shrink? Nuclei  
 What do you want to call the expanded or shrunken objects? ExpandedNuclei  
 Were the objects identified using an Identify Primary or Identify Secondary module (note: shrinking results are not perfect with Secondary objects)? Primary  
 Do you want to expand or shrink the objects? Expand  
 Enter the number of pixels by which to expand or shrink the objects, or "Inf" to either shrink to a point or expand until almost touching, or 0 (the number zero) to simply add partial dividing lines between objects that are touching (experimental feature). 2  
 What do you want to call the outlines of the identified objects (optional)? Do not use

#### Module #11: IdentifySecondary revision - 3

What did you call the primary objects you want to create secondary objects around?  
 ExpandedNuclei  
 What do you want to call the objects identified by this module? Cells  
 Select the method to identify the secondary objects (Distance - B uses background; Distance - N does not): Distance - N  
 What did you call the images to be used to find the edges of the secondary objects? For DISTANCE - N, this will not affect object identification, only the final display. CorrGreen  
 Select an automatic thresholding method or enter an absolute threshold in the range [0,1]. To choose a binary image, select "Other" and type its name. Choosing "All" will use the Otsu Global method to calculate a single threshold for the entire image group. The other methods calculate a threshold for each image individually. Set interactively will allow you to manually adjust the threshold during the first cycle to determine what will work well. Otsu Global  
 Threshold correction factor 1.0  
 Lower and upper bounds on threshold, in the range [0,1] 0,1

For MoG thresholding, what is the approximate fraction of image covered by objects? 0.3

For DISTANCE, enter the number of pixels by which to expand the primary objects [Positive integer] 9

For PROPAGATION, enter the regularization factor (0 to infinity). Larger=distance,0=intensity 0.05

What do you want to call the outlines of the identified objects (optional)? Do not use

Do you want to run in test mode where each method for identifying secondary objects is compared? No

Module #12: IdentifyTertiarySubregion revision - 1

What did you call the larger identified objects? Cells

What did you call the smaller identified objects? ExpandedNuclei

What do you want to call the new subregions? Cytoplasm

What do you want to call the outlines of the identified objects (optional)? Do not use

Module #13: MeasureObjectIntensity revision - 2

What did you call the greyscale images you want to measure? CorrGreen

What did you call the objects that you want to measure? ShrunkenNuclei

Cytoplasm

Cells

Do not use

Do not use

Do not use

Module #14: ExportToExcel revision - 1

Which objects do you want to export? ShrunkenNuclei

Cytoplasm

Cells

Do not use

Do not use

Do not use

Do not use

Do not use

## References

- Adachi, Y., Kindzelskii, A. L., Ohno, N., et al.** (1999). "Amplitude and Frequency Modulation of Metabolic Signals in Leukocytes: Synergistic Role of *Ifn-Gamma* in *Il-6*- and *Il-2*-Mediated Cell Activation." *J Immunol* **163**(8): 4367-74.
- An, G.** (2009). "A Model of *Tlr4* Signaling and Tolerance Using a Qualitative, Particle-Event-Based Method: Introduction of Spatially Configured Stochastic Reaction Chambers (Scsrc)." *Math Biosci* **217**(1): 43-52.
- Baldwin, A. S., Jr.** (2001). "Series Introduction: The Transcription Factor *Nf-Kappab* and Human Disease." *J Clin Invest* **107**(1): 3-6.
- Barken, D., Wang, C. J., Kearns, J., et al.** (2005). "Comment On "Oscillations in *Nf-Kappa B* Signaling Control the Dynamics of Gene Expression"." *Science* **308**(5718).
- Berridge, M. J.** (1997). "The Am and Fm of Calcium Signalling." *Nature* **386**(6627): 759-60.
- Carlotti, F., Chapman, R., Dower, S. K., et al.** (1999). "Activation of Nuclear Factor *Kappab* in Single Living Cells. Dependence of Nuclear Translocation and Anti-Apoptotic Function on *Egfp* Concentration." *J Biol Chem* **274**(53): 37941-9.
- Carpenter, A. E., Jones, T. R., Lamprecht, M. R., et al.** (2006). "Cellprofiler: Image Analysis Software for Identifying and Quantifying Cell Phenotypes." *Genome Biol* **7**(10): R100.
- Chen, F. E. and Ghosh, G.** (1999). "Regulation of DNA Binding by *Rel/Nf-Kappab* Transcription Factors: Structural Views." *Oncogene* **18**(49): 6845-52.
- Covert, M. W., Leung, T. H., Gaston, J. E., et al.** (2005). "Achieving Stability of Lipopolysaccharide-Induced *Nf-Kappab* Activation." *Science* **309**(5742): 1854-7.
- Darveau, R. P. and Hancock, R. E.** (1983). "Procedure for Isolation of Bacterial Lipopolysaccharides from Both Smooth and Rough *Pseudomonas Aeruginosa* and *Salmonella Typhimurium* Strains." *J Bacteriol* **155**(2): 831-8.
- Du, X., Poltorak, A., Silva, M., et al.** (1999). "Analysis of *Tlr4*-Mediated *Lps* Signal Transduction in Macrophages by Mutational Modification of the Receptor." *Blood Cells Mol Dis* **25**(5-6): 328-38.
- Duyao, M. P., Buckler, A. J. and Sonenshein, G. E.** (1990). "Interaction of an *Nf-Kappa B*-Like Factor with a Site Upstream of the *C-Myc* Promoter." *Proc Natl Acad Sci U S A* **87**(12): 4727-31.
- Fischer, C., Page, S., Weber, M., et al.** (1999). "Differential Effects of Lipopolysaccharide and Tumor Necrosis Factor on Monocytic *Ikappab* Kinase Signalsome Activation and *Ikappab* Proteolysis." *J Biol Chem* **274**(35): 24625-32.
- Gilmore, T. D.** (1999). "The *Rel/Nf-Kappab* Signal Transduction Pathway: Introduction." *Oncogene* **18**(49): 6842-4.
- Gilmore, T. D.** (2006). "Introduction to *Nf-Kappab*: Players, Pathways, Perspectives." *Oncogene* **25**(51): 6680-4.
- Gilmore, T. D.** (2009). "Rel-Nf-Kb Transcription Factors: Inhibitors of Rel/Nf-Kb." 2009, from <http://people.bu.edu/gilmore/nf-kb/inhibitors/index.html>.

- Guo, L., Lim, K. B., Poduje, C. M., et al.** (1998). "Lipid a Acylation and Bacterial Resistance against Vertebrate Antimicrobial Peptides." Cell **95**(2): 189-98.
- Hannink, M. and Temin, H. M.** (1990). "Structure and Autoregulation of the C-Rel Promoter." Oncogene **5**(12): 1843-50.
- Harada, H., Takahashi, E., Itoh, S., et al.** (1994). "Structure and Regulation of the Human Interferon Regulatory Factor 1 (*Irf-1*) and *Irf-2* Genes: Implications for a Gene Network in the Interferon System." Mol Cell Biol **14**(2): 1500-9.
- Hirata, H., Yoshiura, S., Ohtsuka, T., et al.** (2002). "Oscillatory Expression of the *Bhlh* Factor *Hes1* Regulated by a Negative Feedback Loop." Science **298**(5594): 840-3.
- Hirschfeld, M., Ma, Y., Weis, J. H., et al.** (2000). "Cutting Edge: Repurification of Lipopolysaccharide Eliminates Signaling through Both Human and Murine Toll-Like Receptor 2." J Immunol **165**(2): 618-22.
- Hiscott, J., Kwon, H. and Genin, P.** (2001). "Hostile Takeovers: Viral Appropriation of the *Nf-Kappab* Pathway." J Clin Invest **107**(2): 143-51.
- Hoffmann, A., Levchenko, A., Scott, M. L., et al.** (2002). "The *I Kappa B-Nf-Kappa B* Signaling Module: Temporal Control and Selective Gene Activation." Science **298**(5596): 1241-5.
- Ihekwa, A. E. C., Broomhead, D. S., Grimley, R., et al.** (2005). "Synergistic Control of Oscillations in the *Nf- Kappa B* Signalling Pathway." IEE Proceedings-Systems Biology **152**(3): 153-60.
- Ihekwa, A. E. C., Broomhead, D. S., Grimley, R. L., et al.** (2004). "Sensitivity Analysis of Parameters Controlling Oscillatory Signalling in the *Nf- Kappa B* Pathway: The Roles of *Ikk* and *I Kappa B Alpha*." IEE Systems Biology **1**(1): 93-103.
- James, C. D., Moorman, M. W., Carson, B. D., et al.** (2009). "Nuclear Translocation Kinetics of *Nf-Kappab* in Macrophages Challenged with Pathogens in a Microfluidic Platform." Biomed Microdevices **11**(3): 693-700.
- Joo, J., Plimpton, S., Martin, S., et al.** (2007). "Sensitivity Analysis of a Computational Model of the *Ikk Nf-Kappab Ikappabalpha A20* Signal Transduction Network." Ann N Y Acad Sci **1115**: 221-39.
- Kawai, T. and Akira, S.** (2007). "*Tlr* Signaling." Semin Immunol **19**(1): 24-32.
- Kearns, J. D., Basak, S., Werner, S. L., et al.** (2006). "*Ikappabepsilon* Provides Negative Feedback to Control *Nf-Kappab* Oscillations, Signaling Dynamics, and Inflammatory Gene Expression." J Cell Biol **173**(5): 659-64.
- Klinke, D. J., 2nd, Ustyugova, I. V., Brundage, K. M., et al.** (2008). "Modulating Temporal Control of *Nf-Kappab* Activation: Implications for Therapeutic and Assay Selection." Biophys J **94**(11): 4249-59.
- Kuprash, D. V., Osipovich, O. A., Pokholok, D. K., et al.** (1996). "Functional Analysis of the *Lymphotoxin-Beta* Promoter. Sequence Requirements for *Pma* Activation." J Immunol **156**(7): 2465-72.
- Lev Bar-Or, R., Maya, R., Segel, L. A., et al.** (2000). "Generation of Oscillations by the *P53-Mdm2* Feedback Loop: A Theoretical and Experimental Study." Proc Natl Acad Sci U S A **97**(21): 11250-5.

- Lipniacki, T., Puszynski, K., Paszek, P., et al.** (2007). "Single Tnfalpha Trimers Mediating Nf-Kappab Activation: Stochastic Robustness of Nf-Kappab Signaling." *BMC Bioinformatics* **8**: 376.
- Miller, S. I., Ernst, R. K. and Bader, M. W.** (2005). "Lps, Tlr4 and Infectious Disease Diversity." *Nat Rev Microbiol* **3**(1): 36-46.
- Miyake, K.** (2006). "Roles for Accessory Molecules in Microbial Recognition by Toll-Like Receptors." *J Endotoxin Res* **12**(4): 195-204.
- Nelson, D. E., Ihekweba, A. E. C., Elliott, M., et al.** (2004). "Oscillations in Nf-Kappa B Signaling Control the Dynamics of Gene Expression." *Science* **306**(5696): 704-8.
- Nelson, D. E., Horton, C. A., See, V., et al.** (2005). "Response to Comment On "Oscillations in Nf-Kappa B Signaling Control the Dynamics of Gene Expression"." *Science* **308**(5718).
- Ogawa, H., Iimura, M., Eckmann, L., et al.** (2004). "Regulated Production of the Chemokine Ccl28 in Human Colon Epithelium." *Am J Physiol Gastrointest Liver Physiol* **287**(5): G1062-9.
- Pahl, H. L.** (1999). "Activators and Target Genes of Rel/Nf-Kappab Transcription Factors." *Oncogene* **18**(49): 6853-66.
- Park, B. S., Song, D. H., Kim, H. M., et al.** (2009). "The Structural Basis of Lipopolysaccharide Recognition by the Tlr4-Md-2 Complex." *Nature* **458**(7242): 1191-5.
- Perkins, N. D.** (2007). "Integrating Cell-Signalling Pathways with Nf-Kappab and Ikk Function." *Nat Rev Mol Cell Biol* **8**(1): 49-62.
- Quitschke, W. W., Lin, Z. Y., DePonti-Zilli, L., et al.** (1989). "The Beta Actin Promoter. High Levels of Transcription Depend Upon a Ccaat Binding Factor." *J Biol Chem* **264**(16): 9539-46.
- Rebeil, R., Ernst, R. K., Gowen, B. B., et al.** (2004). "Variation in Lipid a Structure in the Pathogenic Yersiniae." *Mol Microbiol* **52**(5): 1363-73.
- Scott, M. L., Fujita, T., Liou, H. C., et al.** (1993). "The P65 Subunit of Nf-Kappa B Regulates I Kappa B by Two Distinct Mechanisms." *Genes Dev* **7**(7A): 1266-76.
- Sethi, G., Sung, B. and Aggarwal, B. B.** (2008). "Nuclear Factor-Kappab Activation: From Bench to Bedside." *Exp Biol Med (Maywood)* **233**(1): 21-31.
- Shakhov, A. N., Kuprash, D. V., Azizov, M. M., et al.** (1990). "Structural Analysis of the Rabbit Tnf Locus, Containing the Genes Encoding Tnf-Beta (Lymphotoxin) and Tnf-Alpha (Tumor Necrosis Factor)." *Gene* **95**(2): 215-21.
- Shin, Y. H., Son, K. N., Lee, G. W., et al.** (2005). "Transcriptional Regulation of Human Cc Chemokine Ccl15 Gene by Nf-Kappab and Ap-1 Elements in Pma-Stimulated U937 Monocytoid Cells." *Biochim Biophys Acta* **1732**(1-3): 38-42.
- Stark, J., Chan, C. and George, A. J. T.** (2007). "Oscillations in the Immune System." *Immunological Reviews* **216**: 213-31.
- Villar, J., Maca-Meyer, N., Perez-Mendez, L., et al.** (2004). "Bench-to-Bedside Review: Understanding Genetic Predisposition to Sepsis." *Crit Care* **8**(3): 180-9.
- Werner, S. L., Barken, D. and Hoffmann, A.** (2005). "Stimulus Specificity of Gene Expression Programs Determined by Temporal Control of Ikk Activity." *Science* **309**(5742): 1857-61.



**Wickremasinghe, M. I., Thomas, L. H., O'Kane, C. M., et al.** (2004). "*Transcriptional Mechanisms Regulating Alveolar Epithelial Cell-Specific Ccl5 Secretion in Pulmonary Tuberculosis.*" J Biol Chem **279**(26): 27199-210.

**Worm, M., Ebermayer, K. and Henz, B.** (1998). "*Lymphotoxin-Alpha Is an Important Autocrine Factor for Cd40 + Interleukin-4-Mediated B-Cell Activation in Normal and Atopic Donors.*" Immunology **94**(3): 395-402.

**Wu, H. and Lozano, G.** (1994). "*Nf-Kappa B Activation of P53. A Potential Mechanism for Suppressing Cell Growth in Response to Stress.*" J Biol Chem **269**(31): 20067-74.

